# ZEBRAFISH EXTRACELLULAR MATRIX AS A THERAPEUTIC AGENT FOR ADULT MAMMALIAN CENTRAL NERVOUS SYSTEM REGENERATION

by

**Sung-Min (Terry) Kim**

Bachelor of Science, University of California San Diego, 2013

Submitted to the Graduate Faculty of

Swanson School of Engineering in partial fulfillment

of the requirements for the degree of

Doctor of Philosophy

University of Pittsburgh

2018

UNIVERSITY OF PITTSBURGH

SWANSON SCHOOL ENGINEERING

This dissertation was presented

by

Sung-Min (Terry) Kim

It was defended on

January 24, 2018

and approved by

Ian Conner, MD, Ph.D., Assistant Professor, Ophthalmology & Bioengineering

Tracy Cui, Ph.D., Professor, Bioengineering

Michael Tsang, Ph.D., Associate Professor, Developmental Biology

Dissertation Director: Yadong Wang, Ph.D., Professor, Bioengineering

**ZEBRAFISH EXTRACELLULAR MATRIX AS A THERAPEUTIC AGENT FOR ADULT MAMMALIAN CENTRAL NERVOUS SYSTEM REGENERATION**

Sung-Min (Terry) Kim, Ph.D.

University of Pittsburgh, 2018

Mammalian central nervous system (CNS) has limited capacity for regeneration. Despite numerous efforts in the last few decades, CNS-related injuries remain as detrimental as they were 50 years ago. While some functional recovery can occur, most regenerations are limited by an extracellular matrix (ECM) that actively inhibits axonal repair and promotes glial scarring. In most tissues, the ECM is an architectural foundation that plays an active role in supporting cellular development and regenerative response after injury. In mammalian CNS, however, this is not the case - its composition is not conducive for regeneration, with various molecules restricting plasticity and neuronal growth. In fact, the CNS-ECM alters its composition dramatically following an injury to restrict regeneration and to prioritize containment of injury as well as preservation of intact neural circuitry. Therefore, an ideal solution to limited CNS regeneration would be to modify and supplement the inhibitory extracellular environment so that it becomes more regeneration-permissive. Mammalian nervous tissue cannot provide such ECM, and synthesizing it in a laboratory is beyond current technology. Remarkably however, evolutionarily primitive species possess robust regenerative neural tissue. For example, small tropical freshwater dwelling zebrafish (Danio rerio) can completely regenerate severed spinal cord, re-gaining full motor function in a week. We believe their ECM contributes to its regenerative capability and that it can be harnessed to induce regeneration even in mammalian CNS. The objective of this dissertation was to evaluate the tissue-specific properties of zebrafish CNS-ECM for CNS injuries in terms of (1) influence on neuron viability and network formation, (2) potential for evoking

regenerative CNS traits, and (3) capacity to restore axon connections that translate to meaningful behavioral recovery.

Scaffolds enriched with ECM derived from zebrafish brains (zf-brECM) were used to grow a population of primary cortical neurons. The scaffolds were compared to others that were enriched with ECM derived from mammalian tissue, such as pig brain (p-brECM), pig urinary bladder (p-UBM), and rat brain (r-brECM). The scaffolds themselves were designed to help control the distribution of neuronal bodies and axonal sprouting. Ultimately, zf-brECM promoted significantly more neuron survival and growth than mammalian ECMs. Additionally, zf-brECM significantly increased the overall formation of new axon networks. More importantly, axon networks formed in the presence of zf-brECM resulted in functional propagation of action potential signals. Building upon this, therapeutic efficacy of zf-brECM was explored in vivo using a rodent model of optic nerve crush (ONC). ONC was chosen as a representative model of CNS injury model for two reasons: 1) ONC surgery is reliably replicable, lending itself to minimal surgical variability and intra-animal data noise; 2) optic nerves are small and their neural circuitries are simple, making the resident retinal ganglion cells (RGCs) and their axons easy to analyze. We compared zf-brECM against commercially available mammalian ECMs by looking at the biological response of the optic nerves and observing traits that are considered hallmarks of CNS regeneration: glial scar deposition and expression level of axon inhibitors, namely chondroitin sulfate proteoglycans (CSPG). While ECM technology for CNS injuries has been limited and virtually unstudied in the visual system, it is known that mammalian optic nerves cannot regenerate under normal physiological circumstances. Therefore, we also observed long-distance growth of repairing axons traversing the lesion sites and compared the resulting behavioral recovery. The

final behavioral assays revealed that only zf-brECM was able to restore pupil response as well as depth perception to damaged rodent eyes.

This body of work demonstrates the regenerative potential of zf-brECM, combined with its affordability, easy handling, and fast reproduction, positions zebrafish as an excellent candidate for a novel ECM source in the future. Specifically, it shows that zebrafish ECM holds promising regenerative potential for application in adult mammalian CNS injuries. Future research is necessary to determine the specific factors in zebrafish CNS-ECM responsible for the regenerative events.

## TABLE OF CONTENTS

## LIST OF TABLES

## LIST OF FIGURES

# PREFACE

I would first like to thank Dr. Wang for providing me the opportunity of a lifetime to conduct such exciting work of research. You have fostered a stimulating environment best suited for my growth as a scientist and it was truly a blessing to have worked under your mentorship. I would also like to thank my committee members: Dr. Ian Conner, Dr. Tracy Cui, and Dr. Michael Tsang for their insight and guidance throughout my doctoral degree.

I would also like to thank everyone in Biomaterials Foundry. You guys welcomed me into the lab with such warmth and have taught me so much over the years. You are all excellent colleagues as well as friends. I wish you guys the best of luck at your new university!

I would also like to thank my family. Mom and dad, you may have never pushed me to pursue a doctoral degree, but you were both so supportive of my decision and showed endless support. Coming home every once in a while to your welcoming arms and the delicious food you always had prepared for me was the highlight of my long graduate years. And to my brother Andy, who has now become a distinguished scientist of his own right - you always leave me stunned by how much you have accomplished.

Most importantly, I would like to thank my significant other and my best friend, the brilliant Adelyn Yeoh. Words simply cannot describe the impact you have had on my life and the strength and laughter you have provided me. I am so blessed to have you by my side through this

stage in my life. And of course, how could I forget our adorable companion Bakery whose constant ‘woofs’ filled our apartment with life. Thank you both – you two are my everything.

Finally, I would like to thank the Bioengineering Department of Swanson School of Engineering and its graduate department has also been a wonderful source of support. Dr. Shroff and Nick Mance, thank you for all your support and assistance. To everyone listed here and anyone I may have forgotten – thank you; I will not have made it this far without all of your help and support.

# 1.0 INTRODUCTION

Adult mammalian central nervous system (CNS) possesses poor intrinsic capacity for regeneration. Its axons display limited ability to repair after injury and consequently, most functional deficits after CNS injuries are permanent [1]. The lack of regenerative capacity mainly stems from its repair-inhibitory extracellular matrix (ECM) which actively stops axonal extensions and regrowth [2].

ECM is one of the most important regulators of cellular and tissue function in the body. The ECM plays a vital role in the cell's structural and biochemical integrity, and the right ECM composition is essential for development, tissue repair and organ homeostasis. Sustained disruption of the ECM can result in various pathological conditions and even regenerative shortcomings [3]. However, the reverse is also true – intelligent manipulation and adjustment of ECM composition can instigate growth and regenerative events. Regenerative medicine therapies have actively attempted to harness the healing mechanisms of ECM by isolating the matrix and apply them in a non-regenerative target. The goal is for the foreign ECM to promote tissue reconstruction in the host and eventually restore healthy tissue, both morphologically and functionally. In tissue engineering, this approach is known as "ECM therapy", a subset of regenerative medicine that takes advantage of composition found naturally in cellular environment and utilizes their bioactive molecules that are known to promote healing [4]. By doing so, ECM

therapy seeks to engage "regeneration" in a top-down approach – it begins with a theoretical/conceptual perspective on what constitutes as a regenerative agent, and works 'down' in the direction of increasingly greater organizational and functional detail of the involved biochemical composition and physical mechanisms. Typically, the ECM is harvested from the donor tissue and processed through decellularization [3,4]. The ECM is then transformed into a deliverable form and acts as a bioactive replacement of the host ECM, leading to promotion of site-specific constructive remodeling.

In theory, ECM replacement can be an effective solution to unlocking mammalian CNS regeneration as the repair-hostile CNS-ECM is largely responsible for the lack of regenerative capability. Unfortunately, because current ECM technology derives most, if not all, of its bioactive molecules from mammalian tissue source, ECM therapy has not had much success in jumpstarting CNS regeneration [5]. Interestingly, lower-vertebrates such as the zebrafish possess remarkably regenerative neural tissue but remain largely unexplored by the bioengineering community. One particular specie is especially known for its exceptional CNS regeneration – the zebrafish (Danio rerio). Well-known for their ability to easily regenerate damaged optic nerve and severed spinal cord, these small freshwater-dwelling fish possess CNS-ECM that aids in axonal repair by suppressing glial cell activation and circumventing inflammatory response. Yet, their ECM have yet to be utilized therapeutically. In this dissertation, we report the investigation of CNS-ECM derived from zebrafish brain as a therapeutic agent for constructive remodeling of CNS and axon regeneration. We hypothesize the zebrafish ECM contributes to their natural regenerative capability and may be harnessed to induce similar regeneration in mammalian CNS. We believe their regenerative potential, combined with their affordability, easy handling, and fast reproduction, will make zebrafish an excellent candidate as a novel ECM source.

## 1.1 SIGNIFICANCE

Adult mammalian CNS possesses very small chance for regeneration following an injury. Past the early developmental stage, neurons can no longer divide, and much of the communication needed for regenerative events becomes lost after an injury due to disrupted myelin sheath. Additionally, the complexity of neural circuity found in mammalian CNS includes positional data found in each individual synaptic connection, much of which is lost following an injury. The CNS ultimately prioritizes containment of injury over regeneration, leading to functional deficits involving permanent axonal disconnection. Consequently, CNS-related injuries cause life-long debilitation and lead to over $50B in healthcare costs [6]. Despite numerous scientific strides in the last few decades, CNS injuries remain one of the greatest challenges in the field of medicine.

There is hope however. Neurologic impairment and extent of damage following CNS injuries are known to be highly dependent on the ECM found in the injury location. Studies have shown that with adequate regeneration-permissive environment, CNS injuries can achieve some minor functional recovery in the form of dendritic remodeling, axonal sprouting, and synaptic changes, collectively known as neural plasticity [6,7]. Unfortunately, there are several factors that prevent CNS regeneration, including but not limited to: poor intrinsic regenerative potential of the neurons, hostile immune response leading to inflammation, and suppressed neurotrophic support in the ECM (Figure 1). In fact, most mammalian CNS possess compositionally regeneration-inhibitive ECM that actively stops axonal extension and promotes glial scarring, which suppresses axon repair and reduces neurotrophic support [7-10]. This leads to approximately 12,000 new

individuals who suffer from permanent effects of spinal cord injury every year, along with 80,000 who suffer from traumatic brain injuries and almost 500,000 who suffer from the permanent damage of stroke [6]. These staggering numbers suggest there is an urgent clinical and economic need for a regenerative approach that can promote functional axonal recovery in mammalian CNS injuries.

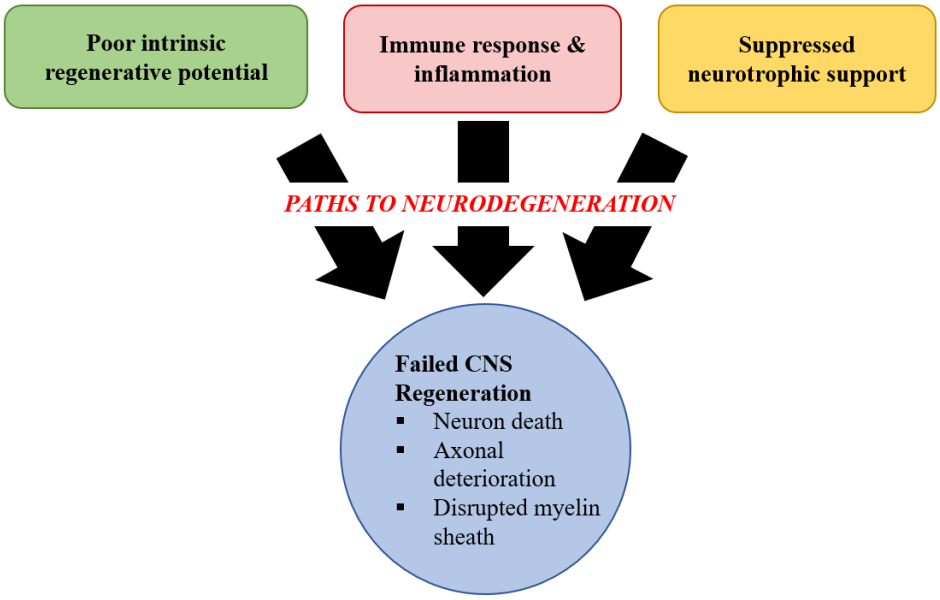


**Figure 1. Neurodegenerative pathways leading to failed CNS regeneration.** There are three major factors leading to neurodegeneration that must be prevented or overcome to engage regenerative events in CNS: poor intrinsic regenerative potential of the neurons, hostile immune response leading to inflammation, and suppressed neurotrophic support in the ECM. An ideal regenerative therapy must prevent one or more of these pathways.

### 1.1.1 CNS Injury Response

In the CNS, there are three cell types - astrocytes, microglia, and oligodendrocytes - which act as support cells. Oligodendrocytes make the myelin sheath responsible for protecting the axons and

propagating signals. Astrocytes and microglia have a variety of support functions required for neuronal function [11-13]. When an injury occurs (ie. spinal cord injury or optic nerve damage), the immune system is activated and sends out phagocytes to clean up the debris. The benefits are temporary however as the phagocytes are non-discriminatory and as a result, become detrimental as they begin to digest healthy tissue and remaining nerve endings as well [14]. To overcome this phenomenon, astrocytes form glial scar around the injury to prevent the phagocytes from damaging the remaining tissue (Figure 2). Astrocytes and microglia cells wall off the areas of damage with factors such as chondroitin sulfate proteoglycans (CSPG) which also happen to inhibit the growth of axons [12-14]. In essence, glial scar operates as a quarantine zone around the nerve damage. Unfortunately, this protective barrier also blocks the nerve from connecting to severed ends and prevent axonal regeneration. Glial scars express several inhibitor molecules which interrupt the signaling pathways responsible for inducing axonal growth and nerve regeneration [15]. Naturally, this has led many to believe glial scar is the main antagonist of achieving CNS regeneration. However, studies have also demonstrated that absence of glial scar is not ideal either as it increases inflammation in injury and thus exacerbates the damage even further [16,17].

Neurons are unique in that they must thrive not only individually but also as a group by forming meaningful synaptic connections with other resident neurons. In the context of clinical application regarding CNS injuries, this holds especially true as the neural connections contain positional data responsible for all learned information and experiences. In other words, for meaningful clinical results, the CNS must achieve regeneration beyond cellular restoration and succeed in replicating lost axon connections as well. Typically, neurons find their targets during development using series of extracellular cues that behave as guidance molecules for dendritic ends [18]. For example, the neurons may follow a specific chemical gradient and take directional

cues from making contact with various membrane proteins until reaching their final target by protein recognition. Unfortunately, these signals are time dependent and cannot be relied on to reconnect the same two ends when an injury occurs.

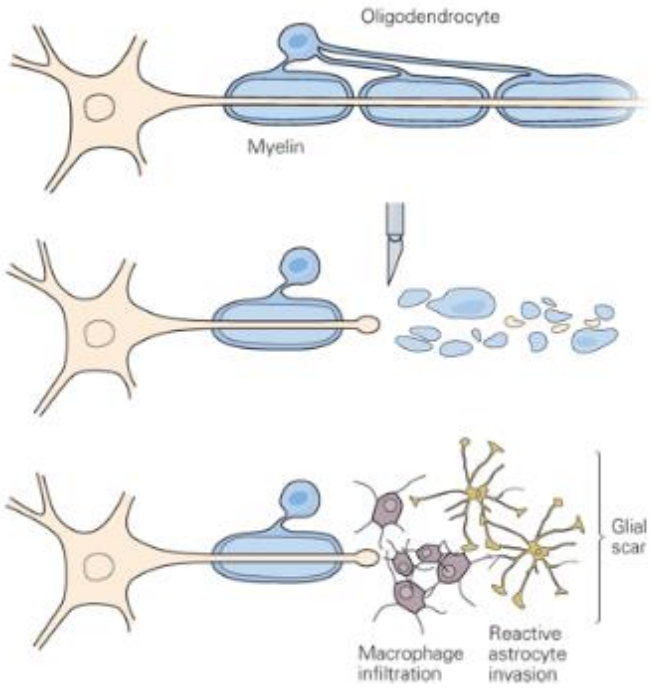


**Figure 2. A simplified depiction of a common injury response in adult mammalian CNS.** The nerve is severed, leaving various cellular debris behind from the destroyed axon and myelin sheath. Macrophage infiltration begins the removal of debris and its activity is kept in check by the deposition of reactive astrocytes, known as glial scar. Reproduced from [19].

### 1.1.2 Neural Plasticity

While adult mammalian CNS has poor capacity for regeneration, CNS injuries can achieve some minor functional recovery in the form of neural plasticity [6,7]. Neural plasticity describes the CNS's ability to change its anatomical, neurochemical, and functional performance status across

the lifespan. Long-term potentiation can result from an increase in receptors on the post-synaptic partner, decrease in enzymes. Long term depression on the other hand is the reverse of these processes and occurs from pulling apart, or degradation, of the dendrites and axons, known as "pruning". Pruning removes unnecessary connections, which is accomplished by microglia within the brain [20]. Combined, neural plasticity describes CNS's ability to rewire itself in response to experiences or injury, and its occurrence indicates a form of CNS regeneration that could theoretically be achieved if provided the right stimulus. Neural plasticity presents itself in various types and they are briefly summarized in the table below **(Table 1)**.

**Table 1. Three major types of neuronal plasticity found in CNS.** There are 3 major types of plasticity that can occur in CNS: enhancement of existing axonal connections, formation of new connections, and formation of new cells, which happens only by presence of stem cells. Existing axonal connections can be enhanced by either synaptic development or synaptic strengthening, whereas formation of new axon connections can occur by unmasking of axons or random dendritic sprouting.

| **Type** | **Mechanism** |
|---|---|
| *1. Enhancement of existing connections* | |
| Synapse development | Physiological |
| Synapse strengthening | Biochemical |
| *2. Formation of new connections* | |
| Unmasking axons | Physiological |
| Dendritic sprouting | Structural |
| *3. Formation of new cells* | |
| Self-replication | Stem cell |

## 1.2 The ROLE OF ECM

In mammalian CNS, the ECM is responsible for prohibiting regeneration by suppressing axonal repair. However, in general biology, the ECM has a much wider and more diverse range of duties, many of them directed towards constructive remodeling and repair [21]. ECM is defined as the diverse collection of proteins and sugars that surround cells in all solid tissues. Typically, ECM plays a critical role in maintaining the structural and compositional integrity of the tissue. When injuries occur, the ECM undergoes several key changes in composition to assist remodeling of the injured site. It is a vital player in the body's natural ability to repair and regenerate. The ECM is mainly composed of an intricate interlocking mesh of fibrillar and non-fibrillar collagens, elastic fibers, and glycosaminoglycan-containing glycoproteins (hyaluronan and proteoglycans). Until recently, it was believed ECM's role was limited primarily to structural and biochemical responsibilities. However, it is now understood that ECM is crucial for providing information necessary for controlling cellular behavior as well [21-28].

Despite its many roles, ECM chiefly serves a structural duty before all else. After the intracellular synthesis of the ECM, its components are secreted into the interstitial matrix surrounding the cells and become the main structural scaffold for the tissue. Another structural duty of the ECM is to act as a compression buffer against deforming stresses. Macroscopically, ECM achieves this by physically segregating cells and organs apart and acting as a protective cushion in-between. ECM also provides mechanical strength to the cellular architecture as the interstitial matrix found in most ECM are composed of fibrous collagen type I and fibronectin. Compositionally, collagens are the most abundant component of most ECMs, but its varying expression level reflects the wide array of specific functions different ECMs serve depending on

the tissue [29-32]. For instance, CNS-ECM lacks much of the structural protein such as collagen. In connective tissues such as cartilage and tendons, the ECM expresses an elevated level of chondroitin sulfate as they help to maintain the structural integrity of the tissue [33]. External mechanical loading of tissues can also alter the ECM composition in some instances. For example, in individuals with limited mobility or mostly sedentary lifestyle, the ECM expresses decreased level of proteoglycan in collagen and in bone mineral. The proteoglycan level however increases with exercise, indicating that ECM composition can be altered both intrinsically and extrinsically [34].

The ECM also serves various non-structural functions. At the molecular level, the ECM is capable of regulating cellular behavior through modulation of cellular proliferation, cytoskeletal organization, cellular differentiation and receptor signaling. The biophysical properties of the ECM also help to regulate cellular mechanosensory pathways via mechanotaxis or extracellular tension, which then prompts the cells to detect and respond to changes in tissue biomechanics [35-41]. Matrix metalloproteinases (MMPs) found in ECM also play a central role in tissue remodeling. MMPs are responsible for cleaving protein components of the ECM. For example, they regulate ECM composition and facilitate cell migration by removing barriers such as collagen. Additionally, MMPs also modulate cellular interaction with the environment by regulating a host of molecules such as growth factors and their receptors, cytokines and chemokines, adhesion receptors and cell surface proteoglycans, and a variety of enzymes. This function is critical for ECM-mediated tissue remodeling [42]. Last but not least, the ECM also houses a large selection of cytokines and growth factors which are readily available in case of tissue injury or infiltration of foreign material [37].

## 1.3 ECM TECHNOLOGY

Expanding appreciation of ECM's role in cellular and tissue function has created a momentum towards engineering a viable ECM therapy in the field of tissue engineering. The ECM technology has been successfully explored for various tissue remodeling applications in a wide range of preclinical and clinical models [43-49]. Currently, all commercially and academically investigated ECMs are derived from mammalian tissue, the most common being porcine small intestinal submucosa and porcine dermis (Table 2) [50]. ECM therapy has been used to successfully facilitate constructive remodeling of numerous tissues such as esophagus, lower urinary tract, muscle and tendon, and myocardium [51-55]. However, there are very few documented attempts at using ECM therapy to treat CNS injuries, and the few that have tried did not achieve much success [56-58].

**Table 2. Partial list of commercially available ECM products and their source of origin.** Current ECM technology is based on matrix isolated from mammalian tissues or organs. Some of the popular species for ECM extraction include pigs, cows, horses, and humans. Reproduced from [50].

| ECM Product | Manufacturer | Tissue Source |
|---|---|---|
| AlloDerm | Lifecell | Human dermis |
| MatriStem | ACell Inc. | Porcine urinary bladder matrix |
| Dura-Guard | Synovis Surgical | Bovine pericardium |
| PriMatrix | TEI Biosciences | Fetal bovine dermis |
| OrthADAPT | Synovis Life Technologies | Equine pericardium |

When applying ECM therapy, biocompatibility of the matrix and the resulting host response are highly dependent on the ECM's decellularization and post-processing protocols [59]. For decellularization, detergents such as triton X-100 or sodium deoxycholate are commonly used. This is combined with enzymatic washing such as trypsin, DNases, or RNases, followed by mechanical perturbation. Quality control is carried out to ensure each batch of ECM has received the same decellularization treatment and that most, if not all, cellular debris have been removed. Otherwise, the ECM can incite pro-inflammatory immune response in the host tissue. Conversely, if the decellularization procedure is too harsh, it can harm the ECM structure and decrease its remodeling efficacy. Therefore, the procedure must balance between the two carefully in order to ensure the matrix interacts seamlessly with the host. ECM post-processing techniques also modify the resulting matrix composition which can alter the host response. For example, degradability of the ECM can have major influence on the resulting tissue remodeling. Decreased degradability, which can result from the ECM being crosslinked, tend to promote chronic inflammatory response [50,60]. On the other hand, non-crosslinked ECM with higher degradability that has been processed using the same protocol tends to leave byproducts capable of promoting constructive remodeling [50,61].

### 1.3.1 Remodeling Mechanisms

Provided appropriate processing and preparation, the ECM scaffold will proceed to promote site appropriate tissue reconstruction via various cellular mechanisms, all of which involves altering the native healing behavior. A well processed ECM scaffold will therefore possess various growth

factors and glycosaminoglycans, and as the ECM degrades, it will release a group of bioactive byproducts capable of influencing native cellular behavior. For example, in osteogenesis, the degradation of cryptic peptides can enhance perivascular stem cell regenerative potential by significantly increasing their proliferation and migration. This leads to bone remodeling and recruitment of endogenous stem cell populations [62-63]. Other factors found in ECM and its degradation byproducts are various growth factors such as VEGF, bFGF, and TGF-β1. Certain ECM molecules also instigate host tissue infiltration and participate in mechanotransduction, which has been shown to be a requirement for constructive remodeling of functional tissue in the urinary bladder and tendon [64-67]. Other mechanisms of ECM remodeling include promoting innervation and modulation of the innate immune response. Innervation is partially controlled by the ECM and is therefore a critical factor in achieving regeneration. In peripheral nervous system (PNS), ECM degradation byproducts have been shown to induce Schwann cell migration which promotes remyelination following injuries. In CNS however, ECM remodeling follows a very different path, one directed towards injury-containment rather than reconstruction and regeneration. While the ability to support infiltrating axons and functional innervation is integral in tissue reconstruction following CNS injuries, CNS-ECM is unfortunately pro-inflammatory and not repair-permissive. To summarize, conventional ECM therapy can support cell infiltration and innervation, degrade to produce bioactive molecules that enhance stem cell regenerative potential, and alter the innate immune response towards functional tissue reconstruction. However, CNS-ECM cannot promote constructive remodeling as its primary function is to halt regeneration and contain the spread of neuronal deterioration.

### 1.3.2 Limitations

While ECM typically provides a supportive framework for cellular repair in most tissue, its role in CNS neurons is highly regulatory. Injury leads to release of growth inhibitors and reduced growth factors. In response, studies have rendered the extracellular environment more repair-friendly by replacing certain key components, namely, the two major classes of CNS regeneration inhibitors, myelin associated inhibitors (MAIs) and CSPGs. However, their individual roles were diminished when targeted individually due to the compensatory nature of protein pathways [68]. There are often multiple proteins responsible for a function and mechanism in place that responds to loss of function with overproduction. In fact, more studies have shown that strategies counteracting specific individual inhibitors of axon growth promote only modest regeneration on their own [69]. Therefore, tackling the issue at a "tissue-level" using ECM replacement as a blanket approach to targeting networks of factors and proteins simultaneously makes logical sense. A complete overhaul of native environment using an alternative ECM would indeed be the most conducive to regeneration. However, for it to be successful, the alternative ECM must possess regenerative potential. Unfortunately, all commercially available ECM are currently derived from mammalian tissue [50]. Some have explored using porcine brain ECM for neural tissue application while select groups have also looked at using *fetal* porcine brain ECM as its relatively primitive status encourages proliferation. While porcine brain ECMs showed slight improvement in neurotrophic potential via retention of growth factors and proteins, none successfully translated to much functional recovery [70].

This limitation can be potentially mitigated by considering alternative sources of ECM outside of the Mammalia class. The restrictive nature against CNS regeneration is believed to have

developed over the course of evolution in order to prioritize safeguarding the body's complex neural circuitry from further damage. Consequently, this has left the more primitive species such as invertebrates and lower-vertebrates with remarkable capacity for CNS regeneration, made possible in large part by their repair-permissive ECM [71-72]. Upon injury, their ECM suppresses inhibitors and promotes neuronal growth while reducing inflammation, glial scarring, and further neuron decay. While most of these alternative species remain unexplored by the bioengineering community, one possible candidate truly stands out - the zebrafish.

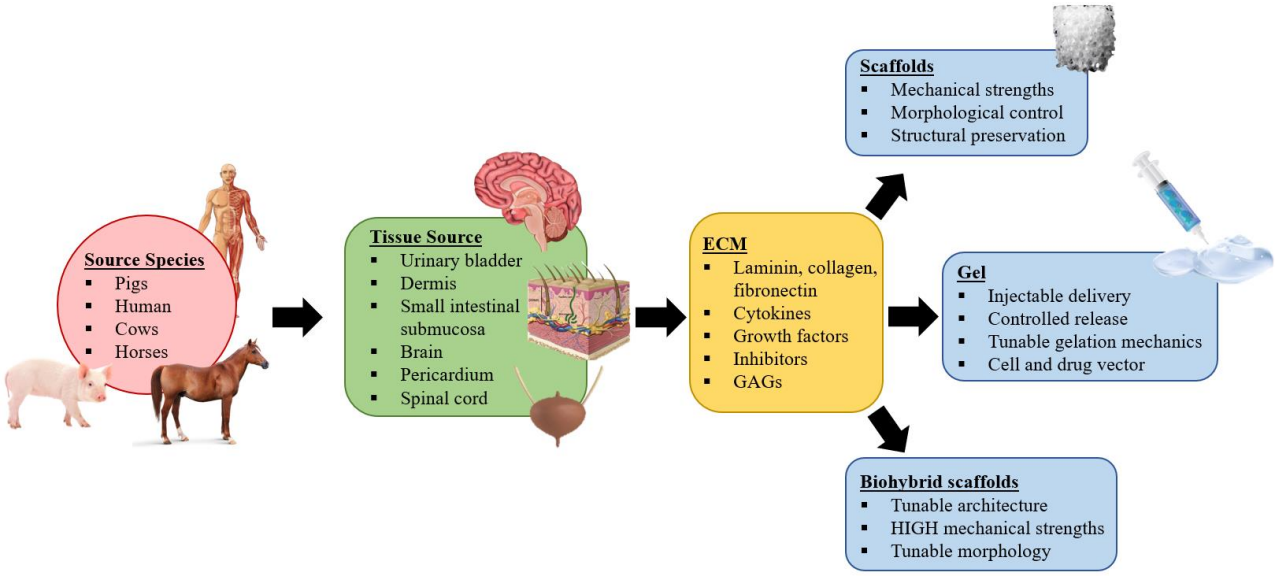


**Figure 3. ECM sources and applications.** Primary species used to derive ECM include humans, pigs, cows, and horses. Common tissue and organ sources used to isolate the matrix range from urinary bladder and dermis to brain and spinal cord. For regenerative applications, the bioactive components of the matrix can be prepared and processed as scaffolds, gel, or biohybrid scaffolds. Each form has its benefits and limitations, as show above.

## 1.4 ZEBRAFISH

### 1.4.1 Lesson in History

Given the limited regeneration seen in mammalian CNS, it is remarkable that many non-mammalian species are able to regenerate substantial parts of their CNS. This ability becomes more pronounced in lower species of the evolutionary hierarchy. In fact, numerous lower vertebrates and almost all invertebrates possess the capacity to partially or completely regenerate their damaged axons. This ability has been documented in various branches of the animal kingdom since the discovery in 1740 that hydra can regenerate itself after bisection [34]. Biologists and evolutionary scientists have since then pondered why this ability eludes mammals and other higher organisms. Current understanding of evolution posits the increased complexity of neural circuitry in higher organisms may have been the driving force. Compositional and architectural complexity of CNS increased exponentially during the course of evolution until eventually, it reached a point where CNS regeneration no longer involved mere few bundles of axons but instead, required restoration of millions of individual connections, each carrying the risk of being wrongfully re-connected. The possible repercussion of wrongly reconnected nerves became more severe as the CNS became more specialized and compartmentalized in highly evolved species. Additionally, the average distance of axonal networks increased proportionally to the complexity of the system, meaning their prospect for proper re-connection waned even further. Thus, the more evolved organisms came to develop a finely controlled ECM catered towards containment of injuries rather than regeneration [73-74]. Although a definitive evolutionary account of CNS regeneration and its natural selection through time cannot be determined, it is timely to address this issue given the

scientific community's increasing cellular and molecular understanding of neuronal development and regeneration in nonconventional species.

Special care must be taken when comparing CNS regeneration between species however. Neurogenesis is a multifaceted trait and its ECM even more so as its composition can vary according to location and type of damage. Within one organism, different regeneration responses can be observed depending on whether the injury is made in the brain, the retina or the spinal cord. Furthermore, different injury paradigms have been used either to selectively remove specific neuronal populations or to non-selectively remove many cell layers [50,75]. Considering the overall structure of neural tissue and the location of the stem cells that will replace the missing cells in injured tissue, this distinction has important mechanistic implications. Additionally, contradictory results have even been reported for the same animal species after brain, retina or spinal cord lesion.

When comparing species for clues to unlocking CNS regeneration, it is also worthwhile to study their wound-healing responses. As wound-healing occurs outside of the developmental stages involved in developing the CNS, it can be considered a regeneration-specific step. Thus, the would-healing response can serve as an ECM-mediated determinant of the specie's regenerative capacity [50,63-65]. Glial cells of ECM should also be carefully observed. They respond to injury within the CNS and their behaviors are vastly different in vertebrates [11-13]. Lower organisms that robustly regenerate injured CNS, such as the zebrafish, show a unique glial cell response at the damaged site [76]. For example, their spinal cord contains two types of glia, myelinating oligodendrocytes and radial glia. Normally, the radial glia expresses glial fibrillary acidic protein (GFAP) and possess proliferative and neurogenic capacity. However, when an injury occurs, the radial glia transiently lose GFAP and begin to express vimentin and nestin. The radial

glia then undergo an epithelial to mesenchymal transition which allows them to migrate into surrounding tissue before reforming a single-cell layered neuroepithelial tube [77,78]. Through series of cell division, the cellular channel undergoes elongation until it reconstructs the spinal cord. The newly constructed spinal cord then provides a permissive environment for axonal growth through the lesion. Unfortunately, the glial cell populations in mammalian spinal cord respond to injury by simply generating a wound [77-80].

### 1.4.2 Regenerative Potential of Zebrafish CNS

The nervous system of zebrafish has a greater capacity to regrow axons, repair circuits, and recover function. Zebrafish CNS-ECM are well-known for exhibiting scar-free healing via suppression of glial cell activation, and for circumventing inflammatory response trigger by relying on apoptosis instead of necrosis. Zebrafish are also capable of regaining full motor function in 7 days following a complete spinal cord transection. They can also regenerate severed optic nerves and brain lesion with incredible ease [77-83].

Many have attempted to understand exactly why axons regenerate so well in the zebrafish CNS [79,83-86]. Exposing mammalian axons to cells of the zebrafish CNS, or exposing zebrafish axons to cells of the mammalian CNS, can help distinguish whether the differences in regeneration are attributable to neurons themselves or to their ECM. Studies show regenerating axons of both mammalian and zebrafish neurons are repelled by mammalian oligodendrocytes and myelin found in mammalian CNS-ECM [87]. However, both can grow in the presence of zebrafish

oligodendrocytes or zebrafish-CNS conditioned media [79,87]. This demonstrates that the differences in axon regeneration stem from compositional difference of the mammalian and zebrafish CNS-ECN. This compositional difference can be one of three scenarios: absence of inhibitory cues, increased presence of factors that block inhibitory cues, or increased growth factors [88-91].

Numerous studies have also analyzed presence of inhibitory factors in zebrafish CNS [83-86,92,93]. The adult mammalian CNS contains multiple molecules inhibitory to axon growth, including glycoproteins found in myelin. It also contains ECM proteins such as CSPGs and Tenascins [92,93]. Myelin associated inhibitors (MAIs) such as mammalian myelin-associated glycoprotein (MAG) and oligodendrocyte myelin glycoprotein (OMgp) activate the growth-inhibiting Nogo receptor (NgR) complex on regenerating axons which halts any axonal outgrowth [94,95]. Remarkably, the zebrafish homolog of mammalian Nogo does not affect its growth of axons, or mammalian axons. Many believe zebrafish simply do not possess Nogo receptor homologs or that they behave functionally different from mammalian Nogo receptor [95,96]. Either way, it suggests that myelin in zebrafish may help propagate signals without serving as axon inhibitors.

The glial scar created by reactive astrocytes is another major obstacle to regeneration in the mammalian CNS. Astrocytes in the glial scar deposit several axon inhibitory molecules at the injury site, including CSPGs. Although there are some reports to the contrary, the zebrafish CNS is thought to lack astrocytes [97]. Accordingly, immunostaining experiments in adult zebrafish found that CSPGs were unchanged at the lesion following ON injury. Although CSPG levels were not altered by injury, they were expressed at the edges of the optic tract, and enzymatic degradation of CSPGs resulted in pathfinding errors by regenerating axons [98-100]. Thus, like in mammals,

CSPGs are growth-inhibitory in zebrafish; however, they are likely produced by non-astrocyte cell types and may help guide axons rather than block their growth [101]. Tenascins, another family of conserved ECM glycoproteins found at glial scars, can also regulate axon growth [92,93,102]. Inhibition of Tenascin-C in zebrafish results in motor axon guidance defects during larval stages and improves axon regeneration and recovery of swimming behavior after spinal cord injury in adults, indicating that the CNS environment of zebrafish does not completely lack inhibitors of axon regeneration [92,93,102,103]. Tenascin-R acts as an inhibitory guidance molecule during initial development of the ON and in adults is expressed at the margins of the optic tract [103]. Thus, similar to CSPGs, Tenascin-R may play a role in guidance during axon regeneration.

Despite the difference in regenerative ability between mammals and zebrafish, many of the molecular and cellular pathways that regulate axon regeneration are conserved [63-65,104]. Zebrafish models have already provided insight into shared mechanisms of axon regeneration and a new ECM technique has the potential to make them even more powerful systems for investigating how molecules and cells regulate neural repair in CNS. Their robust regeneration of optic nerve and spinal cord axons in adult zebrafish have already been studied to identify factors that promote successful regeneration in the CNS [63-65,105-107]. By contrast, most studies using the larval zebrafish model have focused on axon regeneration in the PNS [108]. The amenability of larval zebrafish to live imaging and genetic manipulation makes them ideal for studying dynamic behaviors of regenerating axons and extrinsic cell types [108,109]. Both adult and larval zebrafish have well-defined neural circuits and stereotyped behaviors, making the study of cell biology underlying their incredible axon regrowth and synapse reestablishment possible [108-110].

# 2.0 SPECIFIC AIMS

This dissertation addresses the following specific aims:

**Specific Aim 1: Determine in vitro if zebrafish brain ECM (zf-brECM) promotes more successful cell growth and axon formation in a 3D culture of primary neurons relative to mammalian ECMs.** Specifically, we:

- Designed 3D scaffolds to compartmentalize neuron culture and axonal growths in vitro
- Compared cell retention and viability in zf-brECM vs mammalian ECMs
- Compared lengths of axon growths and network density in zf-brECM vs mammalian ECMs
- Compared axon sprouting frequency and thickness in zf-brECM vs mammalian ECMs
- Demonstrated action potential signal propagation in the new axon networks

**Rationale:** The ideal ECM for CNS regeneration would provide various neuro-supportive proteins and growth factors while circumventing inflammation and glial scarring. In this regard, zebrafish is the perfect specie to explore. Known for their ability to recover motor and sensory function from complete spinal cord and optic nerve injuries, zebrafish possess remarkable ECM [63-65, 78-81]. In fact, any injury to zebrafish spinal cord leads to increased cellular proliferation and neurogenesis rather than neuronal or tissue decay. On top of that, their CNS-ECM components

assist in directing the regenerating motor axons to their original targets, ensuring proper innervation [111]. Rather than follow an intrinsic program, the growth cones of zebrafish neurites are actually guided by extrinsic cues, most likely found in their ECM [112]. Zebrafish CNS-ECM is also ideal for neuronal regionalization and connectivity as it grants many of the properties required to form intricate networks with specificity and reliability [113]. The zebrafish ECM also targets synthesis of inhibitory molecules after injury, and prevent synthesis or deposition of scaffold matrix which holds inhibitory substances [114]. According to our recent finding, it is also likely that healing CNS-ECM may induce stronger regenerative response in mammalian tissue than normal CNS-ECM.

**Hypothesis:** Zf-brECM will outperform mammalian ECM in terms of cell viability and axon network formation.

**Specific Aim 2: Evaluate in vivo the regenerative potential of zf-brECM by identifying key biological traits indicative of CNS regeneration.** Specifically, we:

- Optimized rodent optic nerve crush (ONC) model as a representative CNS injury model of our study
- Developed ECM-fibrin gel delivery for minimally invasive optic nerve treatment
- Quantified and compared glial scar deposition in the optic nerve following zf-brECM treatment vs mammalian ECM treatments, at day 7 and day 28
- Compared chondroitin sulfate proteoglycan (CSPG) expression level at the site of optic nerve injury following zf-brECM treatment vs mammalian ECM treatments, at day 7 and day 28

**Rationale:** Retinal ganglion cells (RGCs) of mammals (including humans) are incapable of regenerating damaged axons across the optic nerve under normal physiological circumstances. Soon after injury, most RGCs undergo apoptosis [115-118]. In some cases, they show minor, transient sprouting but effectively no long-distance regeneration. Numerous studies suggest this failure may be attributed to presence of a non-permissive/inhibitory environment and lack of growth-promoting molecules in the environment [117]. On the other hand, zebrafish can regenerate RGC axon to tectum within 5 days after ONC and regain visual function by day 20. This leads us to believe that replacing the native environment of mammalian tissue with repair-friendly ECM derived from zebrafish CNS can stimulate successful RGC regeneration. Surprisingly, studies have shown that neurogenesis is not truly necessary for visual functional recovery as long as RGC survival is ensured [117,118]. From this, we infer that zebrafish adopts "cell survival" as its primary strategy for visual functional recovery. And since our preliminary data show that zf-brECM can support excellent cell survival in vitro, we believe it will play a key role in stimulating various regenerative events in the CNS.

**Hypothesis:** Zf-brECM treatment will reduce glial scar deposition and CSPG expression at the site of lesion following an optic nerve injury.

**Specific Aim 3: Evaluate in vivo zf-brECM's capacity to promote axonal repair in the optic nerve and restore visually-guided behaviors after an optic nerve injury.** Specifically, we:

- Identified repairing RGC axons of the optic nerves following zf-brECM treatment

- Measured and compared lesion coverage by repairing axons following zf-brECM treatment vs mammalian ECM treatments, at day 7 and 28
- Compared restoration of pupillary reflex to bright light stimulus following zf-brECM treatment vs mammalian ECM treatments, at day 7 and 28
- Compared restoration of depth perception following zf-brECM treatment vs mammalian ECM treatments, at day 7 and 28

**Hypothesis:** Zf-brECM will promote axon repair distally across the injury site and glial scar, leading to mild functional restoration of visually-guided behaviors such as pupillary light reflex and aversion to depth.

# 3.0 Zebrafish Extracellular Matrix Improves Neuronal Viability and Network Formation in a Simple 3-Dimensional Brain-mimetic Culture

## Chapter Aim

The aim of this chapter was to develop a novel zebrafish-based ECM technology for CNS application by evaluating the efficacy of using zebrafish ECM to culture a population of primary cortical neurons. Traditionally, ECM technology is derived from mammalian tissue, and to demonstrate the true advantages of using zebrafish ECM, the results were compared against neuron cultures grown in porcine and rodent ECM. We hypothesized that zebrafish-derived ECM would achieve better neuron survival and axon network formations than the mammalian ECMs. 3D scaffolds were used to provide the cells a physiologically relevant environment for them to grow in, and subsequently, ECM additives were embedded in the scaffolds. Zebrafish ECM significantly increased neuron survival and growth as well as axon formation compared to mammalian ECMs.

## 3.1 INTRODUCTION

Mammalian CNS has poor intrinsic capacity for regeneration. Their axons possess limited ability to repair after injury and consequently, most functional deficits after CNS injuries involving axonal disconnection are permanent [1]. While CNS injuries are difficult to repair or regenerate, studies

have shown that with adequate regeneration-permissive environment, CNS injuries can achieve some minor functional recovery in the form of dendritic remodeling, axonal sprouting, and synaptic changes, collectively known as neural plasticity [2,6,7-10]. Unfortunately, most mammalian CNS possesses regeneration-inhibitive ECM which actively stops axonal extension and promotes glial scarring, suppressing axon repair and reducing neurotrophic support [11-14]. This is in stark contrast to ECM in certain primitive species that plays an active role in supporting cellular development and regenerative response after injury [3,4]. Therefore, we set out to investigate the utility of exposing mammalian neurons to ECMs from primitive species as a means to improve cell survival, axon extension, and neural network formation.

While synthesizing such ECM from scratch is beyond the reach of current technology, ECM derived from various animal tissues has been widely explored as a treatment for various illnesses [3,4,21-28]. Unfortunately, all commercially available ECM are currently derived from mammalian tissue, most prevalent being porcine tissue, and they have shown limited regenerative capacity when applied to CNS injuries [50,69]. Evolutionarily primitive species such as the lizards and goldfish possess remarkably regenerative neural tissue [73,74]. However, these species remain largely unexplored by the bioengineering community and their ECM have yet to be utilized therapeutically. Here, we report the investigation of neural ECM from zebrafish as a matrix for culturing mammalian neurons in a hemi-spherical structure that crudely mimics the structural elements of a brain cortex. Zebrafish are well-known for exhibiting scar-free healing via suppression of glial cell activation and for circumventing inflammatory response [71-74]. Zebrafish are also capable of easily regenerating severed spinal cord and regaining full motor function in 7 days after a complete spinal cord transection.

We investigated zebrafish ECM derived from the brain. The reasons were twofold: 1) zebrafish are small and their brains provide higher matrix yield than other CNS-tissue such as spinal cords and optic nerves, and 2) their brains conserve many of the brain development process with that of mammalian brain development in terms of overall structure and function including neurogenesis and circuit formation. [73,74]. To investigate the regenerative and therapeutic potential of previously unexplored zebrafish brain ECM (zf-brECM), primary cortical neurons of rats were harvested and cultured in different ECMs and compared. The study compared 5 groups: no-ECM control group, porcine brain ECM (p-brECM), porcine urinary bladder matrix (p-UBM), fetal rat brain ECM (r-brECM), and zf-brECM.

To create a physiologically-relevant in vitro environment to study the interaction between the cells and the ECM, we designed a three-dimensional (3D) scaffold that mimics the basic structural elements of the brain [82-84]. Specifically, the scaffolds were made to imitate the gray and white matter separation found in brain cortex, with gray matter possessing dense neuronal cell bodies and white matter composed of axon bundles and networks [83]. To imitate this characteristic in vitro, we used poly(glycerol sebacate) (PGS) to fabricate dome-shaped porous scaffold where the neurons will occupy. The pores in the dome and its hollow core were filled with fibrin gel containing different ECM. The hollow center of the dome provides space for axonal extension [84]. Neuronal viability, axonal extensions, and formation of functional axonal networks showed that the zebrafish ECM outperformed the mammalian ECM in all categories.

## 3.2 EXPERIMENTAL SECTION

### 3.2.1 ECM Production

#### 3.2.1.1 Tissue Decellularization and Characterization

The Institutional Animal Care and Use Committee (IACUC) at University of Pittsburgh approved all animal usage and surgical procedures performed in this study. The ECM utilized in this study were derived from four different tissue sources: porcine brain, porcine urinary bladder, rat brain, and zebrafish brain. Porcine brain and urinary bladder ECM were kindly provided by Dr. Stephen Badylak (University of Pittsburgh) and supplied frozen. For rat brain, pregnant rats were ordered (embryonic-day E18, Sprague Dawley) and upon sacrifice, fresh whole brain tissues were immediately collected from their pups [85]. Zebrafish brains were harvested from colonies of day-60 zebrafish, kindly provided by Dr. Michael Tsang (University of Pittsburgh). They were first numbed using Tricaine solution. Then, their whole brain tissue was collected fresh via their cranium.

Following their harvesting, rat and zebrafish tissue samples were decellularized following our previously-established protocol [86] (Figure 4). Briefly, our unique decellularization method utilizes only freeze-thaw cycles, cryomilling, antibiotic antimycotic solution, lysis buffers, and DNase/RNase to remove DNA in the tissues. This method is thorough enough to remove cellular material but also gentle enough to minimize damage to the tissue's proteins and glycosaminoglycans (GAGs). The final products were freeze-dried as powder and were dissolved in PBS on the day of their use to create ECM solution of desired concentration. To the best of our knowledge, zebrafish tissue, including their brains, have never been thoroughly investigated as a

source of ECM. Consequently, no protocol exists establishing their proper decellularization. Therefore, all ECM were subjected to equal post-decellularization quality control assessment before being deemed viable for the study. Effective removal of cells from the tissue was confirmed via DAPI staining. Briefly, sections were analyzed via immunofluorescent staining where sections were fixed in 4% paraformaldehyde for 10 mins, washed ×3 in PBS, permeabilized in 0.1% Triton X-100, washed ×3 in PBS, blocked in 0.5% normal goat serum (NGS), and incubated with DAPI (1:500) in PBS for 1 h at room temperature (RT), and after further washes in PBS were mounted in Fluorsave (Merck Biosceince, Nottingham, UK). Meanwhile, effective removal of DNA content was measured using PicoGreen assay (Life Technologies). The ECM samples were placed in well-plates and wash 2-3 times with PBS. 200µl of distilled, de-ionized water was added and the samples were frozen at -80°C. 250 µl for each sample was used for cell lysis solution (0.2% of v/v Triton X-100, 10mM Tris, 1mM EDTA). The samples were centrifuged at 12,000 rpm for 10 min at 4°C and the supernatant was collected for assay. Using the PicoGreen kit, the assay buffer 1x TE Buffer was prepared by diluting 20× TE Buffer with deionized distilled DNAase free H2O. Then a 200-fold diluted working solution of the reagent was prepared. Fluorescence was read at excitation of 480 nm and emission at 528 nm for each well in a microplate reader. dsDNA content (ng/ml) was calculated from standard curve. Threshold for acceptable DNA content was less than 50 ng/mg dry weight, which is a commonly cited threshold in industry-grade ECM products as it is close to the value found in commercial-grade Matrigel [87]. Lastly, while brain ECM contains relatively small amounts of fibrous proteins, it also contains large amounts of GAGs and proteoglycans. To determine the sulfated GAG (sGAG) content, Blyscan assay (Biocolor, Carrickfergus, UK) was used. Manufacturer protocol was followed and the samples were measured

in groups of five replicates and averaged. As a negative control of GAG content determination, rat tail known to express large contents of collagen was used.

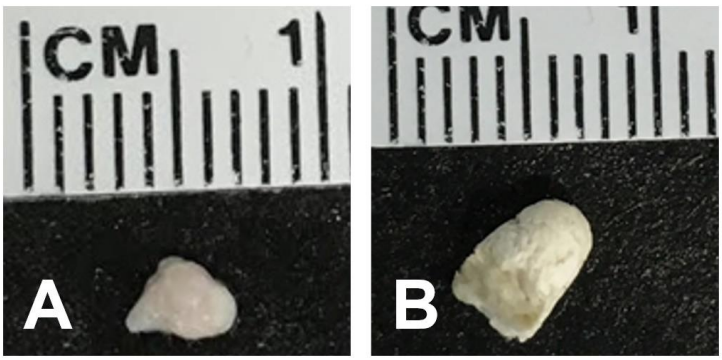


**Figure 4. Brain ECM derived and prepared from adult zebrafish.** The matrix yield of zebrafish ECM is small, and their brain tissue offers the most yield for CNS-ECM. In left, the zf-brECM has been extracted and isolated in lysis buffer (A). To the right, the zf-brECM has been cryomilled and lyophilized before being solubilized into solution form (B).

### 3.2.1.2 Fabrication of 3D Scaffold

The 3D scaffolds were made via modified solvent casting and particulate leaching (SCPL) technique as previously described [86, 88]. Briefly, the technique consists of two parts: 1) solvent casting our PGS with tetrahydrofuran (THF) onto dissolvable salt structures in a mold, and 2) leaching (or dissolving) the salt particles after crosslinking PGS [119]. First, molds were cut from blocks of Teflon. 6 mm diameter hemispheres were then milled into the Teflon blocks, creating a mold. Finely ground salt particles (<32 μm diameter) were then packed into the Teflon mold. A small bead (approximately 2 mm diameter) was then pressed against the surface of packed salt to make hollow core in the center. This formed a bowl-shaped structure with wall thickness of approximately 2 mm made entirely of salt particles. PGS prepolymer solution in THF, synthesized

in-house, was cast onto the salt structure and allowed 30 minutes to absorb. Once the PGS prepolymer had thoroughly permeated the structure, the whole construct was crosslinked by heat curing at 150°C, producing composite construct of PGS and salt, shaped to its final geometry. The composite material was then placed in deionized water bath, dissolving the salt and leaving porous PGS scaffold (Figure 5). The finished scaffolds were frozen for later use. To ensure consistent scaffold dimension, pore size, and porosity, a representative sample from each batch of scaffolds was imaged using scanning electron microscopy (SEM) (Figure 6) and ImageJ software for measurements. This is a crucial step since cells of in vitro exams, especially neurons, may behave sensitively to different structural cues [120]. Following the scaffold construction and sterilization, ECM solutions (8 mg/ml) were prepared and loaded with primary cortical neurons before submerging the scaffolds. Once the solution had appropriately permeated through the scaffolds, fibrin was added to initiate gel formation. Detailed steps are further explained below.

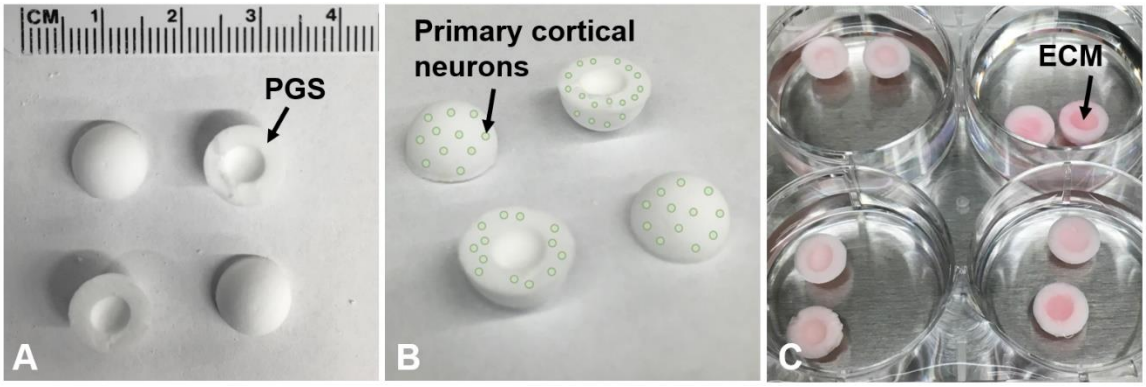


**Figure 5. Fabrication process of ECM-enriched PGS scaffolds with primary neuron culture.** First, dome-shaped PGS scaffolds with hollow cores are fabricated using a salt-leaching method (A). Second, primary cortical neurons are seeded in the 3D scaffolds (B). This is followed by ECM-enrichment of the constructs (as shown by the pink hue) (C).

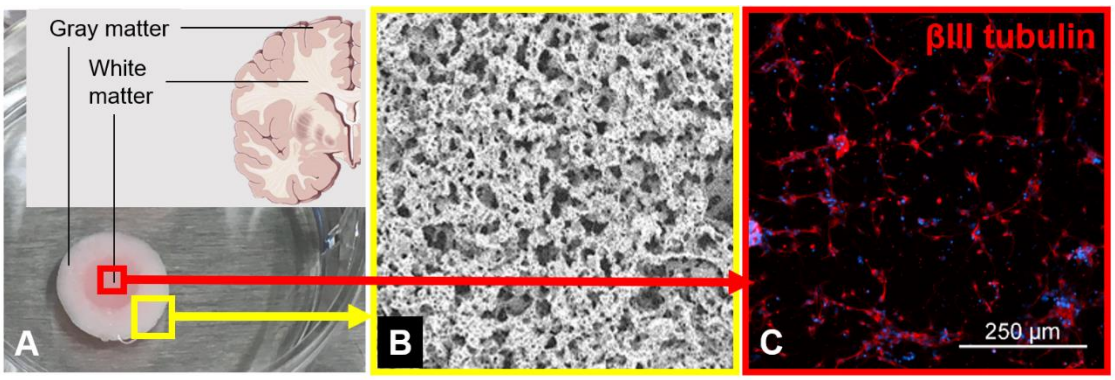


**Figure 6. Design rationale of the 3D scaffold.** The scaffold is designed so that upon seeding of the neurons, the neuron and axon distribution will mimic the gray matter/white matter separation of the brain cortex [82-84]. The scaffold walls holding the cells will resemble neuron body-dense gray matter of brain cortex, while the ECM-rich center will begin to resemble the axon-rich white matter as the neurons begin to sprout axonal bodies towards the core (A). The physiological comparison is depicted in the upper right corner. Then SEM is used to ensure consistent physical properties of all scaffolds (B). Lastly, the activities of the neurons and their axonal growth occurring in the ECM-core are captured and analyzed via immunolabeling (C).

### 3.2.2 Cell Isolation and Seeding

Primary cortical neurons were isolated from rat brains at embryonic day 18 (E18). In short, pregnant rats (Sprague Dawley) were sacrificed and their embryonic pups were immediately extracted [121,122]. Fresh cortex was immediately micro-dissected from the brains of embryonic pups and subjected to 0.25% Trypsin (Life Technologies Corporation, Carlsbad, CA, USA) for 20 min at 37 °C in the CO2 incubator to digest the tissue. This was followed by addition of trypsin inhibitor (Sigma-Aldrich, Milwaukee, WI, USA). The tissue was then disrupted by pipetting up and down 20 times with a 10 mL serological pipet to generate a single cell suspension. The cell suspension was centrifuged for 5 min at 1200 rpm (Centrifuge 5810 R, Eppendorf, Hamburg, Germany) and the pellet was re-suspended in Neurobasal medium (Life Technologies Corporation,

Carlsbad, CA, USA) supplemented with 2% B27 (Life Technologies Corporation, Carlsbad, CA, USA), 0.5 mM GlutaMax (Life Technologies Corporation, Carlsbad, CA, USA) and 1% penicillin/streptomycin (Sigma-Aldrich, Milwaukee, WI, USA). Total cell yield was determined using a hemocytometer. Neuronal purity of the isolated culture was quickly validated by imaging βIII-tubulin immunostained neurons and glial fibrillary acidic protein (GFAP) immunostained astrocytes. These isolated neurons were then seeded on the PGS scaffolds at roughly 1,000,000 cells per scaffold (Figure 5B). After overnight incubation, the PGS scaffolds were submerged in one of the four different ECM solutions for 20 min at 37 °C in the CO2 incubator. The scaffolds were then appropriately gelled using fibrin gel (dilution, 9:1; fibrinogen 5 mg/ml, thrombin 2 mg/ml). ECM presence within the scaffold was quickly confirmed using proteoglycan fluorescence, specifically chondroitin sulfate proteoglycans (CSPGs), specific to the respective animal source of the ECM material. The scaffolds were then fixed with 4% parafolmadehyde (PFA) at day 7 and 14.

### 3.2.3 In vitro Measurements

#### 3.2.3.1 Measurement of Neuron Viability and Axonal Growth

After 7 and 14 days of incubation, initial cell adhesion/retention and survivability were measured using Trypan Blue at a 1:1 dilution to cell suspension using 0.4% Trypan Blue solution, and Countess Counter (ThermoFisher Scientific) for automated cell counting using Countess software (version 1.0.247). The cell suspension for cell count measurement was collected from the ECM center of each scaffold. To ensure the cell retention and viability were a product of each ECM and not due batch differences between the PGS scaffolds or cell seeding density,

measurements were also taken before the ECM was added to each scaffold. Then, immediately after the ECM has been included, 1 cm x 1cm sections were taken from each side of the scaffold and analyzed using DAPI staining to ensure the cortical neurons were seeded homogenously. This was done in order to ensure the following viability and retention differences were not driven by initial differences in cell population in the scaffold walls. Cell viability was then validated by quantifying DNA content release using PicoGreen assay over the course of 25 days. Then, on day 3 and 7, the ECM scaffolds were analyzed for neuron presence and axon growth via immunofluorescent staining of cryosectioned samples. The sections were fixed in 4% paraformaldehyde for 10 mins, washed ×3 in PBS, permeabilized in 0.1% Triton X-100, washed ×3 in PBS, blocked in 0.5% NGS, and incubated with the appropriate primary antibodies diluted in 0.5% NGS PBS overnight. Sections were then washed ×3 with PBS and incubated with the appropriate fluorescent-labeled secondary antibody Alexa 488 diluted 1:100 in PBS for 1 h at room temperature (RT), and after further washes in PBS were mounted in Fluorsave (Merck Biosceince, Nottingham, UK). For evaluation of axon growth, sections were incubated overnight at 4°C with mouse anti-rat βIII-tubulin primary antibody (1:500; BioLegend), followed by goat anti-mouse Alexa-488 immunoglobulin G (IgG) (1:500; Life Technologies) at RT for 1 hour. From the anti-βIII-tubulin images, 500 μm by 500 μm regions representative of the sample was chosen and used to derive the average axon outgrowth length and density. For each ECM group, 7 scaffolds were fabricated, seeded, and analyzed, and from each scaffold, 8 separate 500 μm by 500 μm regions were observed. Axon length was determined by detection of immunofluorescent intensity of individual axon while axon density was determined by taking the ratio of area labeled by immunofluorescence to area of the black background with no immunofluorescence. To detect F-actin presence and global network formation, sections were incubated overnight at 4°C with Alexa

Fluor 488 Phalloidin dye conjugates (1:500; ThermoFisher Scientific), and washed ×3 with PBS. This was then used to identify neurons with successful axonal connections and neurons with no axonal connections with neighboring neurons. Phalloidin labeling was also used to identify presence of myelin and compare the resulting axonal thickness.

#### 3.2.3.2 Measurement of Functional Axon Networks

After 2 weeks of incubation, the scaffolds were observed for functional axon networks as well. This distinction was critical because not all axonal networks exhibit action potential propagation, meaning some could be functionally inconsequential [123]. The network-level activities of the axons were observed using calcium sensitive dye, Fluo-4 (Life Technologies Corporation, Carlsbad, CA, US), which was mixed 1:1 with 20% (v/v) Pluronic F127 (Life Technologies Corporation, Carlsbad, CA, US) [13,14]. Next, Fluo-4 was diluted to final concentration of 1 µM in the extracellular buffer prewarmed to 37 °C. The The 1 µM Fluo-4 solution was applied on the scaffolds and incubated at 37 °C for 1 h. The extracellular solution consisted of NaCl 140 mM, KCl 2.8 mM, CaCl2 2 mM, MgCl2 2 mM, HEPES 10 mM, glucose 10 mM at pH 7.4 (all reagents from Sigma-Aldrich, St. Louis, MO, USA). The Fluo-4 1 µM solution was applied on the scaffold and incubated at 37 °C for 1 h. Upon incubation, the constructs were washed with extracellular buffer to remove excess dye and imaged using an Olympus MVX10 macroscope (Olympus, Japan) at 20× magnification. The samples were subjected to time-lapse fluorescence imaging over 1 min at a rate of 50 ms/frame at RT. Simply, the change in fluorescence over time, indicative of the transient rise in intracellular calcium levels, was measured as electrical activity of the primary neurons. This was done using NIS-Elements AR microscope imaging software and its ROI/Thresholding function [123]. As calcium ion signaling can also

indicate axon guidance, βIII-tubulin labeling was used for further verification of functional axon networks.

### 3.2.4 Statistical Analysis

Graphical representations of all data show means +/- standard deviations. One-way analysis of variance (ANOVA) was performed using general linear model, with Tukey-Kramer post hoc analysis. Outliers greater than three standard deviations from the mean were excluded from data sets.

## 3.3 RESULTS

### 3.3.1 Characterization of ECM and Scaffolds

#### 3.3.1.1 ECM Quality Control

Before the ECM could be used for the study, the residual cellular and DNA content was evaluated to ensure quality control [15]. DAPI staining showed little to no presence of cells in the completely decellularized p-brECM, p-UBM, r-brECM, and zf-brECM (Figure 7). Further quantification of dsDNA content using PicoGreen assay was used to ensure the ECM was sufficiently decellularized. The industry standard accepts threshold of <50 ng/mg dry weight, a value that is found in commercially available Matrigel. The PicoGreen assay results confirmed the sufficient decellularization of our ECM, with less than 30 ng/mg dry weight of tissue being

detected in all lyophilized ECM. The dsDNA levels measured in p-brECM, p-UBM, r-brECM, and zf-brECM were 18 ± 1.4 ng/mg, 14 ± 1.2 ng/mg, 23 ± 0.7 ng/mg, and 16 ± 0.6 ng/mg, respectively (Figure 8). As expected, these readings measured lower than those detected in the whole tissue samples of pigs, rats, and zebrafish. The determination of neuronal purity suggests the percentage of βIII-tubulin immunostained neurons was over 94.8% while GFAP immunostained astrocytes was over 3.1%.

Interestingly, r-brECM showed slightly higher levels of DNA reading than other ECMs. This is most likely because the r-brECM were harvested from E18 pups and during their prenatal life, there is an overproduction of neurons, glial cells, and synaptic connections in the embryonic brain. In fact, >50% of neurons are lost early during the postnatal period [126]. The higher level of DNA content measured in r-brECM which was derived from embryonic brains is consistent with the neuronal pruning during brain development. Lastly, colorimetric Blyscan assay was used to determine sGAG content. The sGAG content for brain matrix materials r-brECM, p-brECM, and zf-brECM was measured at 391 ± 13.5 µg, 385 ± 12.7 µg, and 380 ± 24.7 µg, respectively, per mg dry weight. P-UBM known to express relatively less contents of sGAG and high contents of collagen (types I, II, III, VI, and XIV) contained 110 ± 15.3 µg/mg sGAG [124,125]. No sGAG was found in collagen control of rat tail sample.

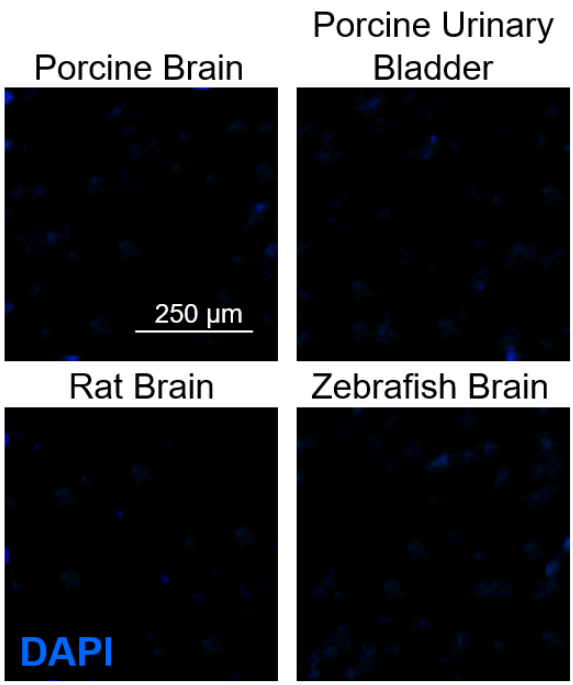


**Figure 7. Residual cellular content of decellularized ECM.** The residual cellular content of the ECM was visualized using DAPI staining. DAPI images revealed little to no cellular content and therefore, all four met the requirement to be safely used for cell culturing.

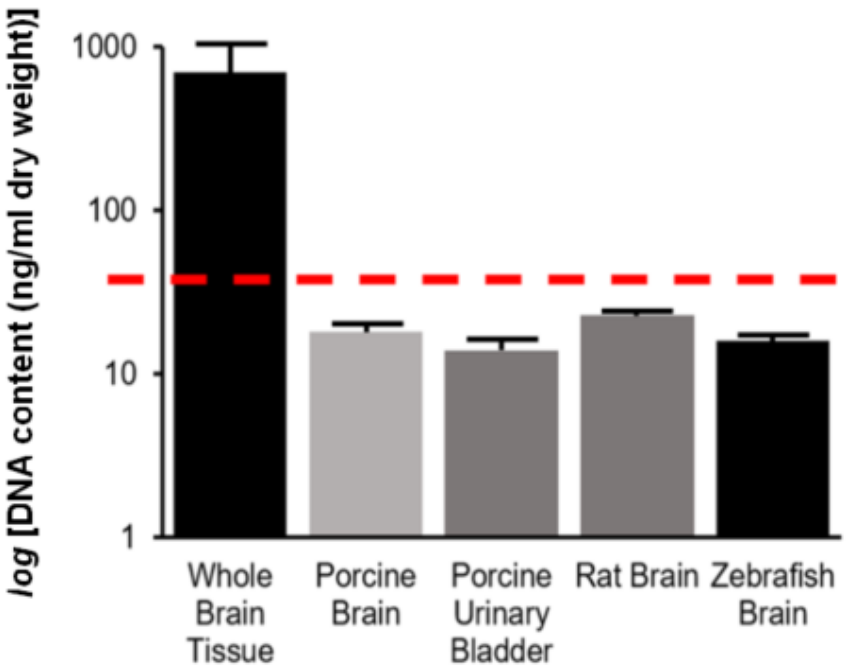


**Figure 8. Residual DNA content of decellularized ECM.** Residual DNA content of the ECM was measured using PicoGreen assay. DNA content plotted in log scale revealed low residual cellular content in all four ECM solutions and all four met the requirement of <50 ng/mg DNA content, as shown by the red dotted line.

### 3.3.1.2 Characterization of PGS scaffolds

The PGS scaffolds were examined using SEM before being embedded with ECM to ensure structural consistency between all scaffolds. The goal was to fabricate scaffolds of approximately 6 mm diameter with pore size of <32 µm diameter and hollow center of approximately 2 mm in diameter (Figure 9).

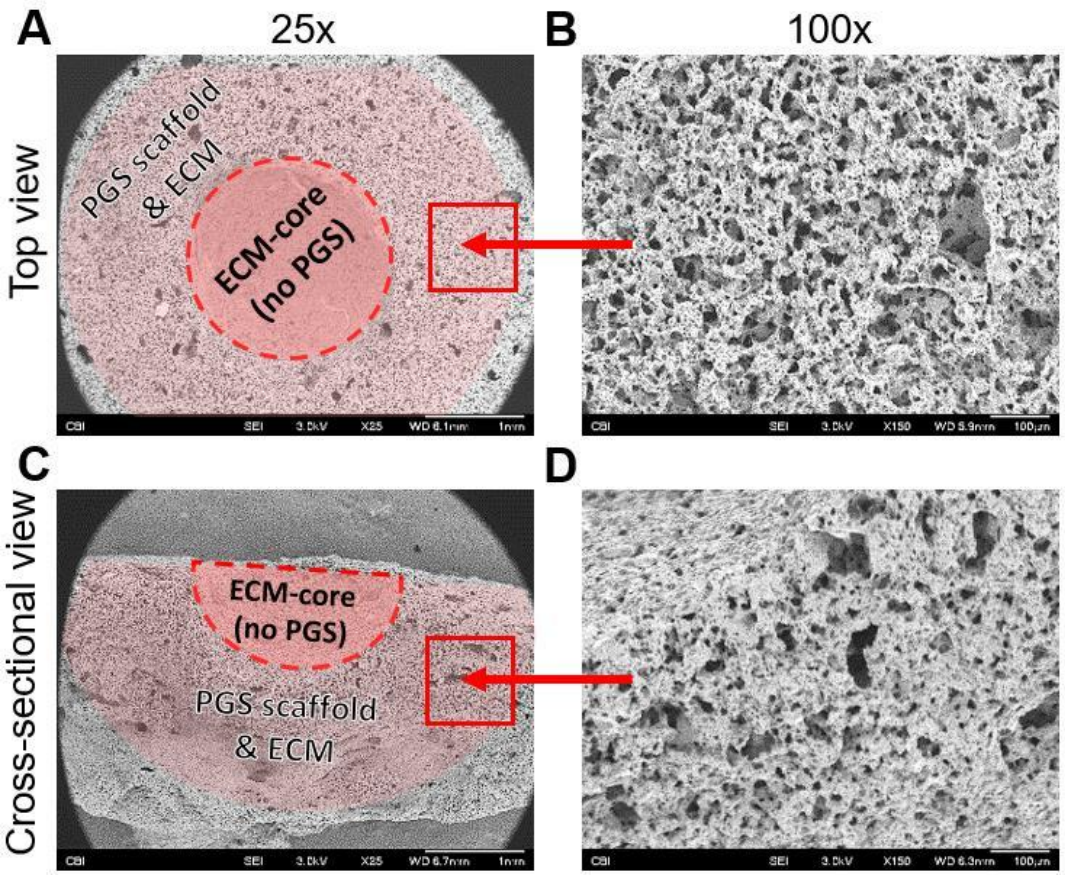


**Figure 9. SEM of the scaffolds.** To ensure structural consistency of all scaffolds, the scaffolds were imaged using SEM. Namely, we looked at their dimension, pore size, and porosity from bird-eye view (A to B) and cross-sectional view (C to D). Upon fabrication, the scaffolds measured at outer diameter of 5.9 ± 0.2 mm with inner diameter of 2.1 ± 0.1 mm, which was deemed acceptable compared to the desired dimension of 6 mm and 2 mm, respectively. The pore sizes measured at 28 ± 2 μm, slightly smaller than the size of salt particles used to salt leach, which could have occurred due to small morphological changes of PGS in response to thermal crosslinking.

### 3.3.2 Growth of Primary Neurons

Different ECM scaffolds affect cell adhesion via combination of different attachment proteins present in the ECM [21-32]. Based on this, initial cell retention was measured despite the consistent physical properties of the scaffolds and gel such as their pore sizes. Primary neurons

grown in the 3D scaffolds embedded with zf-brECM showed significantly higher retention and initial survivability than those grown in scaffolds embedded with p-brECM, p-UBM, and r-brECM (Figure 10). Zf-brECM retained 20,000 cells with 87% survivability, only dropping to 82% by the end of day 14. In contrast, p-brECM, p-UBM, and r-brECM started at 66%, 71%, and 71% respectively, retaining <15,000 cells (Figure 10A), and dropped to 13%, 17%, and 69% respectively at the end of day 14 (Figure 10B). At day 14, r-brECM showed much higher cell viability than p-brECM despite both being derived from mammalian brain tissues. This is most likely because r-brECM was derived from fetal brains and early developmental stage of tissue has shown to augment cell viability [126]. Meanwhile, cells grown in scaffolds with no embedded ECM additives showed 54% initial survivability, decreasing to 30% by the end of day 14.

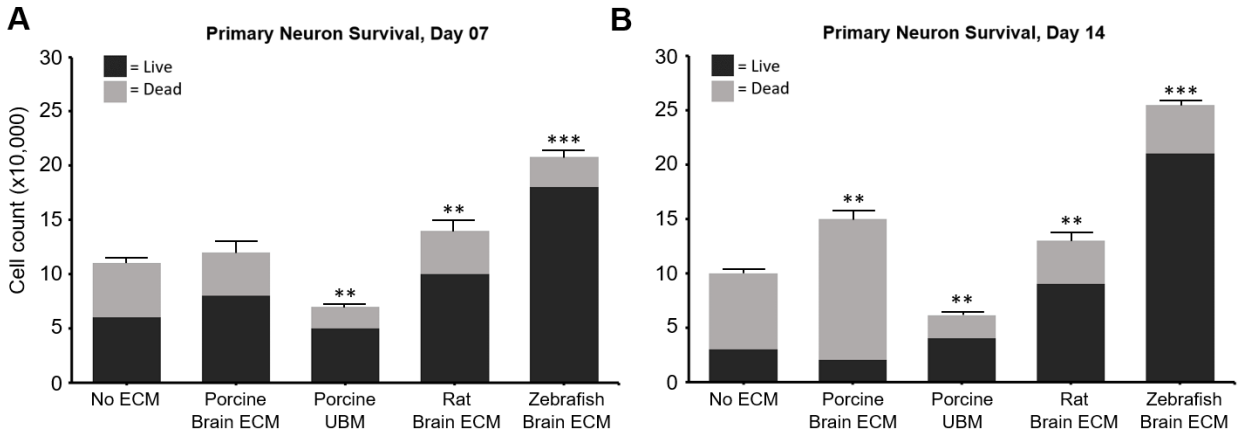


**Figure 10. Trypan blue quantification of cell retention and initial survivability.** Primary neurons were grown in scaffolds with four kinds of ECM and their viability was measured using trypan blue staining. Scaffolds with no ECM additives served as the control group. One-way analysis of variance (ANOVA) between subjects was conducted to compare the effect of different ECM on cell survival in p-brECM, p-UBM, r-brECM, and zf-brECM. Zf-brECM exhibited the highest viability of primary neurons at both day 7 (A) and day 14 (B). At day 7, we observed significant effect on cell survival from p-UBM, r-brECM, and zf-brECM, while p-brECM showed no significant effect.

At day 14 however, all groups exhibited significant effect on cell survival, with zf-brECM showing remarkably improved cell survival than the rest (**P < 0.01, ***P < 0.001 corresponds to all groups).

Viability of the neurons was tracked for 25 days, making note of any sudden changes in the health of overall culture (Figure 11). Around day 5, a significant divergence occurred, with zf-brECM and r-brECM exhibiting viability of over 50%, while the rest showed significant drop in viability of below 20%. Cells grown in scaffolds with no ECM additives showed the largest drop in its viability, from 97% to 10% by day 15. Groups supplemented with p-brECM and p-UBM exhibited slightly higher viability; p-brECM dropped to 66% by day 5 and to 13% by day 15, and b-UBM dropped to 71% and 17% respectively. Zf-brECM displayed the best viability: dropping initially to 87% by day 5 but ultimately stabilizing around 80% by Day 15 and remained so to the end of the experimental window of 25 days. R-brECM performed the second best, with significantly high viability of 71% at day 5 which stabilizes near 53% by end of day 25.

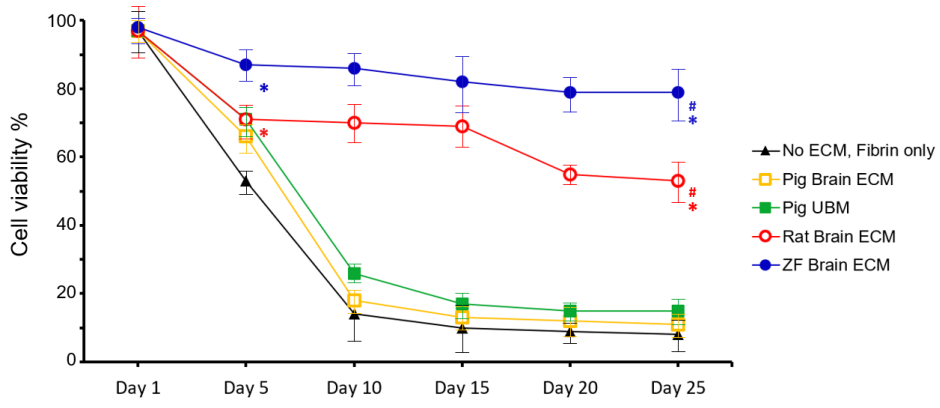


**Figure 11. Continued surveillance of neuron viability.** The neurons and their viability were tracked from day 1 to day 25 after seeding. Neurons grown in zf-brECM and rat-brECM displayed significantly strong viability by end of day 25. Until day 5, all groups maintained above 50% viability, indicating that most ECMs, mammalian derived

or otherwise, can support short-term cell population. Unfortunately, past day 5, the differences in the performance of the different ECMs became much more defined, with p-UBM and p-brECM falling well below 30% viability by day 15. As expected, no-ECM control fared the worst, with most of its population suffering a big loss between day 1 and 5. All groups showed notable change between day 1 and day 25. The difference in cell viability between zf-brECM and r-brECM also proved significant, especially after day 15 (Results were analyzed using two-way repeated-measures ANOVA; *$P < 0.01$ for all groups; #$P < 0.01$ corresponds to day 1 versus day 25).

### 3.3.3 Formation of Axonal Networks

To further analyze neuronal response to different ECMs, evaluation of axonal reach, density, and sprouting frequency was conducted via immunolabeling of βIII-tubulin (Figure 12) and F-actin (Figure 16). First, immunolabeled βIII-tubulin was used to measure average length of axon growths and network density formed in the scaffolds enriched with different ECMs. Specifically, the measurements were taken from the axon-rich ECM-cores. By sampling 500 μm by 500 μm representative regions from immunohistochemical images of each ECM-core (Figure 12 and 13), the average length of axonal growth (Figure 14) and density (Figure 15) in each group were measured at day 3 and day 7. The success of axon network formation can be partially deciphered from the length of axon extensions in a system. Additionally, neurite fate dictates that not all neurites form axons. Based on these, axon lengths are good indication of how well the extracellular environment influences neurite fate. Neurons grown in p-brECM, r-brECM, and zf-brECM core grew the longest axons, reaching up to 95 μm, 100 μm, and 130 μm, respectively, by day 7. Average axons grown in p-brECM and r-brECM both measured around 95 μm by day 3, showing a significant improvement compared to no-ECM group, but did not achieve further growth by day 7. Rather, axons grown in p-UBM, which ultimately measured lower than the rest

at 67 µm, showed more significant growth comparatively, growing more than 10 µm between day 3 and 7 (Figure 14).

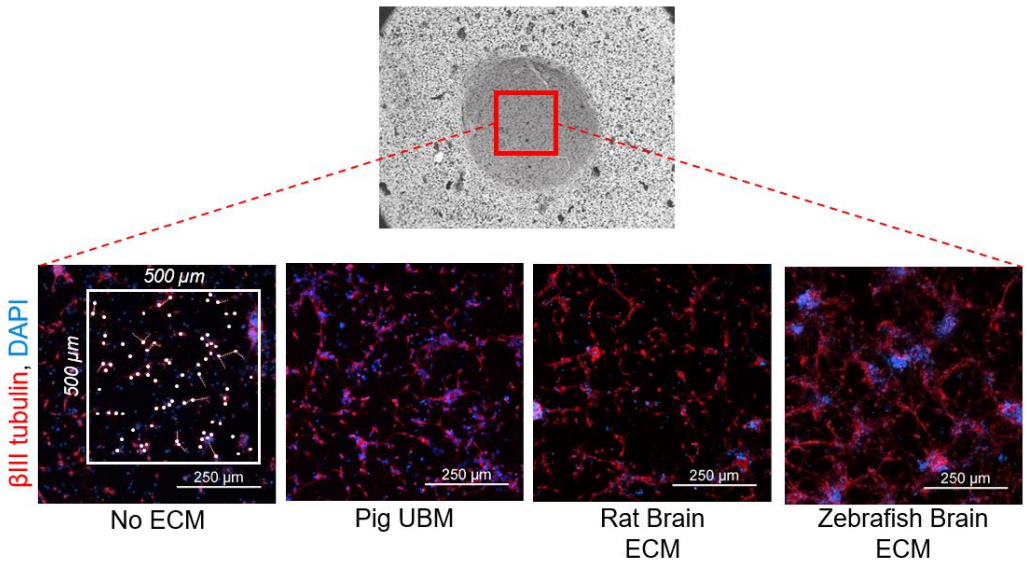


**Figure 12. Axon analysis of ECM cores.** Axon growths were observed by βIII-tubulin labeling. From each group, a representative 500 µm by 500 µm image of immunolabeled βIII-tubulin was captured and analyzed. Using fluorescence intensity to identify the nodes indicating neurons, the sprouting axons were measured computationally.

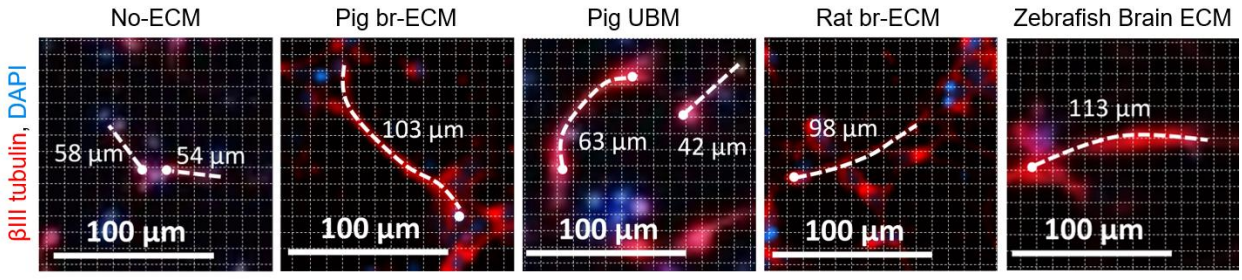


**Figure 13. Lengths of βIII-tubulin labeled axons.** From each group, a representative 500 µm by 500 µm image of immunolabeled βIII-tubulin was captured and used to measure the average length of axonal growth in each

scaffold. Here, examples of axon growth measurements in the five groups are shown, with sampled axon chosen from each group to reflect the group's average length.

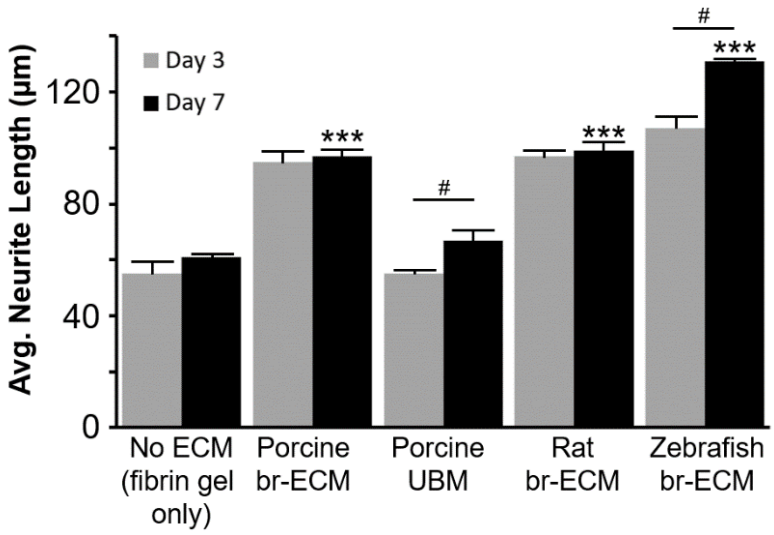


**Figure 14. Measurements of average axonal lengths taken at day 3 and 7.** P-brECM, r-brECM, and zf-brECM exhibited significantly longer average axon length, reaching up to 95 µm, 100 µm, and 140 µm respectively. The success of axon growth in p-brECM was interesting given its cell viability was not remarkably high. Between day 3 and 7, both p-UBM and zf-brECM had significant axon growth.

The axons of zf-brECM also formed the densest network connections, the neural bodies and extensions covering roughly 28% of the surface by day 7 (Figure 15). R-brECM achieved the second densest axonal connections, with the neurons obtaining moderately high axonal density of 18% by day 3 and ultimately stabilizing, making negligible increase by day 7. On the other hand, porcine ECM achieved less dense axon networks, with axons of p-brECM and p-UBM occupying 14% and 15% by day 7, respectively. Interestingly, while the axonal density of p-UBM scored lower than that of zf-brECM, it showed the biggest increase between day 3 and 7, achieving an almost two-fold increase. Unlike axon growth measurements, the effects on density measurement were more significantly pronounced. This tells us that many of the ECMs are moderately

successful at cultivating long axonal growth, but they are not successful at growing too many of them. Therefore, any resulting functional difference of the axonal networks seen in groups may stem from the differences in axonal density more than axonal lengths.

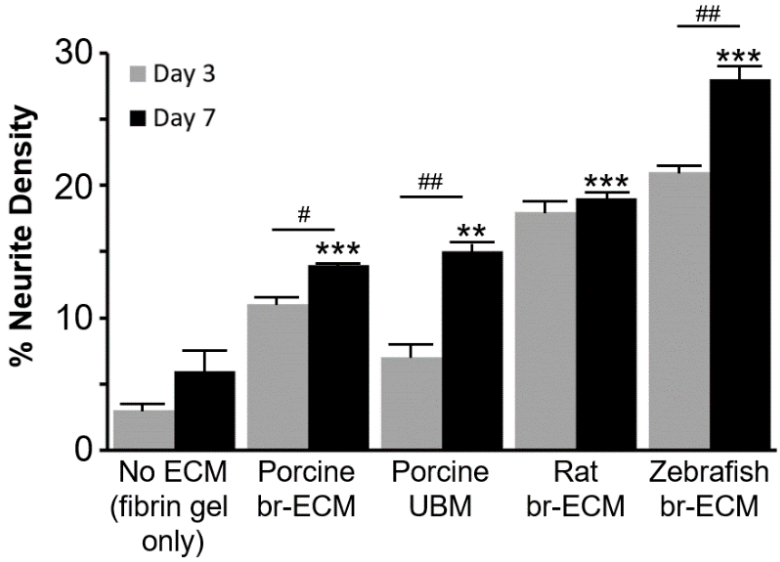


**Figure 15. Complementary measurements of average axon density taken at day 3 and 7.** All groups showed significant increase in axonal density, but only p-brECM, p-UBM, and zf-brECM showed significant increase between day 3 and 7. (**P < 0.01, ***P < 0.001 for all groups; #P < 0.05, ##P < 0.01 corresponds to day 3 versus day 7).

### 3.3.4 Axon Extension Frequency

Secondly, phalloidin-immunolabeled F-actin was used to measure axon sprouting frequency of the primary neurons supplemented with different ECM groups (Figure 16). As phalloidin can be used to label both neuronal bodies and their axonal extensions conjunctively, it is useful for distinguishing neurons that exhibit axon extensions from neurons that do not exhibit axon extensions. Doing so, we could measure the percentage of the neurons in the culture that

successfully sprouted axonal extension (Figure 17). By day 7, almost 72% of the neurons in zf-brECM grew axon extensions, meaning significant number of neurons were involved in the process of axonal branching and network formation. In contrast, approximately 51% and 57% of neurons in p-brECM and r-brECM groups, respectively, displayed axonal sprouting. Lastly, 38% of neurons in p-UBM achieved axonal sprouting, marking the lowest amongst ECM groups, with no-ECM scaffolds showing roughly 29% sprouting frequency of their neurons.

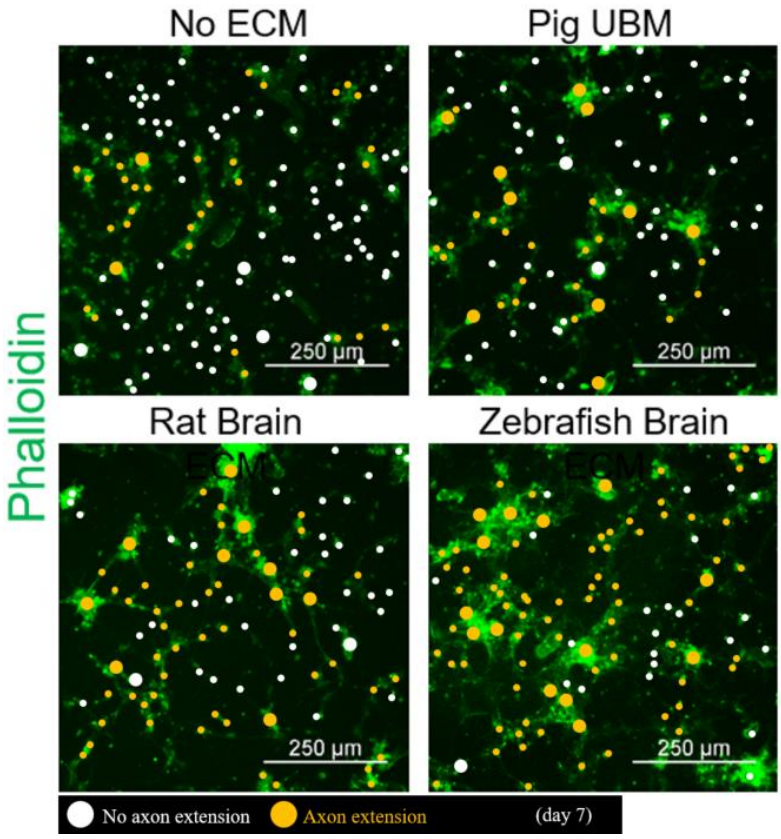


**Figure 16. Axon sprouting frequency.** Immunolabeled phalloidin data was interpreted to quantify axon sprouting frequency amongst the neurons at day 3 and day 7 as well as myelin thickness. Immunolabeling shows difference in abundance of neuronal bodies that achieve axonal sprouting.

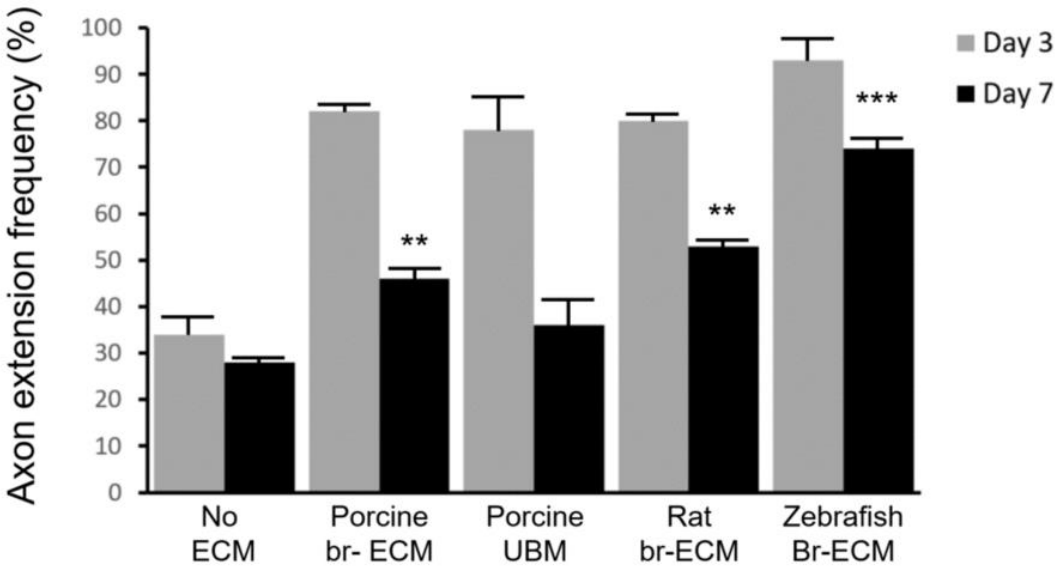


**Figure 17. Axon extension frequency measurement based on phalloidin labeled actin filaments.** Neuronal viability, while crucial, mean little with poor neurite fate. Therefore, the abundance of neuronal body undergoing neurite, and eventually axon, extension must be carefully considered. The quantification of axon sprouting frequency showed significant improvement in p-brECM, r-brECM and zf-brECM groups. All brain ECMs showed high frequency of neuronal extensions, possibly due to their tissue specificity, with all three displaying >50% of neurons with axonal extensions, while the remaining groups displayed less than 40% neurons with axonal extensions. When compared with p-brECM, p-UBM, and r-brECM, axon sprouting frequency of zf-brECM exhibited significant increase. While all groups exhibited marginally increased axon extension frequency at day 7 compared to day 3, no significant effect between the two time points was found (**$P < 0.01$, ***$P < 0.001$ compared to all groups at day 7).

Actin assembly is also known to be involved in myelin wrapping of axons. Thus, our phalloidin results were used to analyze myelin presence as well as axonal thickness. Neuronal bodies of zf-brECM core had the thickest axons of approximately 4.3 ± 0.6 µm, while axons of p-brECM, p-UBM, and r-brECM had 3.7 ± 0.5 µm, 3.1 ± 0.7 µm, and 3.3 ± 0.6 µm (Figure 18). Neurons grown without any ECM supplement had the thinnest axons, measuring approximately 1.2 ± 0.2 µm. Functional CNS networks typically possess abundance of myelin as they are essential for rapid propagation of action potentials but they also operate as inhibitors of axonal repair.

However, studies suggest that uniquely in zebrafish, myelins do not serve as axon inhibitors because their inhibitory domains do not exist. In other words, ECM derived from zebrafish has the potential of supporting myelination while simultaneously supporting rapid action potential propagation without inhibiting axonal outgrowth. Our measurements of axon thickness directly reflect the myelin sheath thickness formed along the axonal extensions, and by comparing this finding to functional analysis of the network, we may draw conclusion regarding action potential propagation. Here we see that zf-brECM significantly increases axon thickness, while no-ECM control group grows axons of approximately 1 μm thickness, a value close to the thickness of average axons with little to no myelin sheath.

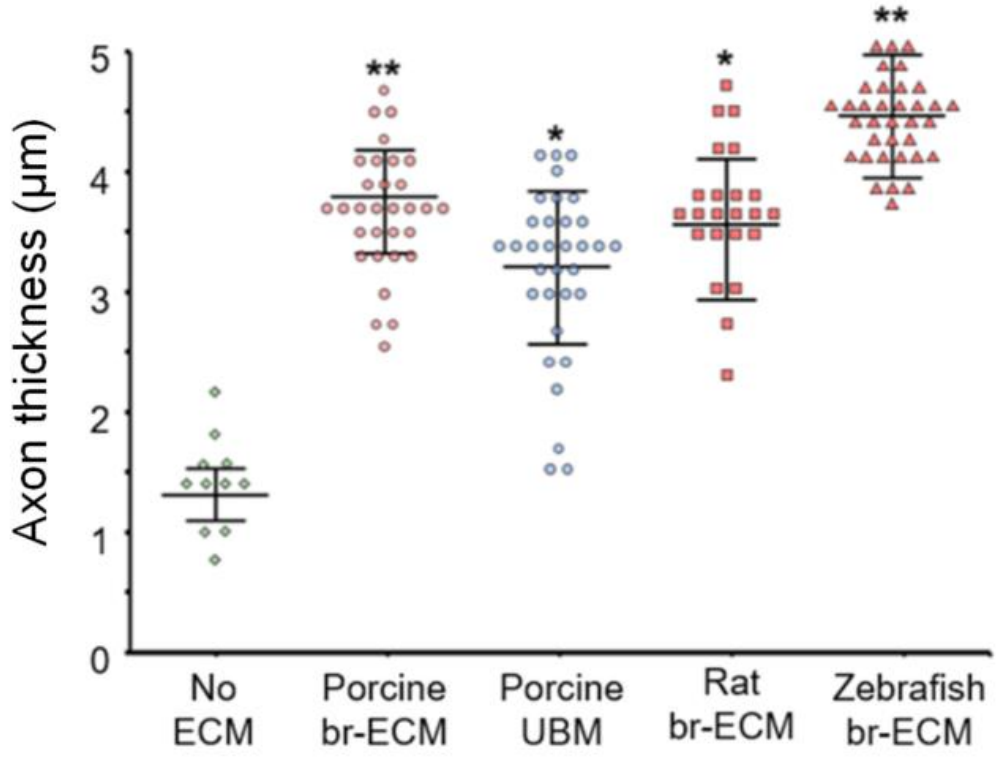


**Figure 18. Myelin presence shown by axon thickness.** Axons labeled using phalloidin was used to measure and distribute axon thickness in each ECM group. Significant increase in axon thickness of neurons grown in scaffolds supplemented with zf-brECM was seen, measuring at 4.3 ± 0.6 μm. This was followed closely by significant increase

in axon thickness found in p-brECM and p-UBM, which measured at 3.7 ± 0.5 μm and 3.1 ± 0.7 μm respectively (The quantitative data represent means ± SD; *P < 0.01 for all groups).

### 3.3.5 Formation of Functional Networks

The neuronal function of the 3D scaffold was probed by live calcium imaging for network activities. Calcium imaging was carried out 1 week after the primary cortical neurons were seeded in the scaffolds by staining the culture with calcium sensitive dye Fluo-4. The cell cultures were then observed using time-lapse fluorescence imaging over 1 min at a rate of 50 ms/frame. The change in fluorescence intensity over time, indicative of the transient rise in intracellular calcium levels, was recorded as a measure of electrical activity of the neurons. From the readings, only the groups r-brECM and zf-brECM showed noticeable change in the fluorescence intensity of Fluo-4 during calcium imaging sessions. In comparison, electrical activities of other ECM groups were negligible, with p-brECM, p-UBM, and no-ECM showing virtually no changes in calcium intensity. Representative fluorescence images of each group and their corresponding intensity traces were recorded (Figure 19). Additionally, individual axons were observed and axon networks supplying action potential propagation were also observed using region of interest (ROI) thresholding to confirm calcium spike readings (Figure 20). From the results, the combinatorial effect of the ECM being both non-mammalian derived (i.e. zebrafish) and tissue-specifically derived (i.e. brain) seems to help generate calcium exchange in the axons and establish the most prominent network activity within their networks.

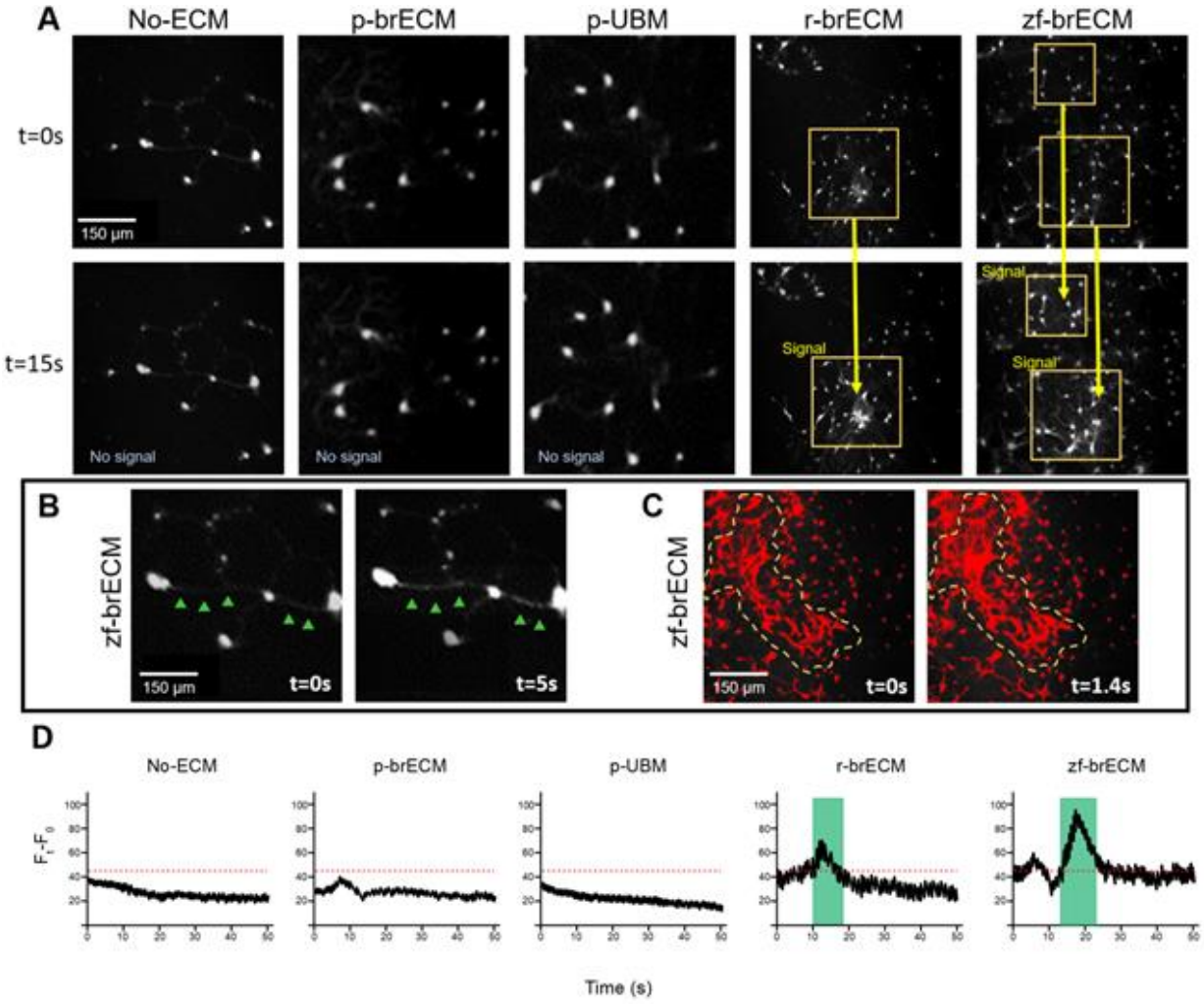


**Figure 19. Live calcium imaging of functional axon networks.** Calcium sensitive dye Fluo-4 was used to identify formation of functional axon networks supplying action potential propagation. Propensity for action potential propagation can be seen by the changes of fluorescence intensity, or the lack thereof, during the sample's time-lapse imaging (A). P-UBM showed no noticeable changes in its calcium exchange, whereas r-brECM and zf-brECM showed clear spikes of fluorescence intensity. The networks were also observed magnified looking at individual axons (B) and via ROI-thresholding (C). Only r-brECM and zf-brECM groups recorded a quantitative spike in fluorescence intensity of calcium sensitive dye indicative of neuronal firing. This measurement was found to be comparable in multiple iterations (D). Scale bar is 150 µm and it is the same for all images.

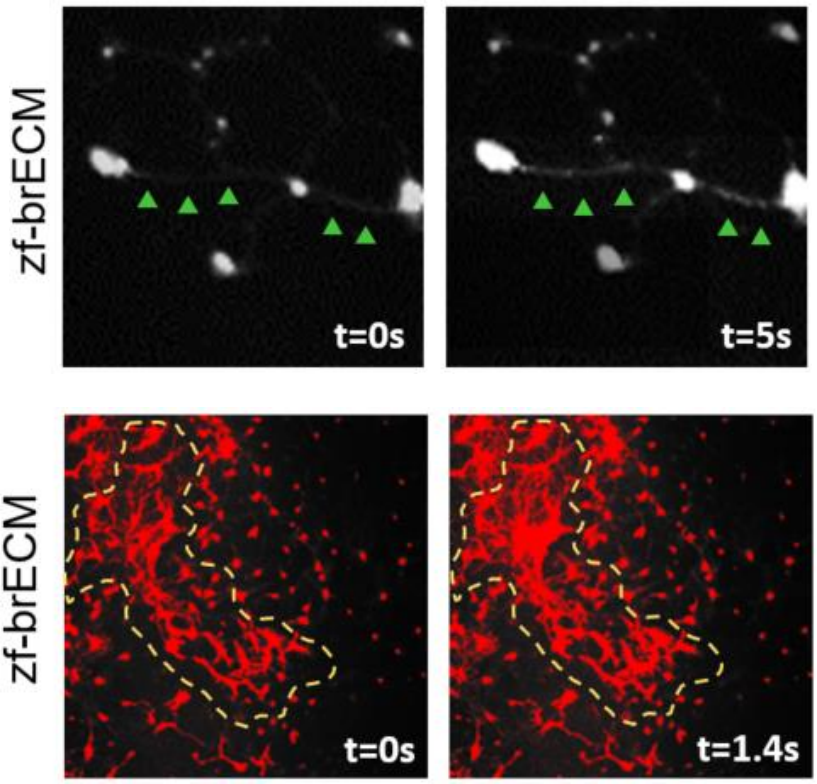


**Figure 20. Alternative visualization of live calcium signals.** Individual axons (top row) were observed to confirm calcium spikes. Axon networks (bottom row) supplying action potential propagation were also observed using region of interest (ROI) thresholding.

## 3.4 DISCUSSION

It has long been assumed that the mammalian CNS is incapable of regenerating neurons. However, it is now widely accepted that adult neurogenesis does exist, and that they have the potential to stimulate regeneration provided the right environment [6,7,43-49]. But without suitable environment, in most cases these neurons do not show long-term survival, and fail to integrate properly into neuronal networks [84-87]. On the contrary, certain anamniotic vertebrates such as the zebrafish regenerate their CNS after transection [34,73-74]. Yet, their ECM is under-explored

in biomedical science and engineering. Herein we demonstrate in vitro using primary rat cortical neurons that ECM derived from zebrafish brain 1) promotes robust cell retention and viability; 2) ensures long-term sustainability of neuronal health; 3) induces significant axonal growth and dense network formation; and 4) produces the most functional axon networks supported by high myelin activity and actin presence.

### 3.4.1 Zf-brECM Promotes Robust Neuronal Retention and Viability

In the case of neurons, cell retention is required for eventual transition from a population of individual neurons to dynamic axonal networks [123-127]. While the scaffolds and fibrin gelation in our study provides physical means of cell retention, different ECM compositions also provide different combinations of adhesive proteins. At day 7 of seeding primary neurons in different ECMs, zf-brECM exhibited significantly improved cell retention of ~20,000 cells, while other ECMs retained below 15,000 cells. Zf-brECM-embedded scaffolds also had the most significantly robust initial cell survivability of 87%, while other ECM groups dropped below 70% by day 5. Cell viability was prominently enhanced by the presence of zf-brECM, with almost twice the viability of the second highest outcome, which was r-brECM. This was a rather unexpected finding as it can be argued that r-brECM, which was derived from embryonic rat brains, is not only tissue-specific to but also from an early developmental stage of our rat neurons. Theoretically, this would make r-brECM the ideal environment for our cells. Yet, by day 25, while r-brECM did display strong cell viability of 53%, zf-brECM possessed extracellular signals necessary for neuronal growth of nearly 80%. This indicates that while ECM derived from tissue-specific source or early

stage tissue are effective, regenerative nature of zf-brECM provides compositional makeup that is significantly conducive to CNS regeneration, invoking strong neuron viability and retention.

A steady neuronal population is also important for CNS regeneration [128-130]. Studies have shown that even after a low initial survival of neurons, a well-sustained, steady population can be crucial for successful neuronal development and proper axonal elongation and pathfinding [131,132]. All ECM groups underwent their largest dip in their viability during the first five days before stabilizing. Day 5 ~ 10 marked a divergence between ECM groups that could promote over 50% viability and ECMs that could not. Near day 5, all groups sustained >50% viability. Immediately after, however, no-ECM, p-brECM, and p-UBM suffered a drop of >40% while r-brECM and zf-brECM maintained steady viability. Eventually, after day 15, each group began to maintain its live-cell population without suffering further damage to neuronal health. In short, zf-brECM achieved the best cellular retention and sustainability of neuron population, demonstrating its efficacy as a possible source of ECM treatment for CNS repair.

### 3.4.2 Zf-brECM Induces Significant Axonal Growth

Along with neuron viability, inductive cues provided by the ECM are thought to be a key mediator of axon extension and pathfinding, leading to eventual network formation capable of neural signals [133]. When combined with our viability analysis, we observed that while axonal activities stabilized early by day 7, overall neuronal health and growth remained in state of fluctuation until later time point. While it is not yet understood what determines neurite fate, it is known that only ~60% of the first neurite that protrudes from cell bodies become axons [134-136]. A minor neurite could extend outward until it touches an already developed axon of another neuron, at which point

the neurite will begin to differentiate into an axon. This crucial process is known as the 'touch and go model', and our results suggest different ECMs utilize the model to a varying degree [137]. Mammalian ECMs struggle to promote neuronal interaction and this lack of cell-cell interaction means neurons lack the signals for axon extensions [134,135,138]. Eventually, the neurons that did not get to 'touch' and 'go' in the first week are pruned from the culture, as reported in the literature and seen in our results [137]. On the other hand, zf-brECM produced strong survivability and high cellular retention, suggesting the ECM enriches neurons with abundant cell-cell interaction with other resident neurons, leading to more opportunities for axon formation.

The different engagement level of the 'touch and go' behavior in different ECM groups is further confirmed by the average axonal growth and network density formation. Zf-brECM exhibited the longest axonal extension as well as the highest density of network formation, while no-ECM and p-UBM exhibited the lowest in both categories. We posit this was possible due to the high cellular retention achieved by zf-brECM. As neurons are highly sensitive to somatosensory cues, the ability of neurons to respond to axon guidance cues are critical for integrating and connecting with other cells [139]. A key mechanism in neuronal development is the ability of the motile growth cone at the tip of a growing process to measure environmental cues and use them to grow accordingly [134,135]. Naturally, neuronal outgrowth is keenly affected by somatosensory response of other neurons. In fact, studies suggest the degree of somatosensory engagement affects not only neuronal adhesion, migration, and shape but also the direction and length of axonal growth [140]. Our results indicate average axonal length and network density are positively correlated to the size of neuron population in each ECM. This is evidenced by p-UBM's odd boost in axon length and two-fold increase in axon density at day 7 despite having the lowest cellular retention. This was possible because it had a well-sustained viability which would have

helped to form successful axon activities. Likewise, zf-brECM which had the highest cell retention as well as the lowest flux of viability, showed the largest increase in both axon length and network density. This leads us to believe neurons engage in highly competitive somatosensory behaviors in zf-brECM where the cells are provided more opportunities for axonal formation through increased chances of neurons engaging other resident neurons. In fact, neurons often demonstrate different growth strategies before and after making contact with other neurons [140]. Before contact, isolated neurons tend to elaborate their dendritic tree, extending more branches and generating more axons to increase their probability of contacting other cells. But after contacting a neighboring neuron, the growth strategy becomes more economic, the dendritic tree tends to simplify and the number of branches and number of axons from the soma decrease [135,140]. In other words, the more frequently and the more early neurons are able to contact other neurons, the more likely they are to build axon networks more economically. Our results suggest that zf-brECM indirectly takes advantage of this behavior early on to create the optimal condition for new axon networks. This is further confirmed by the fact that between day 3 and day 7, there are almost no neurons with new neurites or axons.

### 3.4.3 Zf-brECM Produces Functional Axon Networks

Functional CNS networks possess abundance of myelin as they are essential for rapid propagation of action potentials [141]. However, myelins are infamous inhibitors of axon-formation. Interestingly, while data on how myelin affects axonal regrowth in zebrafish is somewhat unclear, many studies suggest that zebrafish myelins are not axon inhibitors [142,143]. In fact, myelin-associated inhibitory molecules such as Nogo protein and MAG, which are major inhibitors of

axon re-growth in mammals, do exist in zebrafish CNS but their inhibitory domains do not [94-96]. Additionally, other protein domain that is inhibitory in mammals fails to elicit growth cone collapse of regenerating axons in zebrafish. In other words, zf-brECM has the unique potential of possessing myelination that can support rapid action potential propagation without inhibiting axonal outgrowth. To examine this aspect, we observed the phalloidin results highlighting actin assembly required for myelin activities. The highest actin content was seen in zf-brECM, followed by p-brECM and r-brECM, suggesting that efficient myelination of zf-brECM could be pivotal in promoting construction of functional axon networks.

CNS axon outgrowth and myelin wrapping are driven by actin assembly and polymerization. And in neurons, axonal organelle transport occurs via actin [144]. In other words, phalloidin-labeled F-actin in our study indicates myelin activities which are essential for establishing functional axon networks. In fact, live calcium imaging of network-level axon activities using Fluo-4 picked up spikes of action potential propagation in zf-brECM neuron culture. R-brECM exhibited some action potential activities, while the rest showed little to none. Many studies also suggest that the thickness of axons regulates the myelin growth and that as axon diameters grow, neurofilament packing density decreases and cell volume rapidly increases, an effect often seen during myelination [144,145]. During myelination, axons quickly increase in diameter, often doubling the volume of the cell. This consequently implies thicker axons possess more myelin-sheath for signal propagation. As expected, zf-brECM returned the highest average axon thickness, implying zf-brECM promotes the most myelination amongst all ECM groups, allowing it to be highly conducive to action potential propagation. While further investigations are necessary to conclusively declare zf-brECM as the most viable ECM for adult mammalian CNS

repair and to elucidate its exact mechanism, together, our results suggest that zf-brECM possess many promising traits for hosting mammalian neurons.

## 3.5 SUMMARY

Neurons grown with zf-brECM showed more robust survival and network formation compared to those grown in mammalian ECM. Zf-brECM returned the highest initial cell survivability as well as long-term viability, and led to longest axon extensions and densest network formations. The highest actin content observed in zf-brECM suggested successful myelination in zf-brECM group, which could contribute to the formation of functional axon networks. If true, the successful myelination seen in the axon networks of zf-brECM would be accompanied by readings indicating the most action potential propagation. True to our observation, zf-brECM displayed the most distinct calcium signal activity in its axon networks. The findings of this study challenge the long-held notion that ECM should be derived from mammalian tissues. Zebrafish has been extensively studied, yet it was rarely considered as a source for ECM. This in vitro study demonstrated the potential of zebrafish neural ECM and further in vivo study is warranted.

## 3.6 FUTURE WORK

The in vitro examination of zf-brECM is the first study to explore the efficacy of promoting neuronal growth using zebrafish-derived ECM supplements. It demonstrated that extracted non-

mammalian ECM could possess true regenerative potential and that its application deserves to be explored beyond in vitro applications. The success of improving primary neuron survival and their axonal formation using zf-brECM lays a great foundation for further studies utilizing zebrafish ECM. While the exact elements of zf-brECM responsible for the in vitro success are not known, it will be worthwhile to explore zf-brECM's regenerative potential in vivo.

# 4.0 ZEBRAFISH EXTRACELLULAR MATRIX PROMOTES AXON REPAIR AND VISUAL RECOVERY IN RODENT OPTIC NERVE INJURIES

## Chapter Aim

The aim of this chapter was to evaluate the regenerative efficacy of ECM technology derived from zebrafish brain for treating an optic nerve injury. Previously, we showed that compared to mammalian-derived ECM, zf-brECM promotes better neuronal growth and functional axon network formation in vitro. Based on this finding, we hypothesized that zf-brECM would allow injured optic nerves to achieve more robust axonal repair than mammalian ECMs. Other studies have previously established that zebrafish CNS-ECM can circumvent several repair-inhibitory mechanisms of injury response in mammalian CNS. These mechanisms include decreased glial scar deposition over time and suppression of inhibitor molecules. Combined, we hope to observe key biological traits indicative of CNS regeneration in a optic nerve injury model following zf-brECM treatment.

## 4.1 INTRODUCTION

Central nervous system (CNS) injuries remain one of the most difficult medical challenges. Adult mammalian CNS possess limited capacity for regeneration. Much of the limitation is caused by a prioritization on containment of injuries in vital parts of the nervous system over regeneration. Consequently, most functional deficits after CNS injuries involving axonal disconnection are permanent. As a result, CNS-related injuries usually cause life-long debilitation and lead to over $50B in healthcare costs [1]. Mammalian CNS possesses regeneration-inhibitory extracellular matrix (ECM) which actively stops axonal extension and promotes glial scarring, ultimately suppressing axon repair and reducing neurotrophic support [2]. This is in stark contrast to ECM of various lower vertebrate species in which the ECM plays an active role in supporting cellular development and regenerative response after injury [3-5]. Therefore, exposing mammalian neurons to non-mammalian ECM could potentially improve cell survival, axon extension, and neural network formation in CNS injuries.

The spinal cord and optic nerves of zebrafish (Danio rerio) has remarkable regenerative abilities [6]. Zebrafish are capable of regaining full motor function in severed spinal cords 7 days after a complete transection and can achieve scar-free healing via suppression of glial cell activation and circumvent inflammatory response. Much of this is possible due to their repair-permissive ECM designed to promote repairing of damaged axons and synaptic connections [7-9]. Here, we investigated the regenerative potential of zebrafish brain ECM (zf-brECM) in an optic nerve crush (ONC) injury model in rats and compared the results to optic nerves treated with pig derived brain ECM (p-brECM), urinary bladder matrix (p-UBM), and rat derived brain ECM (r-brECM). While application of ECM technology in CNS injuries have been limited and virtually

unstudied in the visual system, we know that mammalian optic nerves cannot regenerate under normal physiological circumstances without assistance (Figure 21). Therefore, several aspects of a successful CNS regeneration were measured. Compared to mammalian ECM controls, the fish ECM greatly reduced spread of glial scarring at the site of injury and led to decreased expression of chondroitin sulfate proteoglycans (CSPG), a well-known source of barrier against axonal regeneration and neurogenesis after CNS injuries. Optic nerves treated with zf-brECM also displayed more successful coverage of lesions with repairing axons as well as restoration of pupillary reflex.

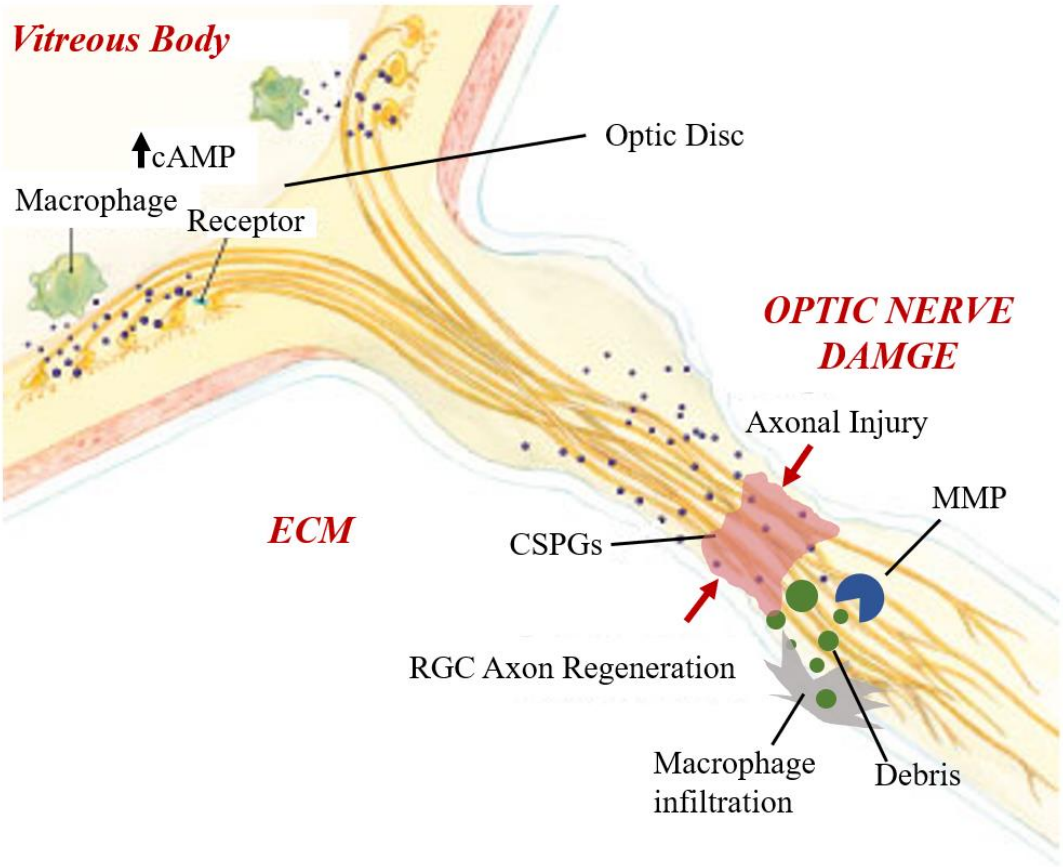


**Figure 21. Injury response of the optic nerve.** The site of the injury is marked by the two red arrows. Damage to the RGC axons and the surrounding myelin sheath leave cellular debris, which trigger macrophage infiltration. In CNS, macrophage recruitment is carried out by oligodendrocytes and is a slow process, taking up to 3

days. In most cases, the cells have already deteriorated by the time of macrophage infiltration and Wallerian degeneration begins to degrade from the axon stump distal to the site of injury. Eventually, glial scar deposition stops the spread of further degradation and releases various axon inhibitors in the process, such as CSPGs.

## 4.2 EXPERIMENTAL SECTION

### 4.2.1 ECM production

The ECM utilized in this study were derived from four different tissue sources: porcine brain, porcine urinary bladder, rat brain, and zebrafish brain. Porcine brain and urinary bladder ECM were kindly provided by Dr. Stephen Badylak (University of Pittsburgh) and supplied frozen. For rat brain, pregnant rats were ordered (embryonic-day E18, Sprague Dawley) and upon sacrifice, fresh whole brain tissues were immediately collected from their pups [85]. Zebrafish brains were harvested from colonies of day-60 zebrafish, kindly provided by Dr. Michael Tsang (University of Pittsburgh). They were first numbed using Tricaine solution. Then, their whole brain tissue was collected fresh via their cranium.

Following their procurement, rat and zebrafish tissue samples were decellularized following our previously-established protocol [86]. Briefly, our unique decellularization method utilizes only freeze-thaw cycles, cryomilling, antibiotic antimycotic solution, lysis buffers, and DNase/RNase to remove DNA in the tissues. This method is thorough enough to remove cellular material but also gentle enough to minimize damage to the tissue's proteins and glycosaminoglycans (GAGs). The final products were freeze-dried as powder and were dissolved in PBS on the day of their use to create ECM solution of desired concentration. To the best of our

knowledge, zebrafish tissue, including their brains, have never been thoroughly investigated as a source of ECM. Consequently, no protocol exists establishing their proper decellularization. Therefore, all ECM were subjected to equal post-decellularization quality control assessment before being deemed viable for the study. Effective removal of cells from the tissue was confirmed via DAPI staining. Briefly, sections were analyzed via immunofluorescent staining where sections were fixed in 4% paraformaldehyde for 10 mins, washed ×3 in PBS, permeabilized in 0.1% Triton X-100, washed ×3 in PBS, blocked in 0.5% normal goat serum (NGS), and incubated with DAPI fluorescent-labeled antibody diluted 1:500 in PBS for 1 h at room temperature (RT), and after further washes in PBS were mounted in Fluorsave (Merck Biosceince, Nottingham, UK). Meanwhile, effective removal of DNA content was measured using PicoGreen assay (Life Technologies). Briefly, the ECM samples were placed in well-plates and wash 2-3 times with PBS. 200µl of distilled, de-ionized water was added and the samples were frozen at -80°C. They were then thawed and transferred to fresh 1.5 ml tube and measured for wet weight. 250 µl for each sample was used for cell lysis solution (0.2% of v/v Triton X-100, 10mM Tris, 1mM EDTA). The samples were centrifuged at 12,000 rpm for 10 min at 4°C and the supernatant was collected for assay. Using the PicoGreen kit, the assay buffer 1x TE Buffer was prepared by diluting 20× TE Buffer with deionized distilled DNAase free H2O. Then a 200-fold diluted working solution of the reagent was prepared. Lastly, the DNA standard solution was prepared for an assay to be run on a 96-well plate. Fluorescence was read at excitation of 480 nm and emission at 528 nm for each well in a microplate reader. dsDNA content (ng/ml) was calculated from standard curve. Threshold for acceptable DNA content was less than 50 ng/mg dry weight, which is a commonly cited threshold in industry-grade ECM products as it is close to the value found in commercial-grade Matrigel [87].

### 4.2.2 Rodent Optic Nerve Crush Model

Healthy adult male rats (Sprague Dawley) were used to create ONC models for the study. All surgeries were performed on the rats' right eyes, while the left eyes were left intact to avoid bilateral impairment [145]. The animals were first anesthetized with intraperitoneal injection of ketamine (80 mg/kg) and xylazine (5 mg/kg). Incisions were then made in the conjunctiva at the limbus, and the Sub-Tenon's space was bluntly dissected posteriorly until reaching the optic nerve. Once the optic nerve was exposed, its optic nerve sheath was fenestrated, and the nerve was crushed 2 mm below the optic disc using fine Yasargil Titanium aneurysm clip (Aesculap, Inc.) for 9 seconds (Figure 22). Special care was taken to not damage the surrounding blood vessels. Then ECM solution was prepared as fibrinogen solution, with fibrinogen concentration of 10 mg/ml and thrombin concentration of 2 mg/ml. The resulting ECM-fibrinogen solution was then delivered as 2 µl injection on the site of lesion of the optic nerve. The surrounding tissue was held and pressed against the gel in place for a minute, or until the ECM had gelled and sealed the tear. Control group received fibrinogen injection with no ECM supplements after the surgical procedure, whereas treatment groups received one of the four ECM treatments. 7 and 28 days after ONC and ECM delivery, the animals were sacrificed using CO2 chamber and secondary method of vertebrae dislocation. Injured eyes were then removed from the dislocated head, taking care to keep the attached optic nerve intact. The collected samples were then immediately fixed in 4% paraformaldehyde before being cryo-sectioned and immuno-stained.

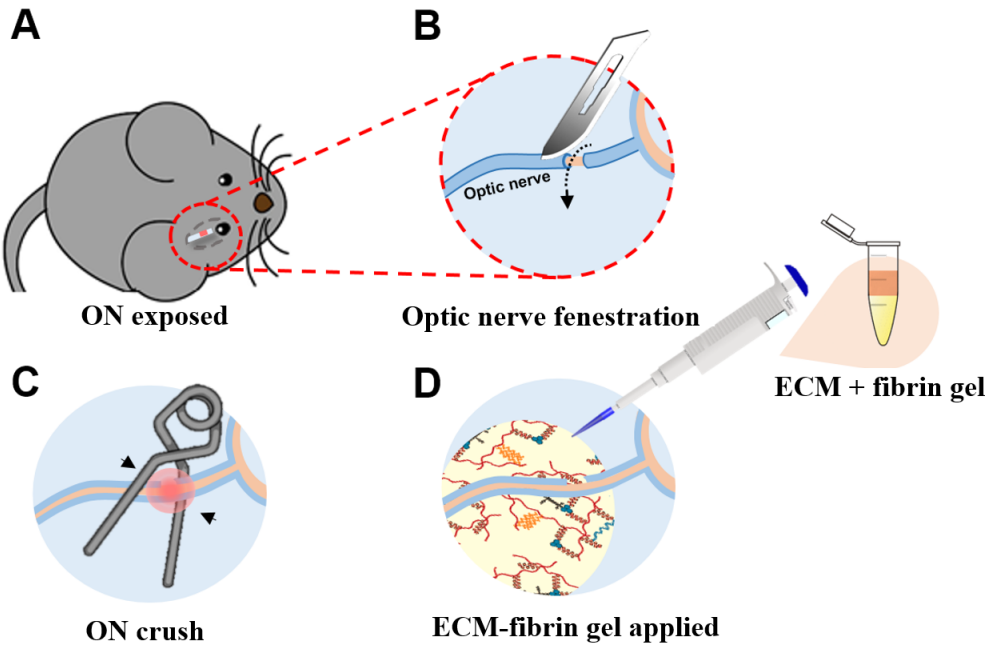


**Figure 22. Schematic of rodent ONC model.** First, the optic nerve is exposed (A), and its optic nerve sheath is fenestrated using a surgical blade (B). Then, using an aneurysm clip, we apply pressure on the optic nerve 2 mm below the optic disc (C), followed by 2 µl delivery of our ECM-fibrin gel (D).

### 4.2.3 Biological Assay

#### 4.2.3.1 Glial Scar Deposition

On day 7 and 28, sections were analyzed via immunofluorescent staining. Sections were fixed in 4% paraformaldehyde for 10 mins, washed ×3 in phosphate buffered saline (PBS), permeabilized in 0.1% Triton X-100, washed ×3 in PBS, blocked in 0.5% normal goat serum (NGS), and incubated with the appropriate primary antibodies diluted in 0.5% NGS PBS overnight. Sections were then washed ×3 with PBS and incubated with the appropriate fluorescent-labeled secondary antibody (either Alexa-488 or Alexa-594) diluted 1:100 in PBS for 1 h at room temperature (RT), and after further washes in PBS were mounted in Fluorsave (Merck Biosceince,

Nottingham, UK). For evaluation of fibrous glial scarring, sections were incubated overnight at 4°C with mouse anti-rat glial fibrillary acidic protein (GFAP) primary antibody (1:1000; Sigma), followed by goat anti-rat Alexa-488 immunoglobulin G (IgG) (1:500; Life Technologies) at RT for 1 hour.

#### 4.2.3.2 Chondroitin Sulfate Proteoglycan Expression

In order to observe CSPG expression, sections were analyzed via immunofluorescent staining at day 7 and 28. The sections were then fixed and washed in PBS, permeabilized, blocked in 0.5% NGS, and incubated with the appropriate primary antibodies diluted in 0.5% NGS PBS overnight. Sections were then washed ×3 with PBS and incubated with the appropriate fluorescent-labeled secondary antibody (either Alexa-488 or Alexa-594) diluted 1:100 in PBS for 1 h at RT, and after further washes in PBS were mounted in Fluorsave (Merck Biosceince, Nottingham, UK). To examine presence of axon inhibitor chondroitin sulfate proteoglycans (CSPGs), sections were incubated overnight at 4°C with mouse anti-rat CS-56 primary antibody (1:200; Sigma), followed by goat anti-mouse Alexa-488 IgG at RT for 1 hour.

#### 4.2.3.3 Axonal Repair Across Lesion

Similarly, on day 7 and 28, sections were analyzed via immunofluorescent staining for analysis of axonal analysis as well. Sections were again fixed in 4% paraformaldehyde for 10 mins, washed ×3 in PBS, permeabilized in 0.1% Triton X-100, washed ×3 in PBS, blocked in 0.5% NGS, and incubated with the appropriate primary antibodies diluted in 0.5% NGS PBS overnight. Sections were then washed ×3 with PBS and incubated with the appropriate fluorescent-labeled secondary antibody (either Alexa-488 or Alexa-594) diluted 1:100 in PBS for 1 h at RT, and after

further washes in PBS were mounted in Fluorsave (Merck Biosceince, Nottingham, UK). To detect axon and activities and repairs over the crush site, sections were incubated overnight at 4°C with mouse anti-rat βIII-tubulin primary antibody (1:500; BioLegend), followed by goat anti-mouse Alexa-488 IgG at RT for 1 hour. Lastly, to visualize the injury sites in all samples, all sections were co-stained with rabbit anti-rat laminin primary antibody (1:200; Abcam), followed by goat anti-rat Alexa-594 IgG (1:500; Life Technologies) at RT for 1 hour.

### 4.2.4 Statistical Analysis

Comparisons of GFAP, CSPG, and βIII-tubulin expression level between groups were made using ANOVA followed by Tukey's post hoc testing for significance. The same method was used to compare differences in thickness of re-myelination and recoveries of visually-guided behaviors, with p-value $<0.05$. The experiment required at least 8 rats per each group to achieve 80% power, with 4 backup rats per group, giving us a total of 60 rats.

### 4.2.5 Behavioral and Functional Assay

#### 4.2.5.1 Pupillary Light Reflex (PLR)

PLR refers to the reflex that controls diameter of pupil in response to intensity of light hitting RGC in retina. This reflex is driven by retino-pretectal connection to olivary pretectal nucleus (OPN) shell and helps eyes adjust to various levels of light, and it can be used as means of behavioral assessment [146-149]. Rats were dark-adapted within their home cage for 1 hour before the experiment for optimal results. All rats were un-anesthetized for the test and simply

restrained by hand for the duration of the experiment. A single blue (470 nm) light was placed in front of the lesioned eye (Figure 23). Normally, when light is shone to eyes, both eyes constrict due to parallel visual pathways. Therefore, to ensure the pupil response in the lesion eye was not driven by light received in the non-lesion eye, the non-lesion eye was covered behind an eye patch. Then pupil constriction and dilation in the light-stimulated eye was recorded with a video camera placed on the side of the head. The pupil was recorded before (baseline) and during (constriction) the light stimulus (30 seconds at intensity of 25 lx). Individual frames of the initial resting pupil size (baseline) and at maximal constriction were extracted from the video recordings and pupil diameters were measured using ImageJ [149]. The percentage of the pupil constriction was calculated from the pupil diameter measurements at the initial resting size and maximal constriction (n = 10 - 12 rats per group). Diminished result indicated relatively low retinal information travelling across the optic tract to the pretectum of the mid-brain, which is responsible for the eye's ability to control pupil and lens reflex.

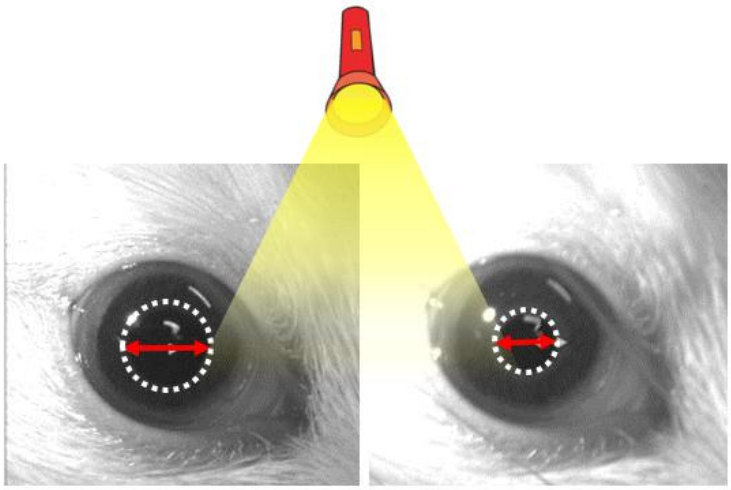

**Figure 23. Schematic overview of pupillary light reflex examination.** PLR was measured as percentage constriction of the rats' eyes following bright light stimuli after receiving ONC procedure and ECM treatments.

#### 4.2.5.2 Visual Cliff Test

Taking advantage of the animal's natural aversion to depth and height, we measured the rat's visual recovery using visual cliff test which works by probing the retino-geniculo-cortical pathway [148,149]. To measure the rats' depth avoidance, their visual cliff behavior was analyzed in an open-top acrylic chamber. While rats do not share the quality of clear vision humans possess, studies have shown that visual cliff can serve as an adequate test of measuring significant differences in depth aversion in rats [150]. Following ONC, their depth aversion is lost and does not return without treatments or intervention. Therefore, the functional recovery of their eyes can be measured by tracking signs of depth aversion they display. A clear platform was placed midway from the bottom. For half of the chamber, the platform was covered with a checkerboard pattern. The other half was left clear but the bottom surface was covered with a checkboard pattern. This set up created a perceivable depth of 1 foot on the 'deep' side of the chamber. The platform in the box, whether it is simulating shallow end or deep end, was level with no slope. The rat was placed on top of the platform in the middle and allowed to choose between the two sides. From the second the rat touched the surface, we measured its time spent on 'shallow' end versus the 'deep' end, and after 5 minutes, the rat was given a score to indicate how much it stayed on one side. To prevent the rats from relying on their healthy eye, as the surgeries were not performed bilaterally, each rat was given a small eyepatch which was fixed in place using tape. Each rat performed this task 5 times per day for 3 days. The visual cliff behavior was averaged to generate mean percentage of trials in which the rat chose to step down to the shallow side (n = 10 - 12 rats per group).

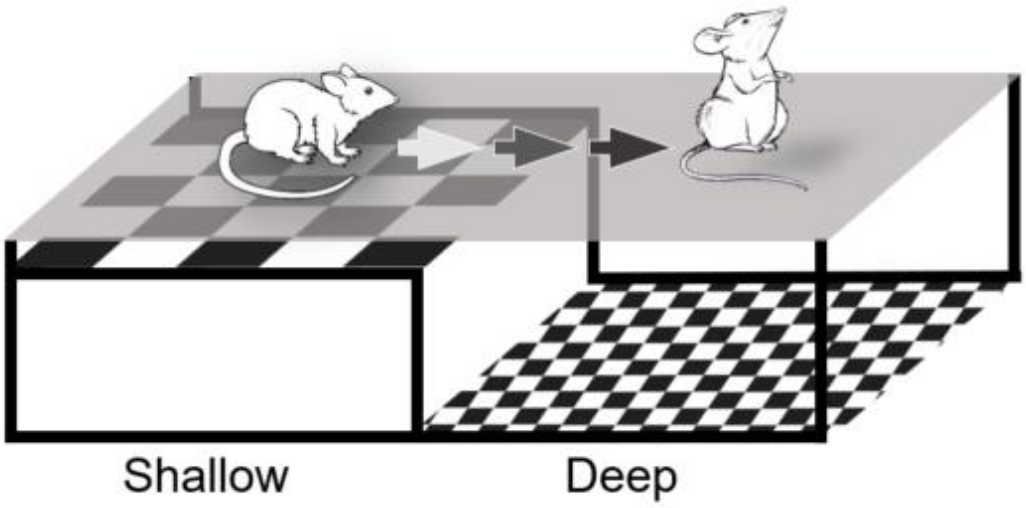


**Figure 24. Schematic overview of visual cliff test.** Using the visual cliff apparatus, we observed the rats' preference to remain in the shallow side as a sign of depth aversion.

### 4.2.6 Statistical Analysis

ANOVA analysis was carried out, followed by Tukey's post hoc testing for significance to determine if the difference is significant with p-value $p<0.05$. This method was used to identify significant difference in the rats' PLR measurements as well as depth avoidance measurements. For PLR, the best visual recovery that has been achieved in rodent ONC records a difference of approximately 20% between treatment and no treatment groups, with SD of 14%. Assuming similar difference, we will need at least 8 animals per group to reach 80% power. In total, the experiment used 60 rats.

## 4.3 RESULTS

### 4.3.1 Glial Scar Measurements

A critical step to a successful CNS regeneration is enabling axons to regrow transverse the site of injury. One of the most prominent obstacles is glial scar deposition which is formed by reactive astrocytes changing their morphology to physically form a barrier. This fibrotic presence of glial scar provides deleterious molecular environment for axonal growth. At day 7 of our study, glial scarring was observed in all groups, with or without ECM supplements as treatments, indicating that none of the ECM treatments completely suppressed glial scar formation (Figure 25). However, the size of the scar seen in zf-brECM group was significantly smaller compared to the scar found in no-ECM group. At day 28, a much more significant difference in the degree of glial scar deposition was observed (Figure 26). Optic nerves that received no ECM additives formed scar deposition of approximately 1700 μm in length, while optic nerves that received zf-brECM formed glial scar deposition of approximately 650 μm in length. This suggests that while zf-brECM may not completely prevent glial scar from forming, it may reduce its spread. Some believe this to be more ideal than eliminating glial scar formation as glial scar also aides the inflammatory response. With compromised astrocytes, inflammation will be unleashed on repairing axons instead [16,17]. However, formation of a glial/collagen scar matrix within CNS lesions is, on balance, detrimental to successful regeneration as it contains a dense array of ECM proteins that impede axon growth, such as CSPG.

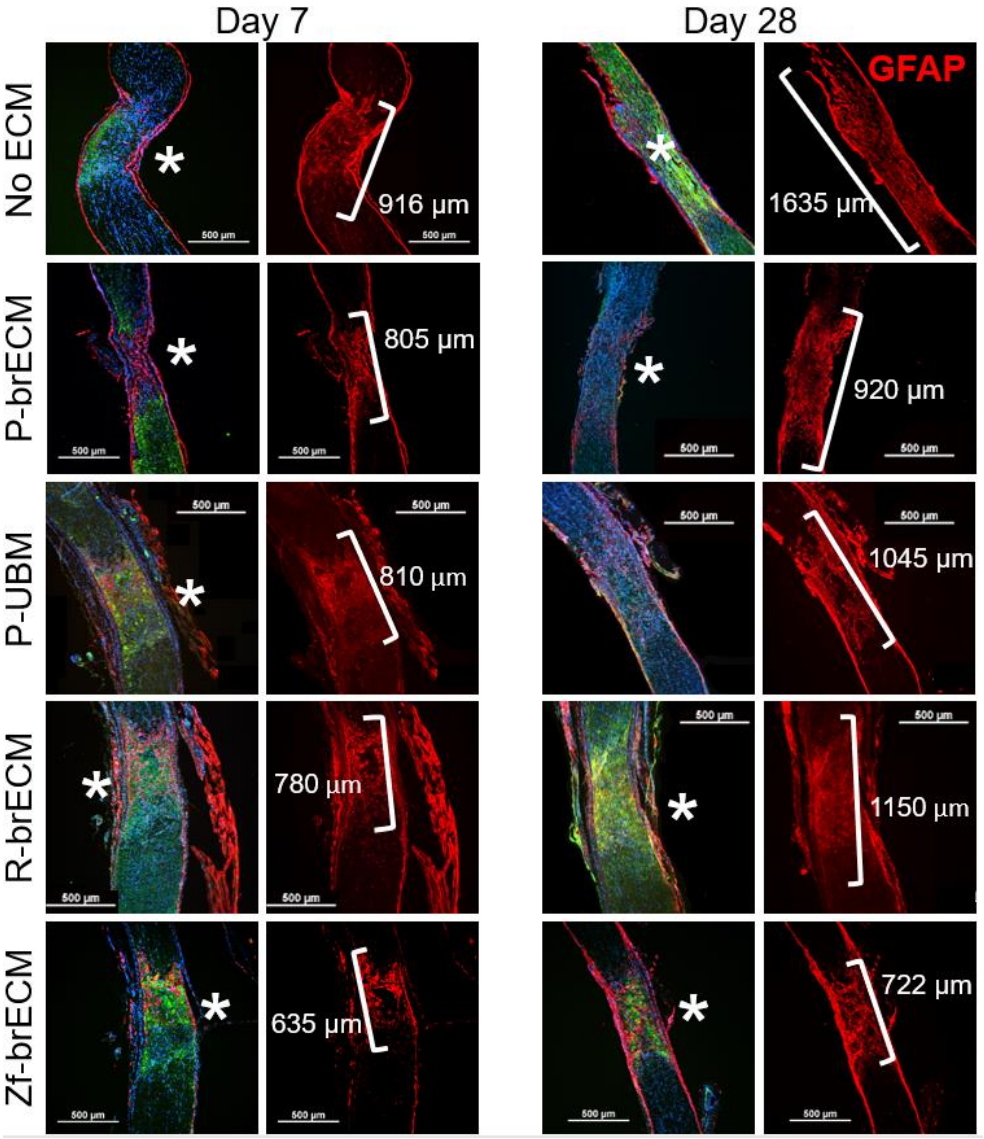


**Figure 25. Glial scar deposition at day 7 and day 28.** GFAP was used to label glial scar deposition, shown in red, at day 7 (left column) and day 28 (right column) following ONC. Following ONC procedure, optic nerves in rats were treated with four kinds of ECM and their reactive astrocytic activity was observed to survey their glial scar formation. Optic nerves with no ECM treatment served as the control group.

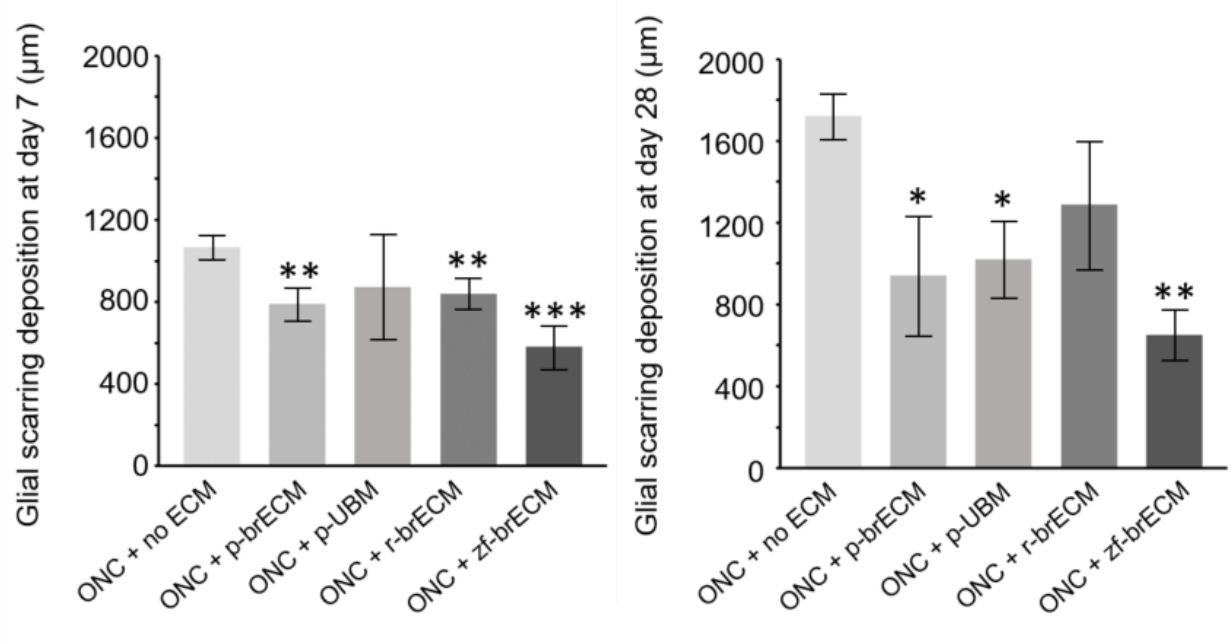


**Figure 26. Quantified measurements of glial scar deposition.** ANOVA between subjects was conducted to compare the effect of different ECM on glial scar deposition in optic nerves treated with p-brECM, p-UBM, r-brECM, and zf-brECM. Zf-brECM exhibited the least glial scar deposition at both day 7 and 28 while no-ECM exhibited the most glial scar formation. However, as seen in day 28, none of the treatment groups was able to completely eradicate glial scar formation. Nonetheless, at day 28, all groups showed increased glial scar deposition while zf-brECM maintained approximately the same level of glial scar deposition as day 7. This suggests that while zf-brECM cannot completely prevent glial scar formation or eliminate them, it can prevent or delay further deposition of reactive astrocytes (*$P < 0.05$, **$P < 0.01$, ***$P < 0.001$ corresponds to all groups).

### 4.3.2 CSPG Expression

Axon inhibitors play a detrimental role in mammalian CNS regeneration. They are abundantly expressed by mammalian ECM and undergo increased release following injuries. CSPGs are one such axon inhibitor that have been shown to greatly limit CNS plasticity. Therefore, a critical milestone for regeneration of mammalian CNS is reduced release of CSPG after injuries. In all groups, we observed CSPG expressions decrease between day 7 and day 28, with or without ECM

treatment. Specifically, at day 7 following ONC, rats receiving no ECM showed very prominent release of CSPGs at the lesion site while p-brECM, p-UBM, and r-brECM groups expressed slightly less. Zf-brECM showed mild expression of CSPG (Figure 27). And by day 28, all groups displayed less CSPG than their day 7 counterparts, with no-ECM displaying moderate level, p-brECM, p-UBM, and r-brECM displaying mild level, and zf-brECM displaying negligible level of CPSG. This suggests CSPG release acts as an early response to injuries and naturally subsides over time without intervention or treatments. Nonetheless, zf-brECM's effect was not insignificant. While all groups showed decreased CSPG by day 28, zf-brECM exhibited noticeably less CSPG presence at day 7. This suggests zf-brECM, unlike mammalian ECM, may be unique in its ability to suppress axon inhibitors before they are naturally removed. While all ECM treatments helped to eventually suppress CSPGs, only zf-brECM was able to engage suppression of inhibitors at early time point. This early role may be pivotal to how zf-brECM affects other regenerative outcomes in vivo.

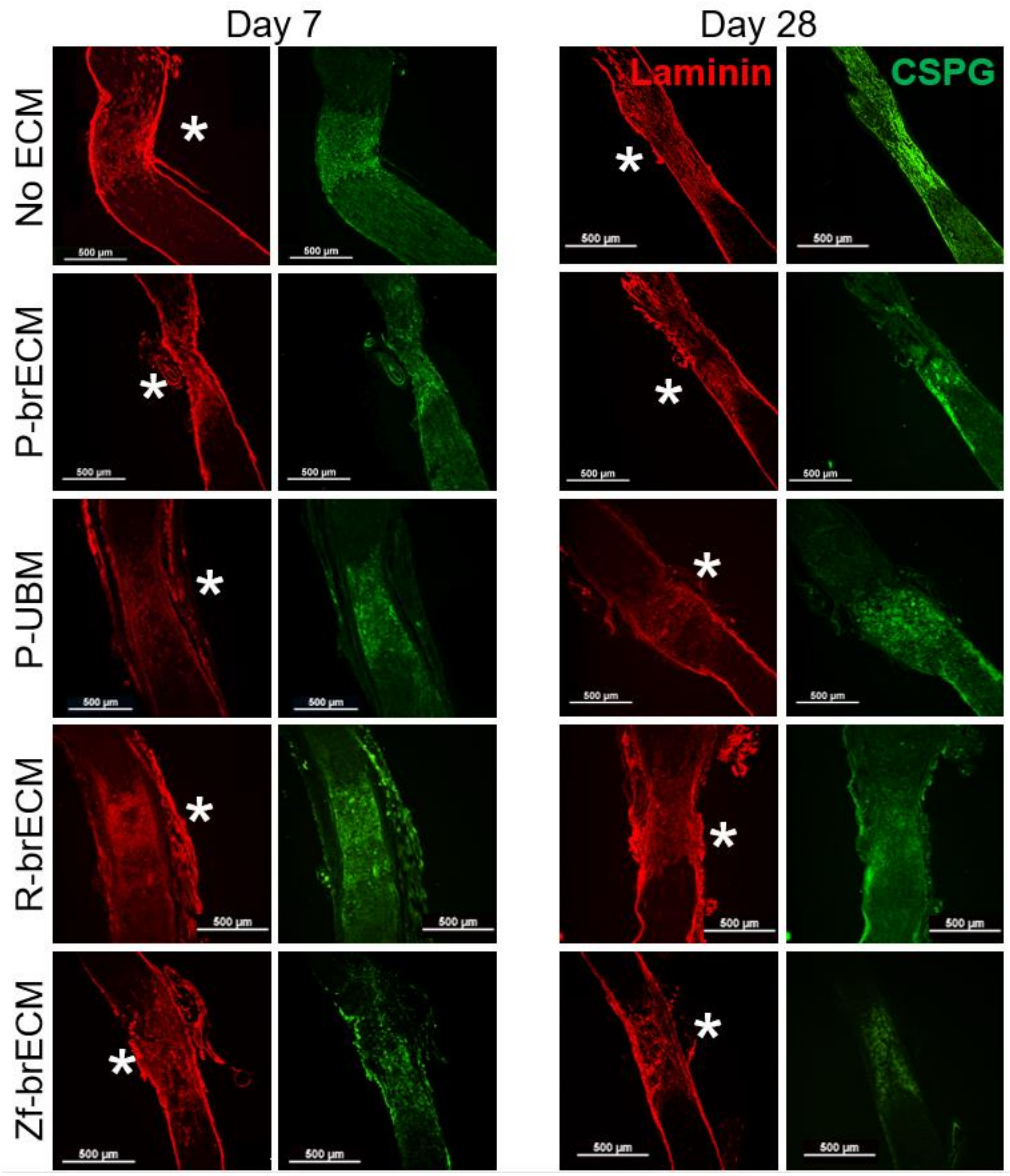


**Figure 27. CSPG release expression at day 7 and day 28.** Following the ONC procedure, optic nerves in rats were treated with four kinds of ECM, and to investigate their effect on expression of axon inhibitors, we observed CSPG presence. CS-56 was used to label expression of CSPGs, shown in green, at day 7 (left column) and day 28 (right column) following ONC. The lesion sites were identified by labeling laminin deposition at the site of crush injuries, shown in red. Asterisks (*) indicate the site of the crush injuries. Rats that received no ECM treatment after ONC served as the control group and ANOVA between subjects was conducted to compare the effect of different ECM on CSPG expression levels. In all groups, we saw CSPG expressions decrease between day 7 and day 28, even without any ECM treatment. This suggests CSPG could be an early response and naturally subside over time without any intervention or treatments. Nonetheless, zf-brECM's effect was not non-negligible. At day 7, zf-brECM exhibited

the least CSPG presence, and while all groups showed decreased CSPG by day 28, only zf-brECM had noticeably minimal CSPG presence. This suggests zf-brECM, unlike mammalian ECMs, may be unique in its ability to suppress axon inhibitors before they are naturally removed. If so, this early role may play a pivotal role in how zf-brECM affects other regenerative outcomes.

### 4.3.3 Repairing Axons Transverse of Crush Site

Any functional recovery of the eyes must stem from underlying biological events. One biological event to note is stimulation of axonal outgrowth across the lesion sites. Following the ONC procedure, the optic nerves in rats were treated with four kinds of ECM and their lesion sites were observed to survey repair activities of their present axons (Figure 28). At day 7, axons of no-ECM measured approximately 14% across the full length of the lesion sites (Figure 29). Axons observed in other ECM groups measured between 30 ~ 35% across the lesion sites at day 7 and roughly the same at day 28. Meanwhile, axons in zf-brECM group boasted approximately 55% lesion coverage at day 7 and 70% at day 28. In the absence of any therapeutic ECM intervention, there was very little lesion coverage at day 28, just as at day 7. In fact, between the two time points, axon extensions with no ECM treatments failed to exceed beyond 15% of the lesion sites. This suggests p-brECM, p-UBM, and r-brECM induce moderate axon repair at an early time point but loses the effect beyond day 7. P-brECM covered approximately 35%, p-UBM covered 31%, and r-brECM covered 29% of the lesion sites by day 7. At day 28, p-brECM and p-UBM showed little improvements, remaining around 35%, while r-brECM displayed approximately 10% improvement. On the other hand, zf-brECM promoted strong axon repair at day 7 and proceeded to support increased repair activity through day 28.

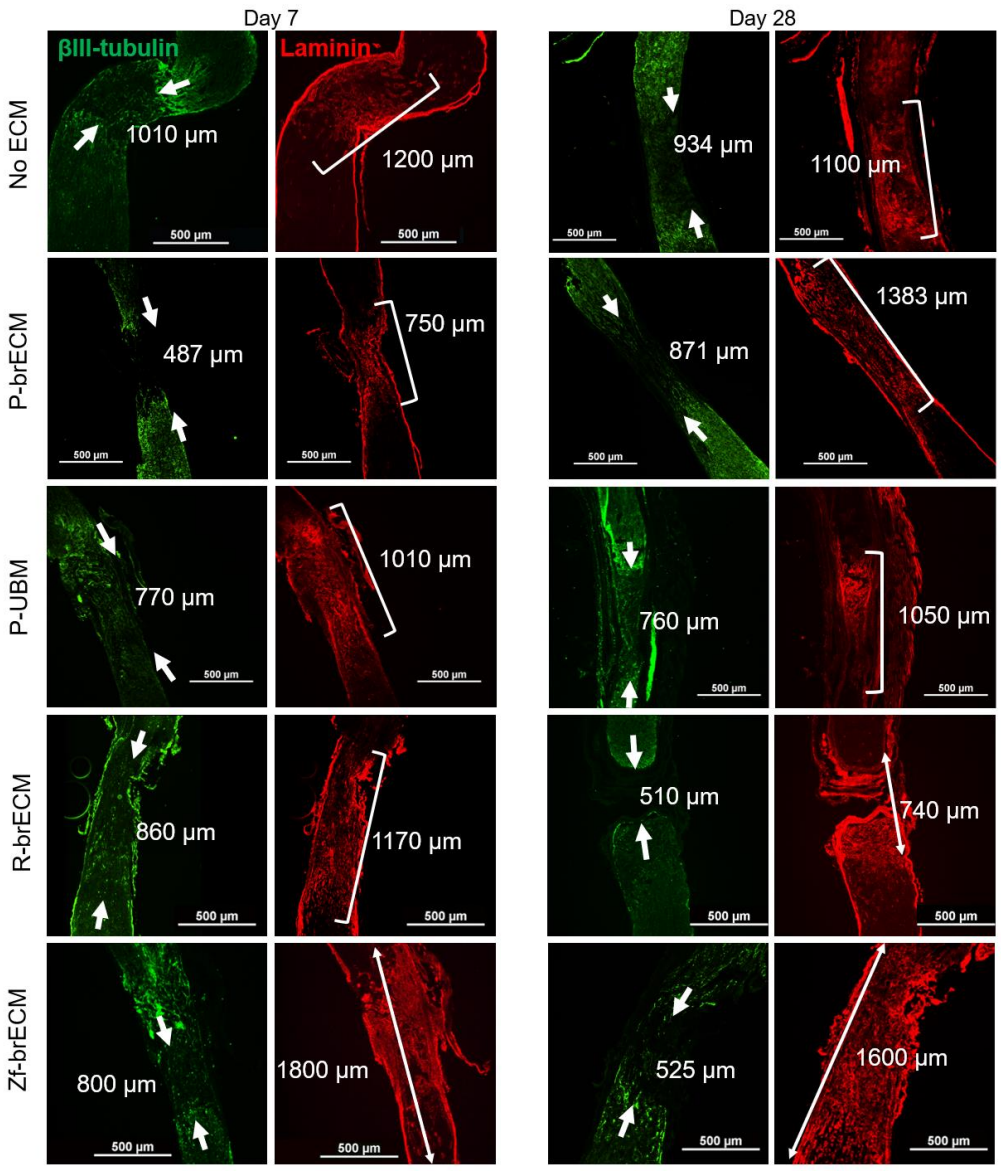


**Figure 28. Axons transverse of lesion sites at day 7 and day 28.** Following ONC procedures, the optic nerves in rats were treated with four kinds of ECM and their lesion sites were observed to survey the repair activities of their present axons. Optic nerves with no ECM treatment served as the control group. βIII-tubulin was used to identify axon repair growth transverse of lesion sites following ONC, shown in green, at day 7 (left column) and day 28 (right column). Laminin deposition was labeled to mark the lesion sites, shown in red.

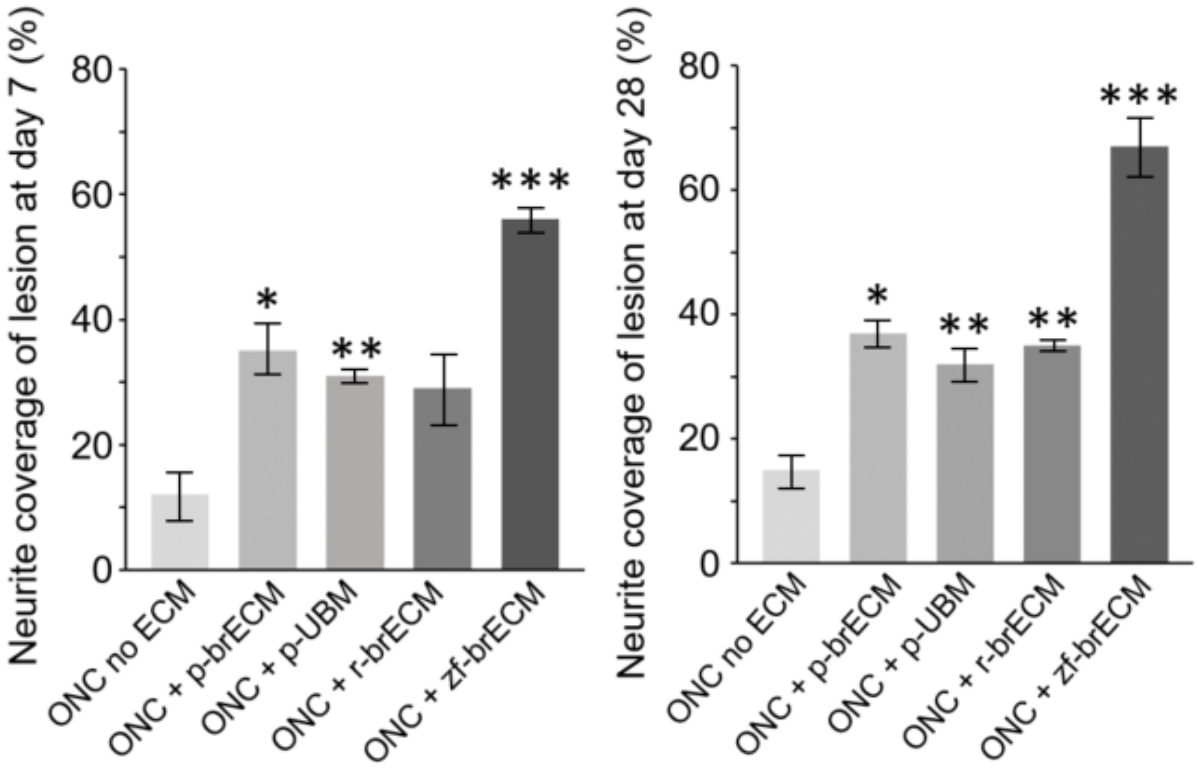


**Figure 29. Percentage coverage of lesion sites by repairing axons.** βIII-tubulin and laminin markers were used to calculate what percentage of the lesions were covered with active axons. ANOVA between subjects was conducted to compare the results following treatment of p-brECM, p-UBM, r-brECM, and zf-brECM. Axons in zf-brECM group boasted approximately 55% lesion coverage at day 7 and 70% at day 28. Meanwhile, axons observed in other ECM groups exhibited between 30 ~ 35% lesion coverage at day 7 and roughly the same at day 28. No-ECM showed very little lesion coverage at both time points, suggesting p-brECM, p-UBM, and r-brECM induce moderate axon repair at an early time point but loses the effect beyond day 7. On the other hand, zf-brECM promotes strong axon repair at day 7 and proceeds to support increased repair activity through day 28 (*$P < 0.05$, **$P < 0.01$, ***$P < 0.001$ for all groups).

### 4.3.4 Restoration of Pupillary Light Reflex

Behavioral performance was assayed in two different tests of visual function. As the biological assays observed in this study portray only a portion of much larger regenerative event, it would be

challenging to understand their roles and relations without adequate behavioral study. The first behavioral test was the PLR test. PLR test probes the retino-pretectal connection to the optic nerve shell and provides insights to the restoration of the eyes' light sensitivity by measuring pupil constriction/dilation. PLR represents constriction of the pupil in the illuminated eye and for the study, it was measured following light stimulus of the lesioned eye at 25 lx for 30 seconds (Figure 30).

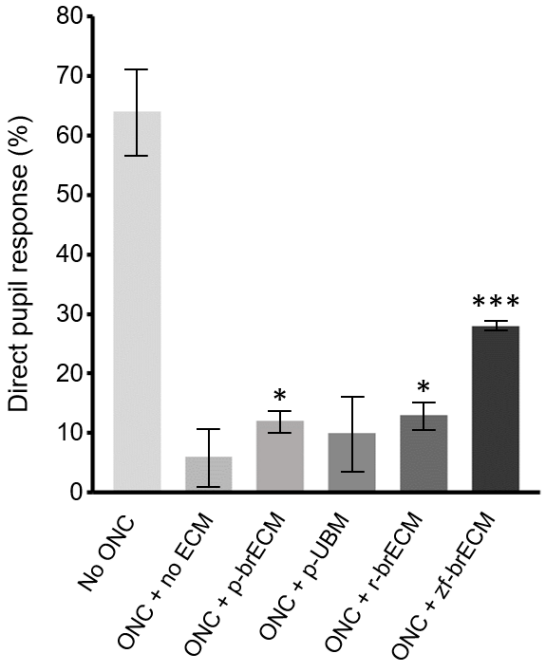


**Figure 30. PLR measurements.** Mean percentage of direct pupil constriction (data presented as mean ± standard error of mean) indicates pupil sensitivity to light stimuli following ONC with various ECM treatments. Following the ONC procedure, optic nerves in rats were treated with four kinds of ECM and their pupil response was observed to survey restoration of functional response. Optic nerves that received no ONC served as the control group. ANOVA between subjects was conducted to compare the results following treatment of p-brECM, p-UBM, r-brECM, and zf-brECM. Result indicates pupil sensitivity to light stimuli is moderately restored following all ECM treatments, with zf-brECM having a significantly higher restoration of pupil response. All mammalian ECM treatments returned

<15% pupil response, whereas zf-brECM was able to return approximately 27% pupil response (*P < 0.01, ***P < 0.001 corresponds to all groups).

PLR response following ONC was markedly heightened following zf-brECM treatment, measuring approximately 27 ± 2 %, meaning a moderate level of light sensitivity had returned to the eye (Figure 30). No-ECM measured 5 ± 4 %, p-brECM measured 12 ± 2 %, p-UBM measured 10 ± 6 %, and r-brECM measured 13 ± 2 %. There was a significant difference in response between zf-brECM and mammalian ECMs, indicating that the regenerated RGC axons in zf-brECM group succeeded in rescuing pupil constriction. Unfortunately, no group was able to achieve complete restoration of PLR. This is in accord with the partial axon repair observed earlier.

### 4.3.5 Restoration of Depth Aversion

The second behavioral test was the visual cliff test, which probes the retinogeniculo-cortical pathway [151,152]. Visual cliff test evaluates depth perception and the functional integrity of the lesioned eyes after different ECM treatments. Rats naturally possess depth aversion that allows them to avoid edges and cliffs and minimize the risk of falling. While rats do not possess the same quality of vision as humans do, studies have shown that visual cliff test can be used to adequately measure significant differences in depth aversion in rats. Following ONC, their depth aversion is lost and does not return without treatments or intervention [153]. Therefore, the functional recovery of their eyes can be measured by tracking signs of depth aversion they display. The same five groups of ECM groups were tested: a unilateral ONC that received fibrinogen gel with 1) no regeneration-enhancing ECM additives, 2) p-brECM, 3) p-UBM, 4) r-brECM, 5) and zf-brECM. To ensure that any observed functional recovery was mediated by regenerated RGC connections

originating from the lesioned eye and not by RGCs from the non-lesioned eye, we covered shut the non-lesioned eye with makeshift eyepatch. Each rat was placed on a platform, below which the floor on one side was painted with a low spatial frequency pattern of large black squares while the other was painted with a high-spatial-frequency pattern of small black squares. This created an illusion of a shallow versus deep drop from the platform, respectively.

Normal non-ONC rats chose to stay on the shallow side of the chamber approximately 70% of the testing period (Figure 31). Regeneration resulting from p-brECM, p-UBM, and r-brECM failed to restore connections that mediate visual cliff avoidance behavior. This could reflect defects in synapse formation and/or insufficient numbers of regenerating axons. Zf-brECM rats chose to step down on the perceived shallow side of the chamber in approximately 25% of trials, which was significantly higher than other ECM groups. This confirmed sufficient number of regenerated axons had formed and that successful synapse formation followed. Overall, these results indicate that zf-brECM treatment leads to axonal regeneration in injured optic nerves that can augment and sustain partial recovery of optical functions and vision-driven behaviors. The corresponding biological signs, while not all necessarily indicative of improvements individually, reveal their combinatorial effect on behavioral recovery.

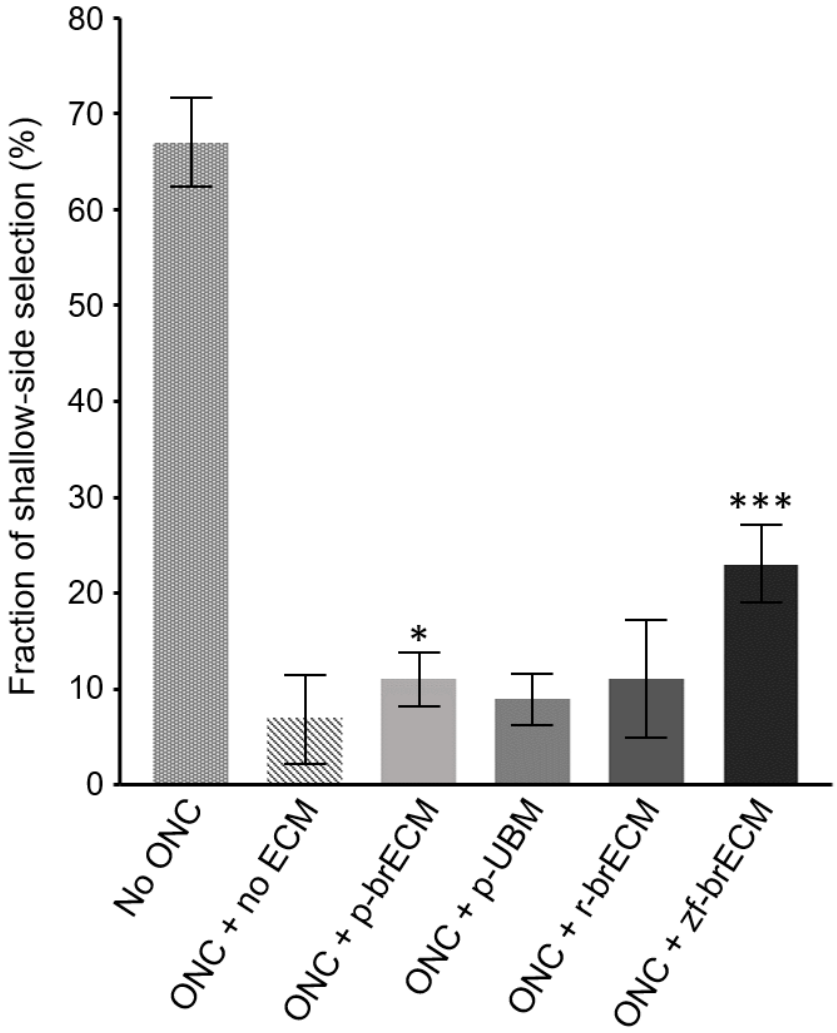


**Figure 31. Depth avoidance following visual cliff test.** We recorded the mean percentage of the shallow-side selection (data presented as mean ± standard error of mean) Rats that received no ONC served as the control group. ANOVA between subjects was conducted to compare the results of visual cliff test following treatment of p-brECM, p-UBM, r-brECM, and zf-brECM. Rats that did not receive ONC chose to remain in the shallow side approximately 70% of the testing period, showing clear preference for the safe side and avoidance of the "deep" end. While p-UBM and r-brECM had no significant effect on depth avoidance, zf-brECM showed moderately higher selection percentage of the shallow end compared to mammalian ECM groups (*$P < 0.01$, ***$P < 0.001$ for all groups).

## 4.4 DISCUSSION

Intelligent manipulation of ECM composition can instigate cellular growth and regeneration in injured tissue. This approach has been actively explored in the field of regenerative medicine by attempting to harness the healing mechanisms of foreign ECM. Unfortunately, it has not had much success in promoting regeneration in CNS injuries. Interestingly, while lower-vertebrate species are known to possess remarkably regenerative neural tissue and ECM, they remain largely unexplored by the bioengineering community. Instead, most ECM treatments are derived from mammalian tissue which have had limited success in promoting neuroregeneration. In our previous study, we explored zebrafish (Danio rerio) as a possible source of lower-vertebrate ECM. Well-known for their ability to easily regenerate damaged optic nerves and severed spinal cords, these small freshwater-dwelling zebrafish possess CNS-ECM that aids axonal repair by suppressing glial cell activation and circumventing inflammatory response. Zf-brECM was able to successfully culture mammalian primary cortical neurons in vitro. Unlike mammalian-derived ECMs, zf-brECM was able to promote robust neuronal survival as well as axonal network formation capable of action potential propagation.

In the present study, regenerative potential of zf-brECM was further investigated in vivo to better understand its viability as an ECM treatment for CNS injuries. Most animal models of CNS injury (eg. spinal cord injury model, brain trauma model, middle cerebral arterial occlusion model) are complex, making the surgeries and the analysis difficult to replicate and analyze. Instead, ONC model was selected as it represents a simplified CNS injury model for the following reasons: 1) ONC surgery is more replicable due to the ease of access to the optic nerves, lending itself to minimal surgical variability and intra-animal data noise; 2) optic nerves are small and their

neural circuitries are simple, making the resident RGCs and their axons easy to analyze [32-34]. Several aspects of a successful CNS regeneration were measured, such as long-distance axons traversing the lesion site, decreased release of axon inhibitors, proper innervation, and ultimately, behavioral recovery.

Zf-brECM was able to positively influence regeneration of axons and their synaptic functionality in the visual pathway. Treatment of ONC with zf-brECM improved long-distance growth and repair of RGC axons compared to mammalian ECMs. In mammalian optic nerve injuries, RGCs typically undergo apoptosis and display transient sprouting, meaning they are incapable of long-distance axon regeneration across the injury site under normal physiological circumstances. Optic nerves treated with zf-brECM however displayed various shifts in their early injury response. For example, a prominent source of inhibition in mammalian CNS regeneration is the glial scar deposition that forms in response to the injury. Rats that received treatments of zf-brECM additives however reduced the spread of glial scarring. While no group completely prevented or eliminated glial scar from forming, by day 28, only zf-brECM group had managed to significantly halt further spread of the scarring. Various studies suggest that presence of glial scar does not necessarily prevent axon and neurite growth, and that absence of glial scar does not guarantee it [124]. Likewise, meaningful CNS regeneration occurred in rats treated with zf-brECM when adequate containment of reactive astrocytes was achieved. As astrocyte scar functions to sequester immune cells, in the absence of astrocytes, inflammation overtakes the axons [137-139]. Therefore, axons of injured optic nerves may find it optimal for growth when glial scar is reduced but not completely eliminated by zf-brECM. Interestingly, this behavior resembles native optic nerves found in zebrafish which are capable of both glial scar development and axonal regeneration [61-63].

The increased axonal coverage of lesion sites following reduced glial scarring in zf-brECM group is also in agreement with the decreased level of initial CSPG expression. A hallmark trait of glial scarring is increased immunoreactivity for CSPGs, which are known to inhibit axonal regeneration [64,121]. In mammals, CSPGs play a direct role in inhibition of axon regeneration. However, in the optic nerve and tract of adult zebrafish, CSPGs are not found directly before or after an ONC, allowing successful regeneration of RGC axons to occur [121,122]. It is speculated that in zebrafish and their ECM, CSPGs act as repellent axon guidance molecules rather than inhibitors that help axons find their correct path to their tectal targets [143,144]. In our study, CSPG expression level decreased between day 7 and 28 for all groups, and in many animals, presence of CSPG was completely removed by the end of day 28, regardless of the type of ECM treatment. This is reasonable as CSPGs are primarily an early injury-response and typically subside on their own without intervention. However, only zf-brECM-treated rats exhibited early suppression of CSPG at day 7. In fact, inhibition of CSPG expression at day 7 following zf-brECM treatment coincided with overexpression of β3-tubulin at both day 7 and 28. As overexpression of β3-tubulin is known to promote sensory axon regeneration, it stands to reason reduced CSPG and increased β3-tubulin would have a positive influence on the rat's visually-guided behaviors.

We then observed two sets of visually-guided behaviors: 1) pupil response using PLR and 2) depth aversion using visual cliff test. The PLR behavior involves retino-subcortical pathways and do not require the cortex whereas the visual cliff depth perception task depends on binocular vision and thus involves the dorsal lateral geniculate nucleus (dLGN) and primary visual cortex (V1). Rats also naturally possess poor, blurry vision and lack the visual acuity of humans due to factors such as small optics, small size of eyes, large depth of focus, and composition of their cones and rods [35]. Even their binocular depth perception is fairly limited compared to that of humans,

with their field of binocular vision measuring at 76° versus 105° of humans [36]. However, depth aversion is driven by various other methods than binocular depth perception, and rats rely on what is known as 'motion parallax' to estimate depth [37]. 'Motion parallax' is a non-binocular method of perceiving depth that relies on perceived change of object's relative position when one's head moves side to side. Rats also orient themselves using distant visual cues, and for very short distances, can rely on whiskers for depth perception [38]. Therefore, test such as the visual cliff test is a reliable means of measuring the rat's recovery of visual prowess and depth aversion.

Zf-brECM promoted moderate restoration of pupil dilation and constriction, and mild recovery of depth aversion in rats after ONC. In contrast, rats treated with mammalian ECMs displayed no sign of improvement in their visually-guided behaviors. Their eyes remained mostly unresponsive to bright light stimuli, showing little to no pupil constriction and dilation. Their near-cliff behaviors also remained unchanged after mammalian ECM treatments, showing visibly no awareness of pending falls or their proximity to the cliff. Zf-brECM succeeded in partial restoration of depth aversion and while the recovery was modest, the implications are promising. For example, even a mild recovery in the visual cliff task suggests that the regeneration of RGC axons could reach the dLGN, the nucleus that relays visual information to V1 [150]. The more significant PLR improvement in zf-brECM can also imply that the threshold for functional recovery of the retino-geniculo-cortical pathway may be higher than that of the other retinofugal parallel pathways for both synapse formation and precision of wiring. Indeed, retinotopic and spatial precision of connections may not be a prerequisite for pathways driving PLR since they can respond just as well to large-field illumination, whereas visual cliff tasks require analysis of spatial frequency and thus higher resolution image-formation [151,152]. It is also possible that the regeneration resulting from zf-brECM treatment failed to restore the connections that mediate

visual cliff avoidance behavior because there were defects in synapse formation and/or insufficient numbers of axons regenerating to the dLGN. It is also possible for functional recovery of retinocollicular connections after distal nerve cut to display anatomical regeneration without functional restoration [36].

## 4.5 SUMMARY

Crushed optic nerves treated with zf-brECM were able to halt glial scar deposition from spreading and suppress early expression of CSPGs. While zf-brECM did not completely prevent glial scar formation or CSPGs release, its effects in controlling the boundaries of their presence distinguished zf-brECM from mammalian ECMs such as p-brECM, p-UBM, and r-brECM. Zf-brECM also returned the highest lesion coverage of repairing neurons. The biological findings supplemented the results of our behavioral assays. For instance, zf-brECM returned the best PLR restoration of the injured eyes. Additionally, zf-brECM achieved the best recovery of depth perception in the rats following ONC. In conclusion, our findings demonstrating the advantages of zf-brECM and the resulting long-distance axon regeneration and partial recovery of visual function may prove informative for devising future treatments for CNS injuries in patients suffering from neurodegenerative diseases or physical trauma.

## 4.6 FUTURE WORK

To further verify the regenerative capacity of zf-brECM, it should be further tested in animal models that represent more complex CNS injury. Furthermore, the study requires a thorough, robust investigation of the ECM's composition and its dynamic in order to delineate key players involved in zf-brECM's regenerative ability.

# 5.0 DISSERTATION SUMMARY

While ECM technology has been successful in restoring cellular and tissue functions in various tissues and organs, it has consistently faced challenges in treating CNS injuries. This limitation stems from the fact that ECM technology currently derives its matrix components exclusively from mammalian tissue. The work presented in this dissertation explores a novel, non-mammalian source of ECM – the zebrafish. Zebrafish are known to have ECM that allows for exceptional axonal regeneration following a CNS injury, and the methods described in this dissertation attempt to harness this ability.

## 5.1 ZEBRAFISH CNS-ECM IMPACT ON NEURON VIABILITY AND AXON FORMATION

To the best of our knowledge, this is the first study using ECM treatment derived from either zebrafish tissue or any lower-vertebrate. With no precedent study serving as a frame of reference on how mammalian cells would behave in the context of zebrafish ECM, the testing of zebrafish ECM had to be thorough and comprehensive. We were primarily interested in the regenerative potential of their CNS-ECM, derived specifically from adult zebrafish brains. Primary cortical neurons were isolated and allowed to grow in scaffolds embedded with either zf-brECM, p-brECM, p-UBM, or r-brECM. The scaffolds themselves were 3D constructs comprised of PGS and hemispherical in shape with a hollow center. This design allowed neurons to populate themselves

in the outer periphery and sprout their axons toward the center, making it easier to isolate neuron analysis from axon observation. Preliminary tests showed that small variation in neuron population density and distribution had amplified effect on eventual axon network formation. This was addressed in subsequent iterations of the 3D constructs by controlling their structural characteristics such as porosity and average pore size. The study demonstrated that zf-brECM achieved better neuron retention and growth than mammalian ECMs. This had a direct influence on axon network formation such as network density and axonal lengths. The initial neuron retention and survival also seem to have a direct effect on the level of functional axons that can be achieved, but it remains to be determined exactly what determines the zf-brECM's ability to support a better thriving neuron population. We suspect various adhesion molecules are at play.

## 5.2 AXON NETWORKS AND SIGNAL PROPAGATION

Additionally, while different ECM promoted varying degrees of axon growth, not all developed the capacity to propagate action potential signals. This required a detailed analysis of functional capacity of the axon networks that were forming. Mainly, we want the newly formed networks to relay action potential signal with minimal loss of information. Oligodendrocytes and their myelin sheath are responsible for ensuring safe passage of neuronal signals, and functional CNS networks typically possess abundance of myelin as they are essential for rapid propagation of action potentials. However, they also operate as inhibitors of axonal repair [73]. In most traumatic CNS injuries such as an optic nerve damage, myelin sheath is destroyed and the involved neurons and axons quickly deteriorate. Studies suggest that uniquely in zebrafish, myelins do not serve as axon

inhibitors because their inhibitory domains do not exist [94-96,124]. In other words, ECM derived from zebrafish has the potential of supporting myelination while simultaneously supporting rapid action potential propagation without inhibiting axonal outgrowth. To test this theory, our measurements of axon thickness were used to compare relative myelin sheath thickness formed along the axonal extensions, and by comparing this finding to functional analysis of the network, we were able to demonstrate that zf-brECM promoted better growth of meaningful axon networks. This was further confirmed by the transient rise in intracellular calcium levels, which was recorded as a measure of electrical activity of the neurons. This established the proof-of-concept of using zebrafish CNS as an alternative ECM source for CNS remodeling and laid the foundation for investigating zf-brECM in vivo. We suspect the level of meaningful axon networks achieved will have direct effect on translational efficacy in animal models.

### 5.3 GLIAL SCAR DEPOSITION AND AXON INHIBITORS

Regenerative potential of zf-brECM was examined using rodent optic nerve as an injury model. CNS regeneration is a multifaceted event marked by several key regenerative traits, and following ECM treatment using zf-brECM, we observed two distinct characteristics of a partial nerve regeneration in an ONC model. First and foremost, zf-brECM decreased the spread of glial scar deposition by reactive astrocytes. Glial scar deposition is a key mechanism of mammalian CNS injury response meant to contain macrophage-driven digestion of the remaining nerve tissue. While this helps to barricade the surviving axons and neurons from further damage, it also forms a barrier that inhibits axonal growth that is needed for nerve regeneration. A key finding from our study was that while zf-brECM did not prevent glial scar deposition, it significantly reduced its

spread. Reduced deposition of glial scar can have several implications, one of which is decreased expression of axon inhibitor molecules. Typically, reactive astrocytes stop axons from growing through the glial scar deposition by releasing several axon inhibitors, such as CSPGs. Thus, we observed CSPG expression following different ECM treatments, and found that zf-brECM decreases initial release of CSPGs following an injury. Overall, zf-brECM promotes several biological characteristics representative of a CNS regeneration, but ultimately, for clinical application, it must achieve axon growth and connections.

## 5.4 AXONAL REESTABLISHMENT AND BEHAVIORAL RECOVERY

We produced ONC models in which to test regenerative efficacy of zebrafish-derived ECM. Given the reduced glial scar from zf-brECM, it is possible to expect more nerve damage caused by unchecked macrophage activities. Thus, we observed axon growth transverse of damage site. While no ECM was able to achieve complete nerve reconnection, the results demonstrated zf-brECM's ability to promote better growth of repairing axons. Several individual axons were even able to cross the entirety of the damage site. But on a macroscopic scale, zf-brECM achieved partial recovery of axon growth. Behavioral analysis showed that partial axon regeneration from zf-brECM still led to improved optical functions as well as restoration of depth aversion.

Several challenges still remain in the development of zebrafish brain as a viable source for ECM technology. We do not yet know how much axons will regrow in a larger CNS model such as a spinal cord injury. We have also yet to determine what growth factors are present to help the axon growth, what inhibitors are absent to allow repair, and what external cues exist to guide the

axons. To address this gap in our knowledge, a comprehensive proteomic test aimed at characterizing the ECM is needed.

## 5.5 FINAL CONCLUSIONS

The intricate design of ECM found in adult mammalian CNS is a complex double-edged sword – it ensures the detrimental effects of traumatic injuries are kept minimal, but at the same time limits all regenerative response. While targeting individual components of the ECM to render it more repair-permissive may be an enticing approach, the effects are negated by the compensatory nature of ECM composition. This indicates the ECM must be completely overwritten, but synthesizing a network of proteins and biomolecules is an arduous task, constrained by our limited understanding of what evokes regeneration in CNS in the first place. This leads us to believe ECM technology is the most viable approach to unlocking CNS regeneration, but traditional ECM products derived from mammalian tissue hold little promise for CNS. As a response, in the course of this dissertation, we explored the possibility of using ECM derived from zebrafish brain for CNS regeneration. The methods described in this dissertation are comprehensive in demonstrating zf-brECM's ability to support neurons and axons in vitro. This finding was taken farther by looking at biological response in an animal using rodent ONC. Major finding included reduced spread of glial scar deposition and decreased level of CSPGs. Finally, repairing axonal growth transverse of damage site demonstrated zf-brECM's ability to promote meaningful regeneration in vivo. Behavioral analysis showed that partial axon regeneration from zf-brECM led to moderate recoveries of visually-guided functions such as pupil dilation and depth aversion. We anticipate the field of CNS

regeneration and ECM technology will both benefit from this research as it opens the possibility of investigating numerous nonconventional species for biomedical applications.

## BIBLIOGRAPHY

[1] Marr, A. L. C. V., and Victor G. Coronado. "Central nervous system injury surveillance data submission standards-2002." (2004).

[2] Shashoua, Victor E. "The role of brain extracellular proteins in neuroplasticity and learning." Cellular and molecular neurobiology 5.1 (1985): 183-207.

[3] Mora, Francisco, Gregorio Segovia, and Alberto del Arco. "Aging, plasticity and environmental enrichment: structural changes and neurotransmitter dynamics in several areas of the brain." Brain research reviews 55.1 (2007): 78-88.

[4] Barros, Claudia S., Santos J. Franco, and Ulrich Müller. "Extracellular matrix: functions in the nervous system." Cold Spring Harbor perspectives in biology 3.1 (2011): a005108.

[5] Burnside, E. R., and E. J. Bradbury. "Manipulating the extracellular matrix and its role in brain and spinal cord plasticity and repair." Neuropathology and applied neurobiology 40.1 (2014): 26-59.

[6] Hay, Elizabeth D., ed. Cell biology of extracellular matrix. Springer Science & Business Media, 2013.

[7] Busch, Sarah A., and Jerry Silver. "The role of extracellular matrix in CNS regeneration." Current opinion in neurobiology 17.1 (2007): 120-127.

[8] Zimmermann, Dieter R., and María T. Dours-Zimmermann. "Extracellular matrix of the central nervous system: from neglect to challenge." Histochemistry and cell biology 130.4 (2008): 635-653.

[9] Rasmussen, Jeffrey P., and Alvaro Sagasti. "Learning to swim, again: axon regeneration in fish." Experimental neurology 287 (2017): 318-330

[10] Fleisch, Valerie C., Brittany Fraser, and W. Ted Allison. "Investigating regeneration and functional integration of CNS neurons: lessons from zebrafish genetics and other fish species." Biochimica et Biophysica Acta (BBA)-Molecular Basis of Disease 1812.3 (2011): 364-380.

[11] Stocum, David L. Regenerative biology and medicine. Academic Press, 2012.

[12] Becker, Thomas, et al. "Axonal regrowth after spinal cord transection in adult zebrafish." Journal of Comparative Neurology 377.4 (1997): 577-595.

[13] Mokalled, Mayssa H., et al. "Injury-induced ctgfa directs glial bridging and spinal cord regeneration in zebrafish." Science 354.6312 (2016): 630-634.

[14] Sood, Disha, et al. "Fetal brain extracellular matrix boosts neuronal network formation in 3d bioengineered model of cortical brain tissue." ACS Biomaterials Science & Engineering 2.1 (2015): 131-140.

[15] Draganski, Bogdan, et al. "Neuroplasticity: changes in grey matter induced by training." Nature 427.6972 (2004): 311-312.

[16] Wang, Yadong, et al. "A tough biodegradable elastomer." Nature biotechnology 20.6 (2002): 602-606.

[17] Brewer, Gregory J. "Isolation and culture of adult rat hippocampal neurons." Journal of Neuroscience Methods 71.2 (1997): 143-155.

[18] Chen, William CW, et al. "Decellularized zebrafish cardiac extracellular matrix induces mammalian heart regeneration." Science Advances 2.11 (2016): e1600844.

[19] Crapo, P. M., Medberry, C. J., Reing, J. E., Tottey, S., van der Merwe, Y., Jones, K. E., & Badylak, S. F. (2012). Biologic scaffolds composed of central nervous system extracellular matrix. Biomaterials, 33(13), 3539-3547.

[20] DeQuach, Jessica A., et al. "Decellularized porcine brain matrix for cell culture and tissue engineering scaffolds." Tissue Engineering Part A 17.21-22 (2011): 2583-2592.

[21] Forsey RW, Chaudhuri JB. “Validity of DNA analysis to determine cell numbers in tissue engineering scaffolds.” Biotechnol Lett. (2009):819-23.

[23] Paolicelli, Rosa C., et al. "Synaptic pruning by microglia is necessary for normal brain development." science 333.6048 (2011): 1456-1458.

[24] Marçal, Helder, et al. "A comprehensive protein expression profile of extracellular matrix biomaterial derived from porcine urinary bladder." Regenerative medicine 7.2 (2012): 159-166.

[25] Zhang, Yuanyuan, et al. "Tissue-specific extracellular matrix coatings for the promotion of cell proliferation and maintenance of cell phenotype." Biomaterials 30.23 (2009): 4021-4028.

[26] Eytan, Danny, and Shimon Marom. "Dynamics and effective topology underlying synchronization in networks of cortical neurons." Journal of Neuroscience 26.33 (2006): 8465-8476.

[27] Myers, Jonathan P., Miguel Santiago- Medina, and Timothy M. Gomez. "Regulation of axonal outgrowth and pathfinding by integrin–ECM interactions." Developmental neurobiology 71.11 (2011): 901-923.

[28] Raper, Jonathan, and Carol Mason. "Cellular strategies of axonal pathfinding." Cold Spring Harbor perspectives in biology 2.9 (2010): a001933.

[29] Santiago-Medina, Miguel, et al. "Regulation of ECM degradation and axon guidance by growth cone invadosomes." Development 142.3 (2015): 486-496.

[30] Gompel, Nicolas, Christine Dambly-Chaudière, and Alain Ghysen. "Neuronal differences prefigure somatotopy in the zebrafish lateral line." Development 128.3 (2001): 387-393.

[31] Kalil, Katherine, and Erik W. Dent. "Touch and go: guidance cues signal to the growth cone cytoskeleton." Current opinion in neurobiology 15.5 (2005): 521-526.

[32] Baranes, Koby, et al. "Interactions of neurons with topographic nano cues affect branching morphology mimicking neuron–neuron interactions." Journal of molecular histology 43.4 (2012): 437-447.

[33] Kalil, Katherine, Gyorgyi Szebenyi, and Erik W. Dent. "Common mechanisms underlying growth cone guidance and axon branching." Journal of neurobiology 44.2 (2000): 145-158.

[34] Fox, Kevin, and Rachel OL Wong. "A comparison of experience-dependent plasticity in the visual and somatosensory systems." Neuron 48.3 (2005): 465-477.

[35] Romo, Ranulfo, and Emilio Salinas. "Touch and go: decision-making mechanisms in somatosensation." Annual review of neuroscience 24.1 (2001): 107-137.

[36] Ebner, Ford F., ed. Neural plasticity in adult somatic sensory-motor systems. CRC Press, 2005.

[37] Yiu, Glenn, and Zhigang He. "Glial inhibition of CNS axon regeneration." Nature Reviews Neuroscience 7.8 (2006): 617-627.

[38] Filbin, Marie T. "Myelin-associated inhibitors of axonal regeneration in the adult mammalian CNS." Nature Reviews Neuroscience 4.9 (2003): 703-713. [39] myelin in ZF

[40] Bastmeyer, Martin, et al. "Growth of regenerating goldfish axons is inhibited by rat oligodendrocytes and CNS myelin but not but not by goldfish optic nerve tract oligodendrocytelike cells and fish CNS myelin." Journal of Neuroscience 11.3 (1991): 626-640.

[41] Lee, John, et al. "Process outgrowth in oligodendrocytes is mediated by CNP, a novel microtubule assembly myelin protein." The Journal of cell biology 170.4 (2005): 661-673.

[42] Suter, Daniel M., and Kyle E. Miller. "The emerging role of forces in axonal elongation." Progress in neurobiology 94.2 (2011): 91-101.

[43] Mosconi, Tony, and Lawrence Kruger. "Fixed-diameter polyethylene cuffs applied to the rat sciatic nerve induce a painful neuropathy: ultrastructural morphometric analysis of axonal alterations." Pain 64.1 (1996): 37-57.

[44] Mora, Francisco, Gregorio Segovia, and Alberto del Arco. "Aging, plasticity and environmental enrichment: structural changes and neurotransmitter dynamics in several areas of the brain." Brain research reviews 55.1 (2007): 78-88.

[45] Barros, Claudia S., Santos J. Franco, and Ulrich Müller. "Extracellular matrix: functions in the nervous system." Cold Spring Harbor perspectives in biology 3.1 (2011): a005108.

[46] Burnside, E. R., and E. J. Bradbury. "Manipulating the extracellular matrix and its role in brain and spinal cord plasticity and repair." Neuropathology and applied neurobiology 40.1 (2014): 26-59.

[47] Kim, Long, Tsang, and Yadong Wang. "Zebrafish Extracellular Matrix Improves Neuronal Viability and Network Formation in a 3-Dimensional Culture."

[48] Fleisch, Valerie C., Brittany Fraser, and W. Ted Allison. "Investigating regeneration and functional integration of CNS neurons: lessons from zebrafish genetics and other fish species." Biochimica et Biophysica Acta (BBA)-Molecular Basis of Disease 1812.3 (2011): 364-380.

[49] Pawar, Kiran, et al. "Intrinsic and extrinsic determinants of central nervous system axon outgrowth into alginate-based anisotropic hydrogels." Acta biomaterialia 27 (2015): 131-139.

[50] Burnside, E. R., and E. J. Bradbury. "Manipulating the extracellular matrix and its role in brain and spinal cord plasticity and repair." Neuropathology and applied neurobiology 40.1 (2014): 26-59.

[51] Ahmed, Zubair, et al. "Matrix metalloproteases: degradation of the inhibitory environment of the transected optic nerve and the scar by regenerating axons." Molecular and Cellular Neuroscience 28.1 (2005): 64-78.

[52] de Lima, Silmara, et al. "Full-length axon regeneration in the adult mouse optic nerve and partial recovery of simple visual behaviors." Proceedings of the National Academy of Sciences 109.23 (2012): 9149-9154.

[53] Klöcker, Nikolaj, et al. "Morphological and functional analysis of an incomplete CNS fiber tract lesion: graded crush of the rat optic nerve." Journal of neuroscience methods 110.1-2 (2001): 147-153.

[54] Koch, Jan C., et al. "Upregulation of reggie-1/flotillin-2 promotes axon regeneration in the rat optic nerve in vivo and neurite growth in vitro." Neurobiology of disease 51 (2013): 168-176.

[55] Kurimoto, Takuji, et al. "Long-distance axon regeneration in the mature optic nerve: contributions of oncomodulin, cAMP, and pten gene deletion." Journal of Neuroscience 30.46 (2010): 15654-15663.

[56] Mead, Ben, et al. "Intravitreally transplanted dental pulp stem cells promote neuroprotection and axon regeneration of retinal ganglion cells after optic nerve injury." Investigative ophthalmology & visual science 54.12 (2013): 7544-7556.

[57] Morishita, Seita, et al. "Systemic simvastatin rescues retinal ganglion cells from optic nerve injury possibly through suppression of astroglial NF-κB activation." PloS one 9.1 (2014): e84387.

[58] Brewer, Gregory J. "Isolation and culture of adult rat hippocampal neurons." Journal of Neuroscience Methods 71.2 (1997): 143-155.

[59] Chen, William CW, et al. "Decellularized zebrafish cardiac extracellular matrix induces mammalian heart regeneration." Science Advances 2.11 (2016): e1600844.

[60] Crapo, P. M., Medberry, C. J., Reing, J. E., Tottey, S., van der Merwe, Y., Jones, K. E., & Badylak, S. F. (2012). Biologic scaffolds composed of central nervous system extracellular matrix. Biomaterials, 33(13), 3539-3547.

[61] Rousseau, Valerie, Ralf Engelmann, and Bernhard A. Sabel. "Restoration of vision III: soma swelling dynamics predicts neuronal death or survival after optic nerve crush in vivo." Neuroreport 10.16 (1999): 3387-3391.

[62] Schols, Saskia EM, et al. "Increased thrombin generation and fibrinogen level after therapeutic plasma transfusion: relation to bleeding." Thrombosis and haemostasis 99.01 (2008): 64-70.

[63] Young, M. J., and R. D. Lund. "The anatomical substrates subserving the pupillary light reflex in rats: origin of the consensual pupillary response." Neuroscience 62.2 (1994): 481-496.

[64] Chen, S-K., T. C. Badea, and S. Hattar. "Photoentrainment and pupillary light reflex are mediated by distinct populations of ipRGCs." Nature 476.7358 (2011): 92.

[65] González Fleitas, María Florencia, et al. "Effect of retinal ischemia on the non-image forming visual system." Chronobiology international 32.2 (2015): 152-163.

[66] Lim, Jung-Hwan A., et al. "Neural activity promotes long-distance, target-specific regeneration of adult retinal axons." Nature neuroscience 19.8 (2016): 1073.

[67] Ahmed, Zubair, et al. "Matrix metalloproteases: degradation of the inhibitory environment of the transected optic nerve and the scar by regenerating axons." Molecular and Cellular Neuroscience 28.1 (2005): 64-78.

[68] Sofroniew, Michael V. "Reactive astrocytes in neural repair and protection." The Neuroscientist 11.5 (2005): 400-407.

[69] Silver, Jerry, and Jared H. Miller. "Regeneration beyond the glial scar." Nature reviews neuroscience 5.2 (2004): 146.

[70] Busch, Sarah A., and Jerry Silver. "The role of extracellular matrix in CNS regeneration." Current opinion in neurobiology 17.1 (2007): 120-127.

[71] Li, Ying, et al. "Transplanted olfactory ensheathing cells promote regeneration of cut adult rat optic nerve axons." Journal of Neuroscience 23.21 (2003): 7783-7788.

[72] Weibel, Doris, Danielle Cadelli, and Martin E. Schwab. "Regeneration of lesioned rat optic nerve fibers is improved after neutralization of myelin-associated neurite growth inhibitors." Brain research 642.1-2 (1994): 259-266.

[73] Lim, Jung-Hwan A., et al. "Neural activity promotes long-distance, target-specific regeneration of adult retinal axons." Nature neuroscience 19.8 (2016): 1073.

[74] Morigiwa, K., et al. "Retinal inputs and laminar distributions of the dorsal lateral geniculate nucleus relay cells in the eastern chipmunk (Tamias sibiricus asiaticus)." Experimental brain research 71.3 (1988): 527-540.

[75] Campos, Joseph J., et al. "The emergence of fear on the visual cliff." The development of affect. Springer, Boston, MA, 1978. 149-182.

[76] Gibson, Eleanor J., and Richard D. Walk. "The visual cliff"." Scientific American 202.4 (1960): 64-71.

[77] Block M. T. 1969. “A note on the refraction and image formation of the rat's eye.” Vision Res. 9(6):705-11.

[78] Heffner, R. S, and H. E. Heffner. 1992. “Visual factors in sound localization in mammals.” J. Comp. Neurol. 317: 219-232.

[79] Kral, K. 2003. “Behavioural-analytical studies of the role of head movements in depth perception in insects, birds and mammals.” Behavioral Processes. 64: 1-12.

[80] Herdegen, Thomas, et al. "Expression of JUN, KROX, and CREB transcription factors in goldfish and rat retinal ganglion cells following optic nerve lesion is related to axonal sprouting." Developmental Neurobiology 24.4 (1993): 528-543.

[81] Becker, Catherina G., and Thomas Becker. "Adult zebrafish as a model for successful central nervous system regeneration." Restorative neurology and neuroscience 26.2, 3 (2008): 71-80.

[82] Udvadia, Ava J., R. W. Koster, and J. H. Skene. "GAP-43 promoter elements in transgenic zebrafish reveal a difference in signals for axon growth during CNS development and regeneration." Development 128.7 (2001): 1175-1182.

[83] Bastmeyer, Martin, et al. "Growth of regenerating goldfish axons is inhibited by rat oligodendrocytes and CNS myelin but not but not by goldfish optic nerve tract oligodendrocytelike cells and fish CNS myelin." Journal of Neuroscience 11.3 (1991): 626-640.

[84] Goldman, D., et al. "Transgenic zebrafish for studying nervous system development and regeneration." Transgenic research 10.1 (2001): 21-33.

[85] Becker, Thomas, et al. "Axonal regrowth after spinal cord transection in adult zebrafish." Journal of Comparative Neurology 377.4 (1997): 577-595.

[86] Reimer, Michell M., et al. "Motor neuron regeneration in adult zebrafish." Journal of Neuroscience 28.34 (2008): 8510-8516.

[87] Becker, Thomas, et al. "Readiness of zebrafish brain neurons to regenerate a spinal axon correlates with differential expression of specific cell recognition molecules." Journal of Neuroscience 18.15 (1998): 5789-5803.

[88] Veldman, Matthew B., et al. "Gene expression analysis of zebrafish retinal ganglion cells during optic nerve regeneration identifies KLF6a and KLF7a as important regulators of axon regeneration." Developmental biology 312.2 (2007): 596-612.

[89] Becker, Catherina G., and Thomas Becker. "Repellent guidance of regenerating optic axons by chondroitin sulfate glycosaminoglycans in zebrafish." Journal of Neuroscience 22.3 (2002): 842-853.

[90] Guo, Yuji, et al. "Transcription factor Sox11b is involved in spinal cord regeneration in adult zebrafish." Neuroscience 172 (2011): 329-341.

[91] Hatta, Kohei. "Role of the floor plate in axonal patterning in the zebrafish CNS." Neuron 9.4 (1992): 629-642.

[92] Panula, P., et al. "The comparative neuroanatomy and neurochemistry of zebrafish CNS systems of relevance to human neuropsychiatric diseases." Neurobiology of disease 40.1 (2010): 46-57.

[93] Grandel, Heiner, et al. "Retinoic acid signalling in the zebrafish embryo is necessary during pre-segmentation stages to pattern the anterior-posterior axis of the CNS and to induce a pectoral fin bud." Development 129.12 (2002): 2851-2865.

[94] Cui, Wilson W., et al. "The zebrafish shocked gene encodes a glycine transporter and is essential for the function of early neural circuits in the CNS." Journal of Neuroscience 25.28 (2005): 6610-6620.

[95] Myers, Paul Z., Judith S. Eisen, and Monte Westerfield. "Development and axonal outgrowth of identified motoneurons in the zebrafish." Journal of Neuroscience 6.8 (1986): 2278-2289.

[96] Varga, Zoltán M., et al. "Zebrafish smoothened functions in ventral neural tube specification and axon tract formation." Development 128.18 (2001): 3497-3509.

[97] Kawai, Hitomi, Noriko Arata, and Hiroshi Nakayasu. "Three- dimensional distribution of astrocytes in zebrafish spinal cord." Glia 36.3 (2001): 406-413.

[98] Ghosh, Chandramallika, et al. "Cell cultures derived from early zebrafish embryos differentiate in vitro into neurons and astrocytes." Cytotechnology 23.1-3 (1997): 221-230.

[99] Koke, Joseph R., Amanda L. Mosier, and Dana M. García. "Intermediate filaments of zebrafish retinal and optic nerve astrocytes and Müller glia: differential distribution of cytokeratin and GFAP." BMC research notes 3.1 (2010): 50.

[100] Grupp, Larissa, Hartwig Wolburg, and Andreas F. Mack. "Astroglial structures in the zebrafish brain." Journal of Comparative Neurology 518.21 (2010): 4277-4287.

[101] März, Martin, et al. "Regenerative response following stab injury in the adult zebrafish telencephalon." Developmental Dynamics 240.9 (2011): 2221-2231.

[102] Baumgart, Emily Violette, et al. "Stab wound injury of the zebrafish telencephalon: a model for comparative analysis of reactive gliosis." Glia 60.3 (2012): 343-357.

[103] Zhuo, Lang, et al. "Live astrocytes visualized by green fluorescent protein in transgenic mice." Developmental biology 187.1 (1997): 36-42.

[104] Herbomel, Philippe, Bernard Thisse, and Christine Thisse. "Zebrafish early macrophages colonize cephalic mesenchyme and developing brain, retina, and epidermis through a M-CSF receptor-dependent invasive process." Developmental biology 238.2 (2001): 274-288.

[105] Mouriec, Karen, et al. "Androgens upregulate cyp19a1b (aromatase B) gene expression in the brain of zebrafish (Danio rerio) through estrogen receptors." Biology of reproduction 80.5 (2009): 889-896.

[106] Lam, Chen Sok, Martin März, and Uwe Strähle. "GFAP and nestin reporter lines reveal characteristics of neural progenitors in the adult zebrafish brain." Developmental Dynamics 238.2 (2009): 475-486.

[107] Lam, Chen Sok, Martin März, and Uwe Strähle. "GFAP and nestin reporter lines reveal characteristics of neural progenitors in the adult zebrafish brain." Developmental Dynamics 238.2 (2009): 475-486.

[108] Lee- Liu, Dasfne, et al. "Spinal cord regeneration: lessons for mammals from non-mammalian vertebrates." Genesis 51.8 (2013): 529-544.

[109] Ghosh, Chandramallika, et al. "Cell cultures derived from early zebrafish embryos differentiate in vitro into neurons and astrocytes." Cytotechnology 23.1-3 (1997): 221-230.

[110] Gestri, Gaia, Brian A. Link, and Stephan CF Neuhauss. "The visual system of zebrafish and its use to model human ocular diseases." Developmental neurobiology 72.3 (2012): 302-327.

[111] Westerfield, Monte, James V. McMurray, and Judith S. Eisen. "Identified motoneurons and their innervation of axial muscles in the zebrafish." Journal of Neuroscience 6.8 (1986): 2267-2277.

[112] McLean, David L., and Joseph R. Fetcho. "Ontogeny and innervation patterns of dopaminergic, noradrenergic, and serotonergic neurons in larval zebrafish." Journal of Comparative Neurology 480.1 (2004): 38-56.

[113] Gamse, Joshua T., et al. "Directional asymmetry of the zebrafish epithalamus guides dorsoventral innervation of the midbrain target." Development 132.21 (2005): 4869-4881.

[114] Olsson, Catharina, Anna Holmberg, and Susanne Holmgren. "Development of enteric and vagal innervation of the zebrafish (Danio rerio) gut." Journal of Comparative Neurology 508.5 (2008): 756-770.

[115] Fricke, Cornelia, et al. "Astray, a zebrafish roundabout homolog required for retinal axon guidance." Science 292.5516 (2001): 507-510.

[116] Mumm, Jeff S., et al. "In vivo imaging reveals dendritic targeting of laminated afferents by zebrafish retinal ganglion cells." Neuron 52.4 (2006): 609-621.

[117] Laessing, Ute, and Claudia Stürmer. "Spatiotemporal pattern of retinal ganglion cell differentiation revealed by the expression of neurolin in embryonic zebrafish." Journal of neurobiology 29.1 (1996): 65-74.

[118] Kay, Jeremy N., et al. "Retinal ganglion cell genesis requires lakritz, a Zebrafish atonal Homolog." Neuron 30.3 (2001): 725-736.

[119] Gao, Jin, Peter M. Crapo, and Yadong Wang. "Macroporous elastomeric scaffolds with extensive micropores for soft tissue engineering." Tissue engineering 12.4 (2006): 917-925.

[120] Flax, Jonathan D., et al. "Engraftable human neural stem cells respond to development cues, replace neurons, and express foreign genes." Nature biotechnology 16.11 (1998): 1033.

[121] Brewer, Gregory J. "Isolation and culture of adult rat hippocampal neurons." Journal of neuroscience methods 71.2 (1997): 143-155.

[122] Huettner, James E., and Robert W. Baughman. "Primary culture of identified neurons from the visual cortex of postnatal rats." Journal of Neuroscience 6.10 (1986): 3044-3060.

[123] Whittington, Miles A., and Roger D. Traub. "Interneuron diversity series: inhibitory interneurons and network oscillations in vitro." Trends in neurosciences 26.12 (2003): 676-682.

[124] Gilbert, Thomas W., et al. "Collagen fiber alignment and biaxial mechanical behavior of porcine urinary bladder derived extracellular matrix." Biomaterials 29.36 (2008): 4775-4782.

[125] Badylak, Stephen F., Donald O. Freytes, and Thomas W. Gilbert. "Extracellular matrix as a biological scaffold material: structure and function." Acta biomaterialia 5.1 (2009): 1-13.

[126] Chiquet-Ehrismann, Ruth, et al. "Tenascin: an extracellular matrix protein involved in tissue interactions during fetal development and oncogenesis." Cell 47.1 (1986): 131-139.

[127] Gupta, Madan, Liang Jin, and Noriyasu Homma. Static and dynamic neural networks: from fundamentals to advanced theory. John Wiley & Sons, 2004.

[128] Aguayo, Albert J. "Axonal regeneration from injured neurons in the adult mammalian central nervous system." Synaptic plasticity (1985): 457-484.

[129] Silver, Jerry, and Jared H. Miller. "Regeneration beyond the glial scar." Nature reviews neuroscience 5.2 (2004): 146.

[130] Lu, Paul, and Mark H. Tuszynski. "Growth factors and combinatorial therapies for CNS regeneration." Experimental neurology 209.2 (2008): 313-320.

[131] Aguayo, Albert J., et al. "Degenerative and regenerative responses of injured neurons in the central nervous system of adult mammals." Phil. Trans. R. Soc. Lond. B 331.1261 (1991): 337-343.

[132] David, Samuel, and Albert J. Aguayo. "Axonal elongation into peripheral nervous system" bridges" after central nervous system injury in adult rats." Science 214.4523 (1981): 931-933.

[133] Strittmatter, Stephen M., et al. "Neuronal pathfinding is abnormal in mice lacking the neuronal growth cone protein GAP-43." Cell 80.3 (1995): 445-452.

[134] Baird, Douglas H., M. E. Hatten, and C. A. Mason. "Cerebellar target neurons provide a stop signal for afferent neurite extension in vitro." Journal of Neuroscience 12.2 (1992): 619-634.

[135] Arlotta, Paola, et al. "Neuronal subtype-specific genes that control corticospinal motor neuron development in vivo." Neuron 45.2 (2005): 207-221.

[136] Twiss, Jeffery L., and Jan Van Minnen. "New insights into neuronal regeneration: the role of axonal protein synthesis in pathfinding and axonal extension." Journal of neurotrauma 23.3-4 (2006): 295-308.

[137] Song, Hong-jun, and Mu-ming Poo. "Signal transduction underlying growth cone guidance by diffusible factors." Current opinion in neurobiology 9.3 (1999): 355-363.

[138] Saueressig, Harald, John Burrill, and Martyn Goulding. "Engrailed-1 and netrin-1 regulate axon pathfinding by association interneurons that project to motor neurons." Development 126.19 (1999): 4201-4212.

[139] Dodd, Jane, and Thomas M. Jessell. "Axon guidance and the patterning of neuronal projections in vertebrates." Science 242.4879 (1988): 692-699.

[140] Maness, Patricia F., and Melitta Schachner. "Neural recognition molecules of the immunoglobulin superfamily: signaling transducers of axon guidance and neuronal migration." Nature neuroscience 10.1 (2007): 19.

[141] McKerracher, Let al, et al. "Identification of myelin-associated glycoprotein as a major myelin-derived inhibitor of neurite growth." Neuron 13.4 (1994): 805-811.

[142] Brösamle, Christian, and Marnie E. Halpern. "Characterization of myelination in the developing zebrafish." Glia 39.1 (2002): 47-57.

[143] Pogoda, Hans-Martin, et al. "A genetic screen identifies genes essential for development of myelinated axons in zebrafish." Developmental biology 298.1 (2006): 118-131.

[144] Mikelberg, Frederick S., et al. "The normal human optic nerve: axon count and axon diameter distribution." Ophthalmology 96.9 (1989): 1325-1328.

[145] Barazany, Daniel, Peter J. Basser, and Yaniv Assaf. "In vivo measurement of axon diameter distribution in the corpus callosum of rat brain." Brain 132.5 (2009): 1210-1220.

[146] Grozdanic, Sinisa D., et al. "Temporary elevation of the intraocular pressure by cauterization of vortex and episcleral veins in rats causes functional deficits in the retina and optic nerve." Experimental eye research 77.1 (2003): 27-33.

[147] Grozdanic, Sinisa D., et al. "Functional evaluation of retina and optic nerve in the rat model of chronic ocular hypertension." Experimental eye research 79.1 (2004): 75-83.

[148] Grozdanic, Sinisa D., et al. "Functional characterization of retina and optic nerve after acute ocular ischemia in rats." Investigative ophthalmology & visual science 44.6 (2003): 2597-2605.

[149] Whiteley, S. J. O., et al. "Extent and duration of recovered pupillary light reflex following retinal ganglion cell axon regeneration through peripheral nerve grafts directed to the pretectum in adult rats." Experimental neurology 154.2 (1998): 560-572.

[150] Díaz, Florentina, et al. "Experimental model of ocular hypertension in the rat: study of the optic nerve capillaries and action of hypotensive drugs." Investigative ophthalmology & visual science 51.2 (2010): 946-951.

[151] Díaz, Florentina, et al. "Experimental model of ocular hypertension in the rat: study of the optic nerve capillaries and action of hypotensive drugs." Investigative ophthalmology & visual science 51.2 (2010): 946-951.

[152] Fox, M. W. "The visual cliff test for the study of visual depth perception in the mouse." Animal behaviour 13.2-3 (1965): 232-IN3.

[153] Walk, Richard D. "The development of depth perception in animals and human infants." Monographs of the Society for Research in Child Development 31.5 (1966): 82-108.